im2np

Institut Matériaux Microélectronique Nanosciences Provence

La préparation des substrats de silicium pour la croissance de nanostructures SiGe

L. Favre[1], J.-B. Claude[1], T. Bottein[1], M. Naffouti[1], K. Liu[1], T. David[1], A. Benkouider[1], G. Amiard[1], E. Ruiz-Gomes[1], A. Delobbe[2], P. Sudraud[2], J.-N. Aqua[3], M. Abbarchi[1], D. Grosso[1], A. Ronda[1], I. Berbezier[1]

(1)IM2NP, UMR CNRS 7334, Aix-Marseille Université, France
(2)Orsay Physics, Fuveau, France
(3)INP, UMR CNRS 75252, Université Pierre et Marie Curie Paris, France

Atelier GDR Pulse 2018

22 – 24 mai, Villeneuve d'Ascq (IEMN), France

cnrs
Aix*Marseille université
Initiative d'excellence
UNIVERSITÉ DE TOULON
ISEN
ALL IS DIGITAL!
MÉDITERRANÉE
yncréa
Association INSTITUTS CARNOT

Institut Matériaux Microélectronique
Nanosciences de Provence

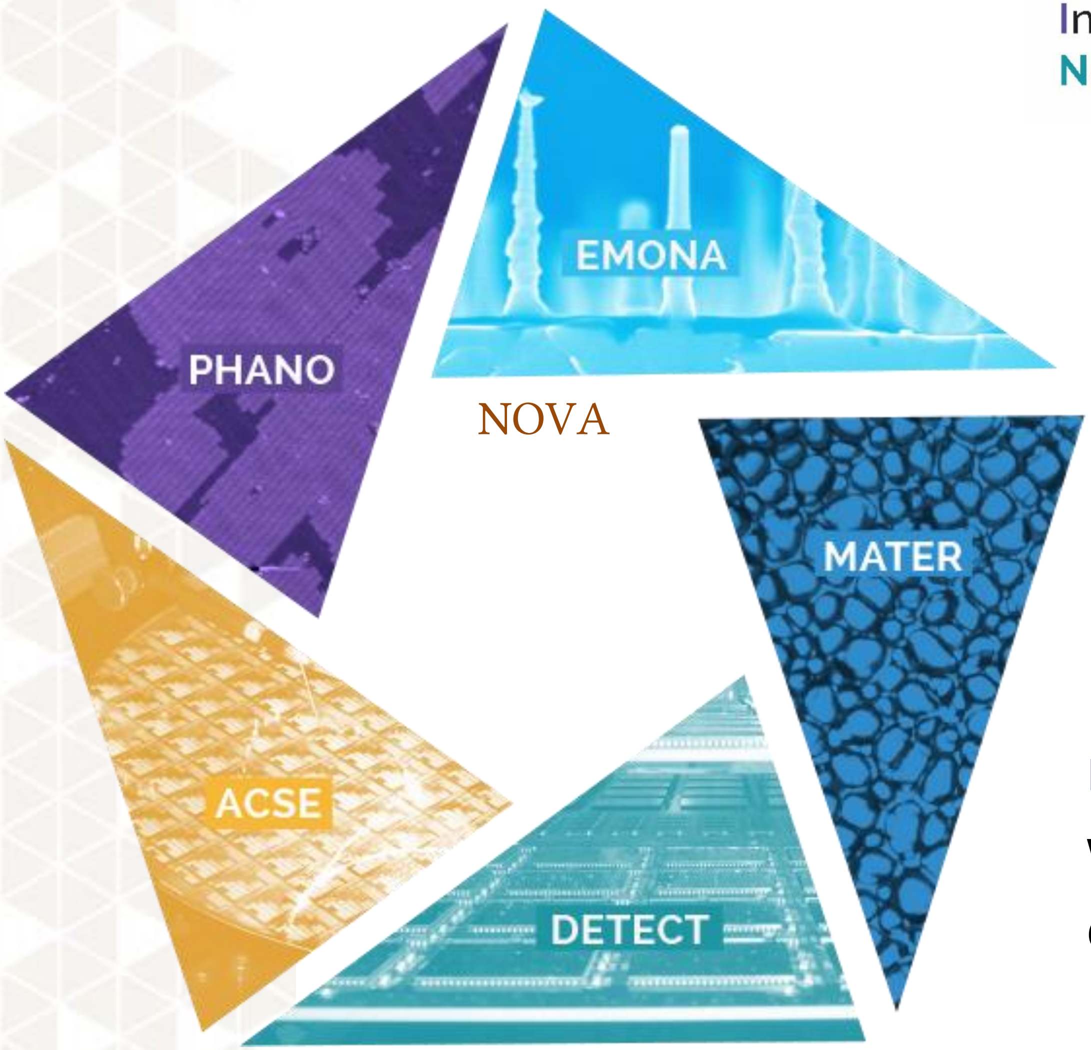

Linking fundamental research to applications within our fields of expertise

www.im2np.fr

Introduction

Development of new technologies: 2D, 1D, 0D and strain

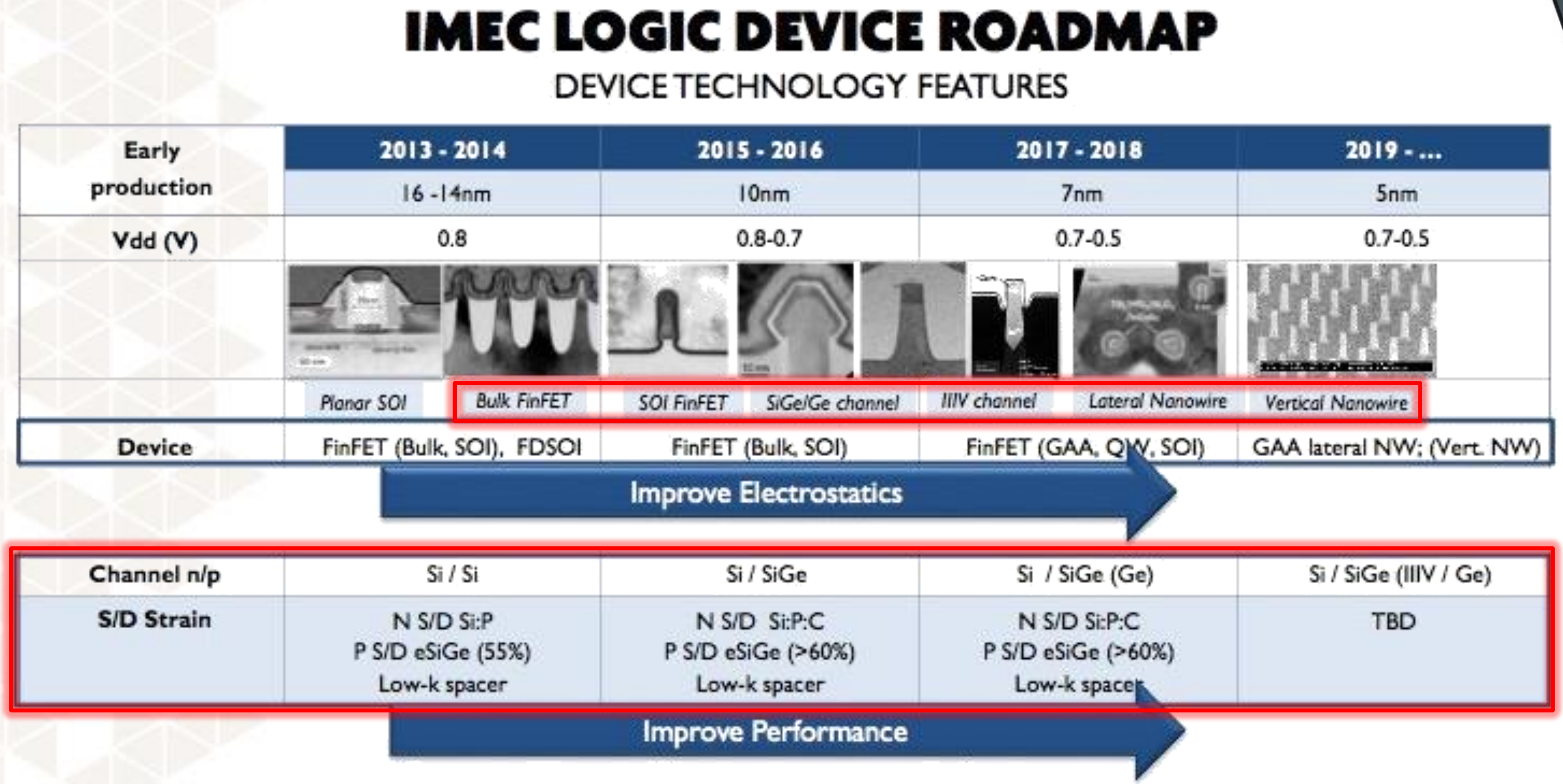

IMEC LOGIC DEVICE ROADMAP

DEVICE TECHNOLOGY FEATURES

Early production	2013 - 2014	2015 - 2016	2017 - 2018	2019 - ...
	16 -14nm	10nm	7nm	5nm
Vdd (V)	0.8	0.8-0.7	0.7-0.5	0.7-0.5
	Planar SOI *Bulk FinFET*	*SOI FinFET* *SiGe/Ge channel*	*IIIV channel* *Lateral Nanowire*	*Vertical Nanowire*
Device	FinFET (Bulk, SOI), FDSOI	FinFET (Bulk, SOI)	FinFET (GAA, QW, SOI)	GAA lateral NW; (Vert. NW)

Improve Electrostatics

Channel n/p	Si / Si	Si / SiGe	Si / SiGe (Ge)	Si / SiGe (IIIV / Ge)
S/D Strain	N S/D Si:P P S/D eSiGe (55%) Low-k spacer	N S/D Si:P:C P S/D eSiGe (>60%) Low-k spacer	N S/D Si:P:C P S/D eSiGe (>60%) Low-k spacer	TBD

Improve Performance

In new strategies: 3D structures and Strain engineering

Introduction

Development of new technologies: 2D, 1D, 0D and strain

STMICROELECTRONICS LOGIC DEVICE ROADMAP

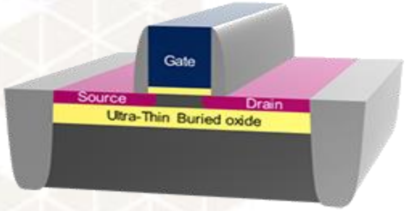

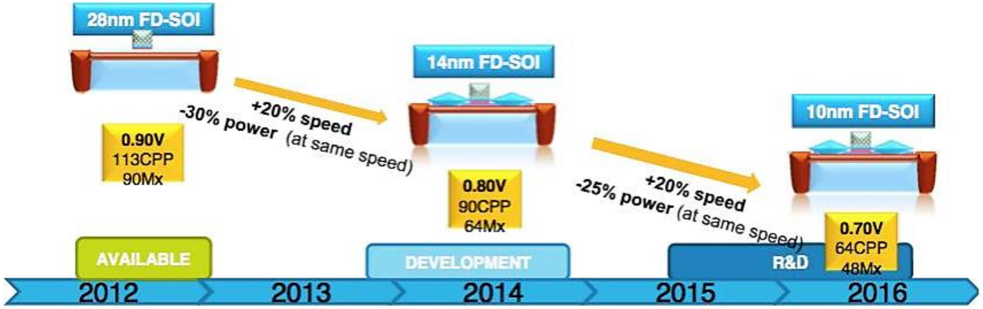

FD-SOI

INTEL LOGIC DEVICE ROADMAP

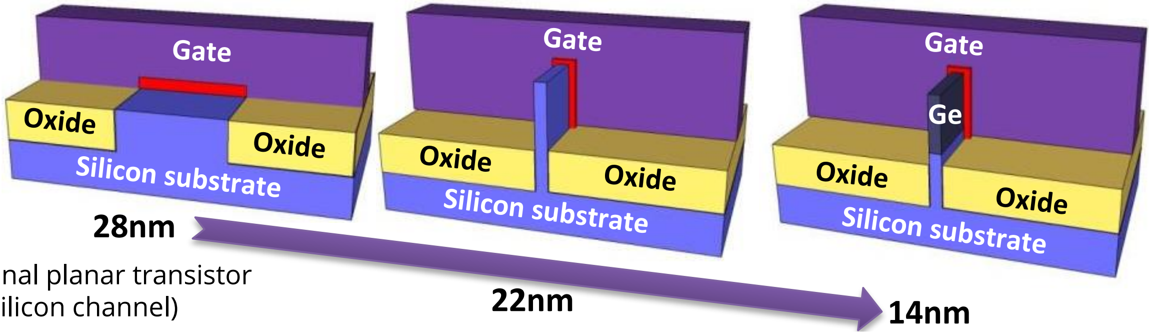

FIN-FET

28nm
Traditional planar transistor
(silicon channel)

22nm
3D FinFET
(vertical Si fin on oxide)

14nm
3D FinFET
(Ge new fin material)

Introduction

Example: nanowires application

Synthetizing a single device

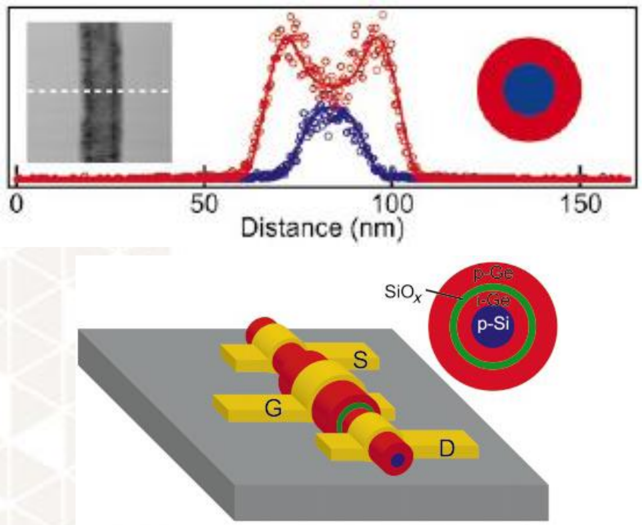

Lincoln J. Lauhon *et al.*, Nature (2002)

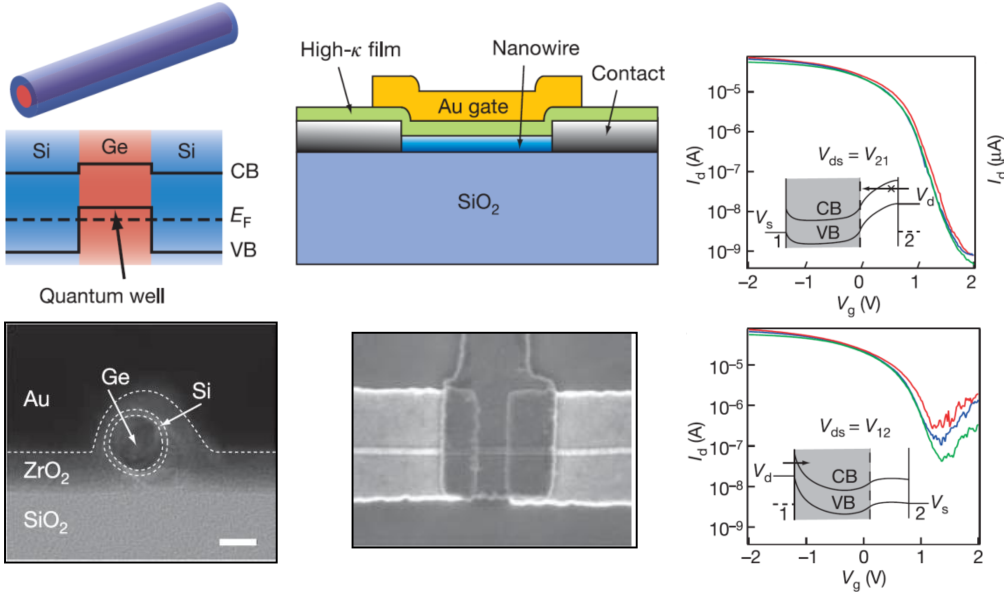

Jie Xiang *et al.*, Nature (2006)

- Ge/Si nanowires ⇒ one-dimensional hole-gas
- One-dimensional quantum confinement effects ⇒ reduced carrier scattering
- Enhanced gate coupling with high-k dielectrics give high-performance FETs
- Intrinsic switching delay comparable to similar length carbon nanotube FETs

J.-N. Aqua, *et al.*, Phys. Rep., **522**, 59 (2013)

Introduction

Example: nanowires application

Organizing multiple objects

Si cells absorption spectrum

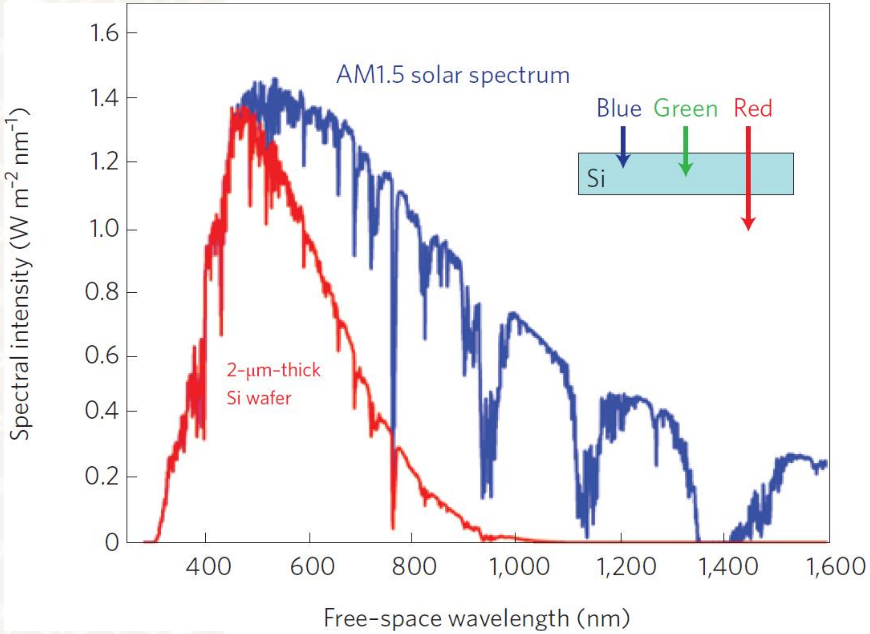

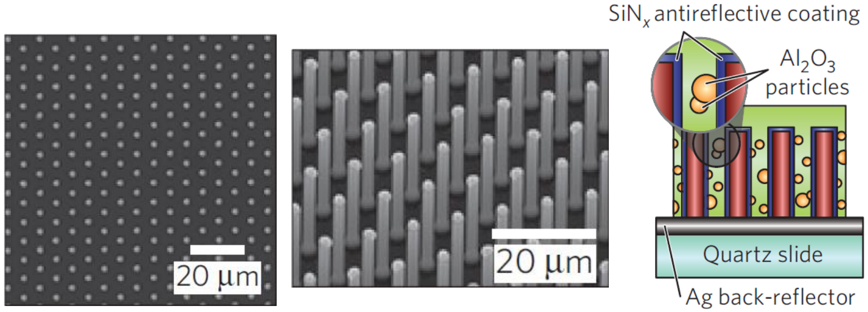

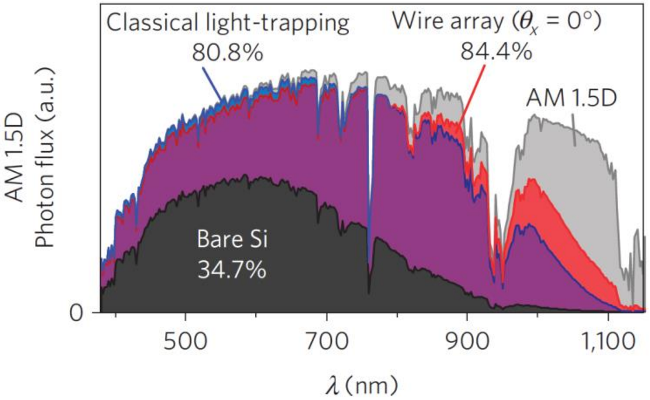

Large unused spectrum range

H. Atwater, A. Polman, Nat. Mater., **9**, 10, 865 (2010)

Nanowires arrays enhance absorption

Kelzenberg *et al.*, Nat. Mater., **9**, 3, 239 (2010)

Introduction

Example: nanowires organization

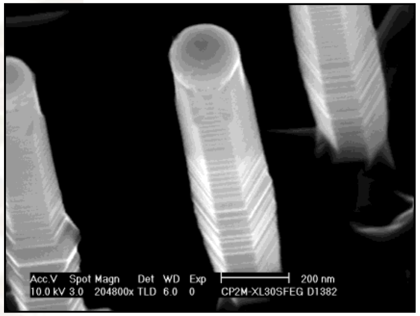

Metallic droplets act as a catalyst in NW growth

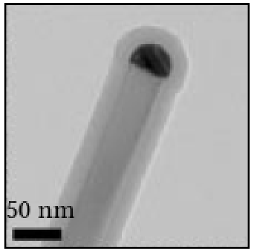

L. J. Lauhon *et al.*, *Nature*, **420**, 6911, 57 (2002)

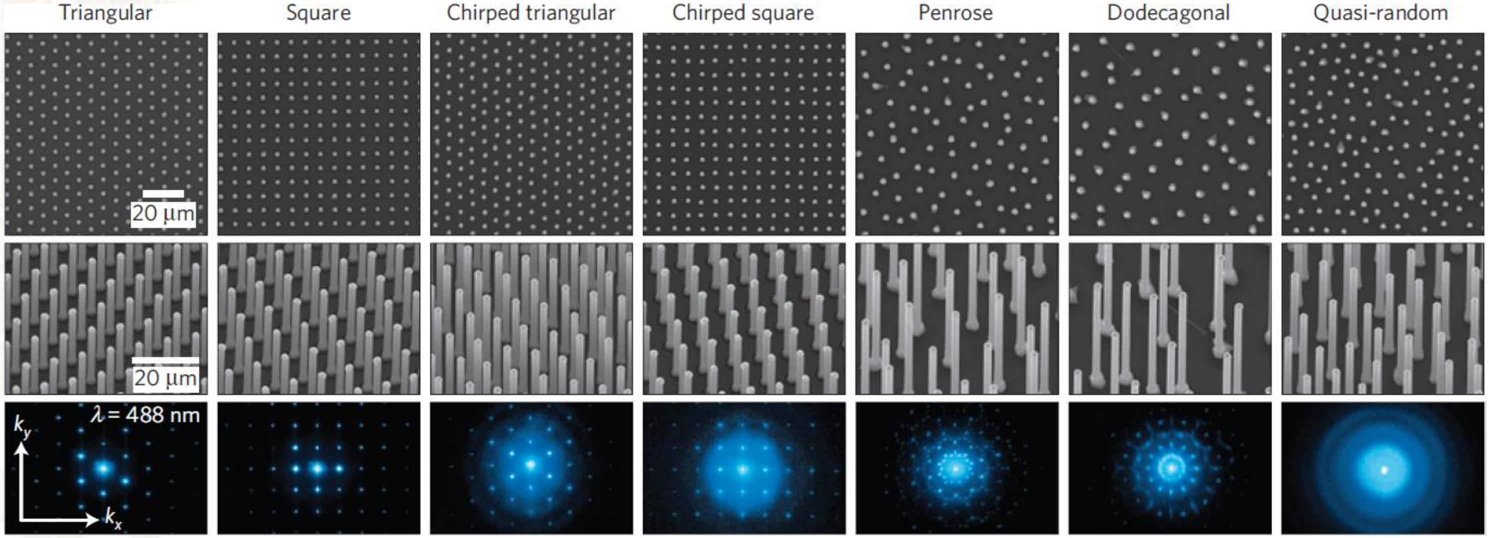

Kelzenberg *et al.*, Nat. Mater., **9**, 3, 239 (2010)

Lithography: for organisation

Introduction

Other examples: Quantum dots applications

Floating gate memories

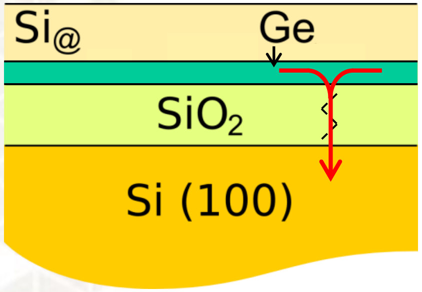

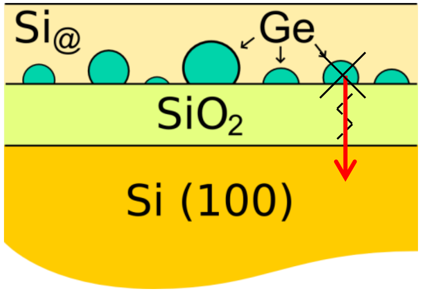

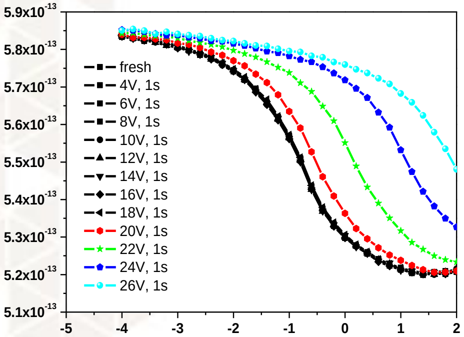

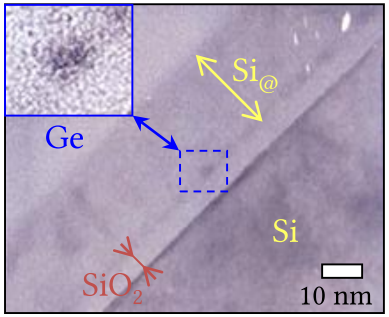

TEM cross section

Quantum dots: light-emitting diodes

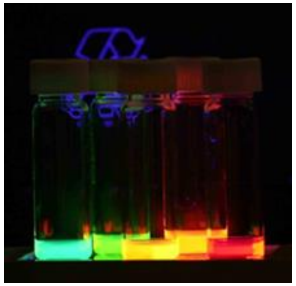

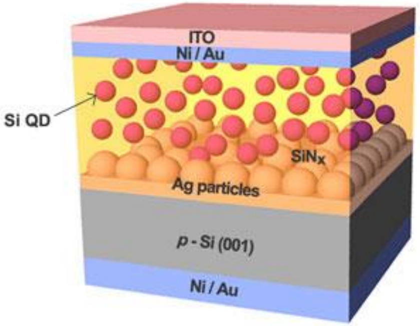

Kim *et al.*, Adv. Mater., **20**, 24, 1521 (2008)

Introduction

Silicon substrate preparation for SiGe nanostructures growth

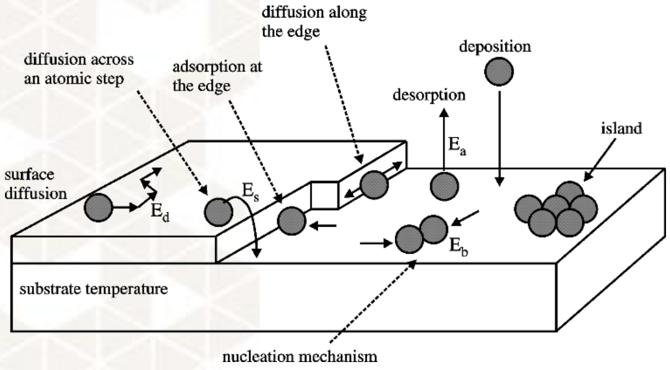

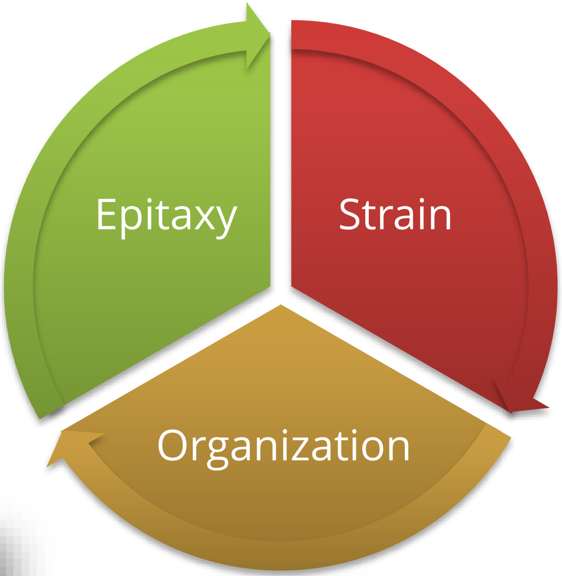

Epitaxy

Strain

Organization

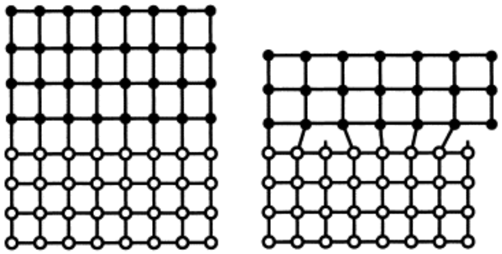

Pseudomorphic

Relaxed

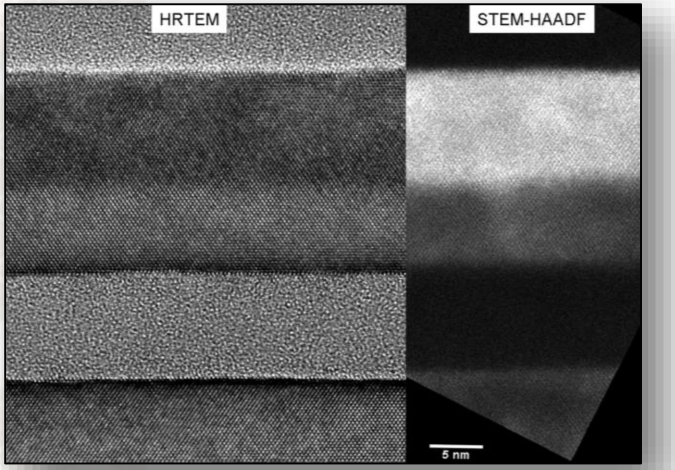

2D

1D

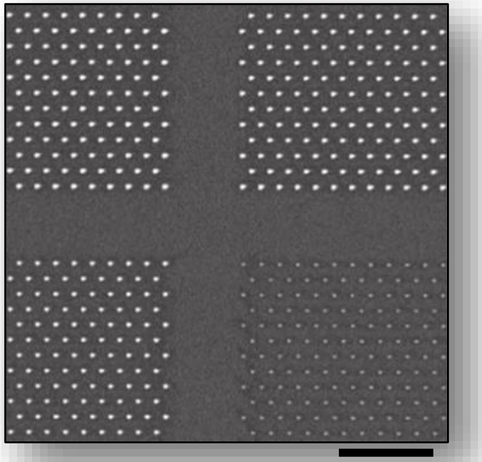

0D

Synopsis

Introduction

- Usual Si cleaning process
- Bottom-up is not, yet, efficient

Ion beam lithography

- Fast review of lithography technics
- Focused Ion Beam principles
- High resolution
- Limits: surface and volume defects

Using Focus Ion Beam for surface preparation

- Gold dewetting
- Au dots
- Silicon dewetting

Conclusion

Usual Si substrate cleaning processes

Wet cleaning : industrial solutions

Name	Diluted HF	Caro	RCA 1	RCA 2	Aqua Regia	…
Solutions	HF 1% T=20°C t=1min	H_2SO_4 (d=1,83) 3 vol. H_2O_2 30% 1 vol. T=140°C t=10min	NH_4OH 0.25 to 1 vol. H_2O_2 30% 1 vol. H_2O_5 vol. T=70°C to 80°C t=10min Rinsing DI 5 to 10 min	HCL 37% 1 vol. H_2O_2 30% 1 vol. H_2O 5 to 6 vol. T 70°C to 80°C t=10min	HCl (d= 1,19) 2 to 4 vol. HNO_3 (d= 1,40) 1 vol. T= room to boiling	
Target	Native SiO_2 Ti, TiN	Organic materials (Metallic particles)	Particles	Metallic materials		
Principe	Acid dissolution	Oxidization followed by acid dissolution		Acid dissolution		
Advantage	High dilution	Low roughness	Eliminate particles			
Limits	No action on plentiful metallic particles and organic particles	Difficult rinsing possible particle redeposition	Weak efficiency on organic and metallic materials	Difficult rinsing possible particle redeposition		

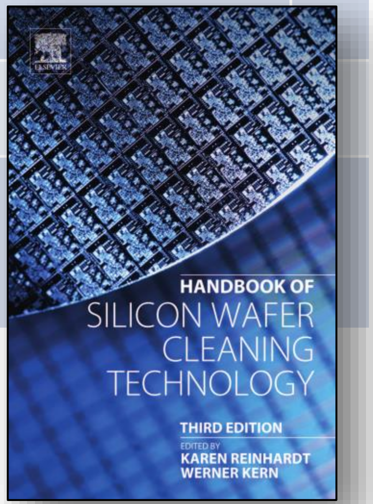
HANDBOOK OF
SILICON WAFER
CLEANING
TECHNOLOGY
THIRD EDITION
EDITED BY
KAREN REINHARDT
WERNER KERN

CARO cleaning: DHF + CARO
RCA cleaning: SC1 + SC2
Clean B: CARO + (D)HF + RCA

Usual Si substrate cleaning processes

Dry cleaning

Categories

- Physical interactions
- Physically-enhanced chemical reactions
- Chemical thermal reaction
- Mechanical process

Contaminants removal by dry cleaning

- **Organic contaminants**: volatilization, UV/O_3 reaction, remote or downstream oxygen plasma treatment
- **Native, chemical, thermal oxide, silicate glasses**: chemical etching, physical sputter etching, low-energy ECR plasma etching
- **Metal and absorbed ions**: remote plasma, photo-induced reaction
- **Particle**: vapor etching

Thermal Desorption and Oxidation

- 700°C: reduce carbon contamination
- 800°C: eliminate carbon contamination and oxide
- 900°C: oxide and a carbon contamination below detection limit

Dewetting process organization

Chemical potential

$$\mu^\beta = \underbrace{\mu^\beta_\mathrm{m}(T)}_{\text{Original } \beta \text{ phase chemical potential}} + \underbrace{\frac{1}{2}C^\beta\varepsilon^2}_{\text{Elastic strain energy density}} - \underbrace{\sigma_\mathrm{n}\Omega^\beta}_{\text{Work (pV)}} + \underbrace{\left[\left(\gamma^{\alpha\beta} + \frac{\mathrm{d}^2\gamma^{\alpha\beta}}{\mathrm{d}\theta_1^2}\right)\frac{1}{R_1} + \left(\gamma^{\alpha\beta} + \frac{\mathrm{d}^2\gamma^{\alpha\beta}}{\mathrm{d}\theta_2^2}\right)\frac{1}{R_2}\right]}_{\text{Surface energy (including anisotropy)}}\Omega^\beta$$

- Ω: atomic volume (or molecular)
- R_i: main radius of curvature
- θ_i: surface orientation

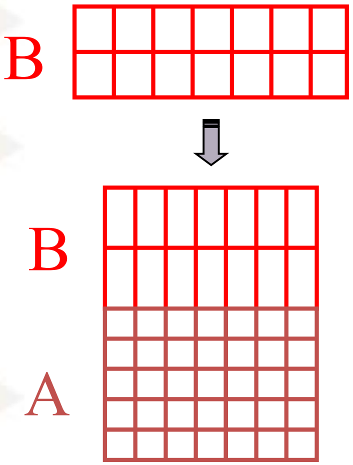

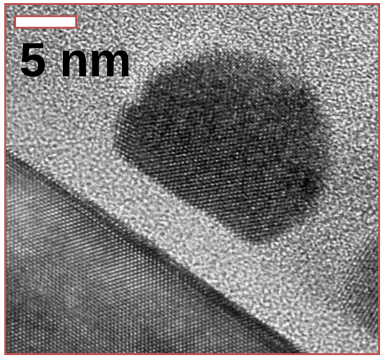

\+ Scattering Barriers

Surface defects, steps, …

Growth and self-organisation of SiGe nanostructures
J.N. Aqua, I. Berbezier, L. Favre, T. Frisch, A. Ronda, Phys. Rep. (2013)

SiGe Nano-structures organization

Self organization strategies

- Vicinal surfaces
- Vicinal reconstructed surfaces
- Surfactant effects

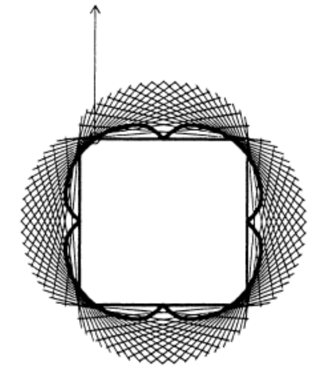

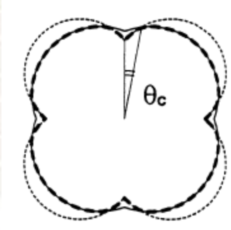

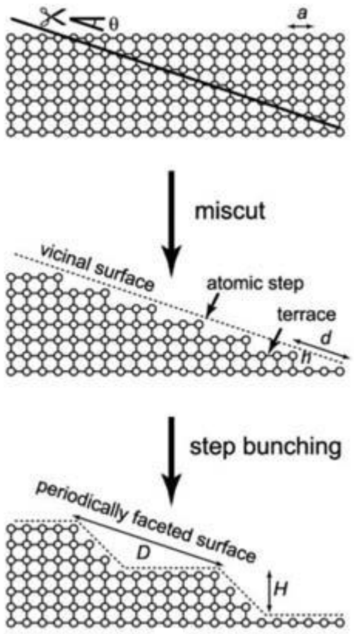

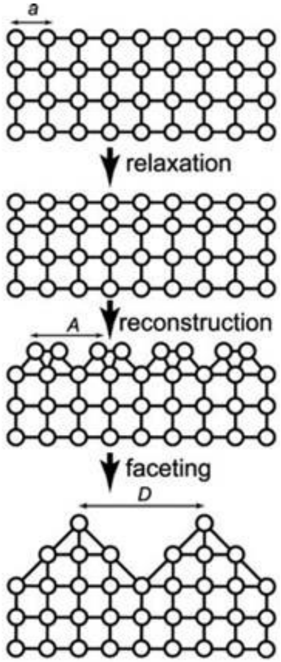

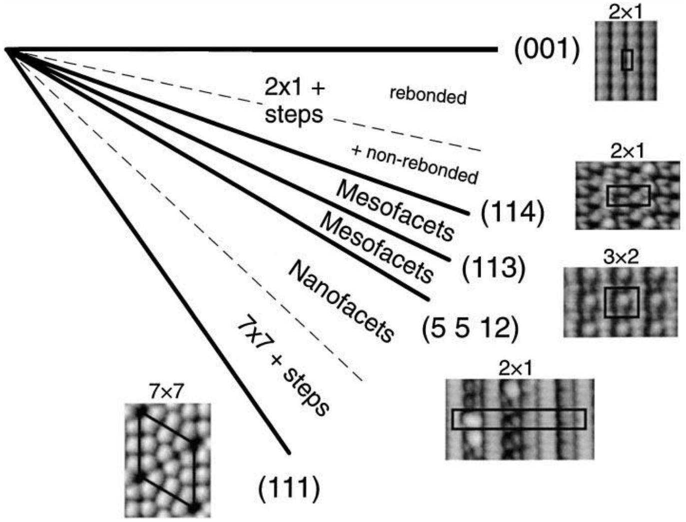

H.-C. Jeong and E.D. Williams, Surface Science Reports **34**, 171–294 (1999)

SiGe Nano-structures organization

Vicinal surfaces

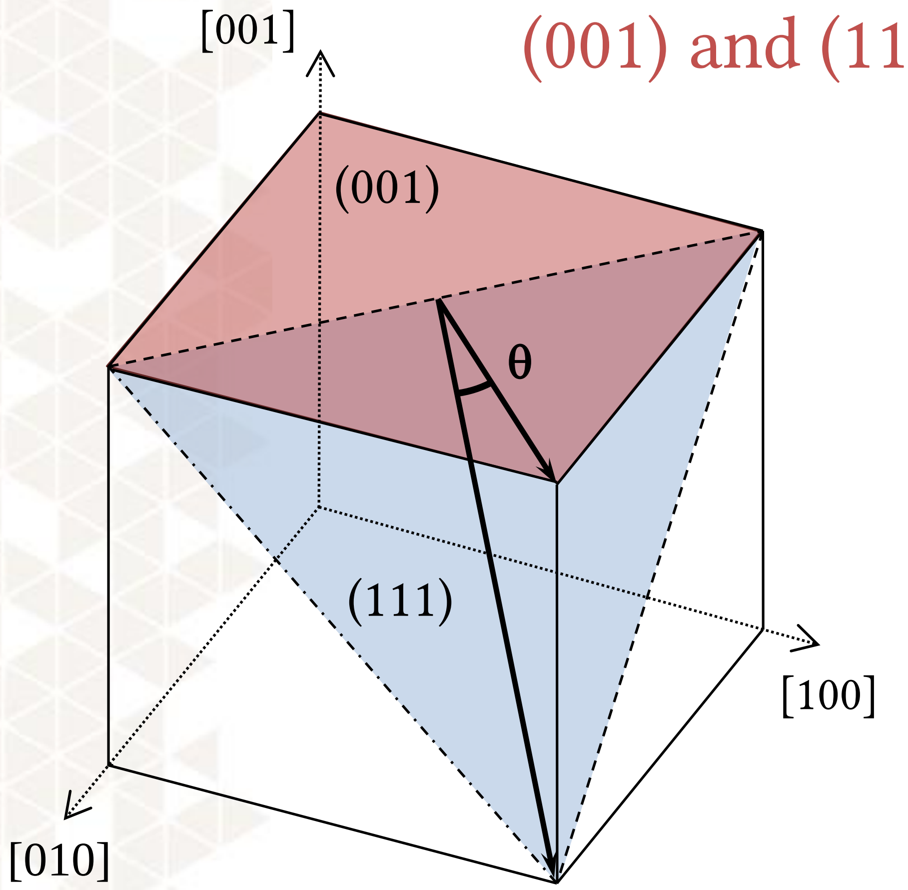

(001) and (111) misoriented surfaces

θ: from 0° to 10°

(001) plane misorientation:
- around $[1\bar{1}0]$ axis
- to (118) plane

(111) plane misorientation:
- around $[\bar{1}10]$ axis
- to $[11\bar{2}]$ and $[\bar{1}\bar{1}2]$ axis

SiGe Nano-structures organization

Homoepitaxy on vicinal surfaces: Si/Si(111)-(11$\bar{2}$) vicinal

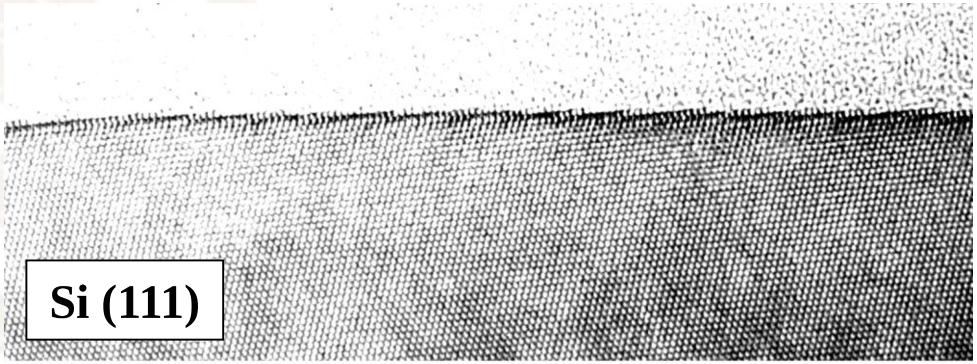

cut surface

(111) misoriented around [$\bar{1}$10]
in direction of [11$\bar{2}$]

faceting process

After
annealing
or growth

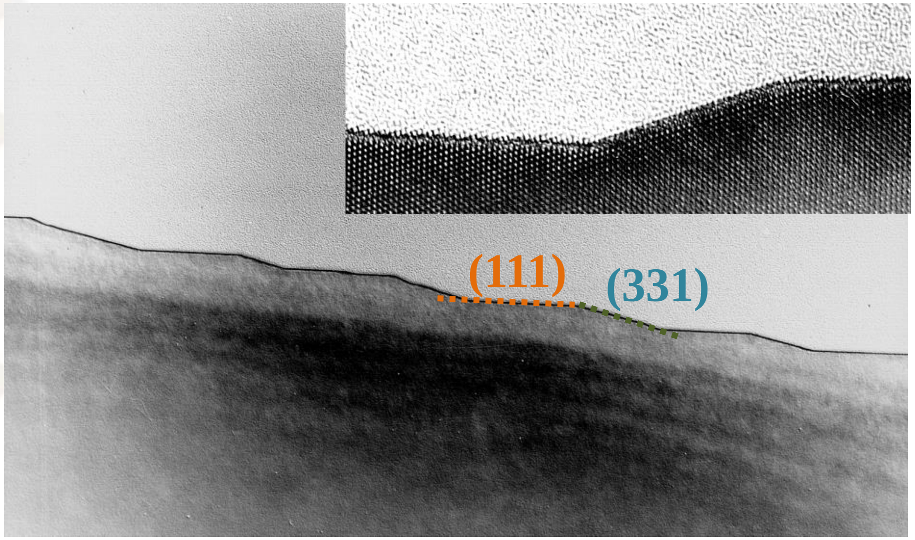

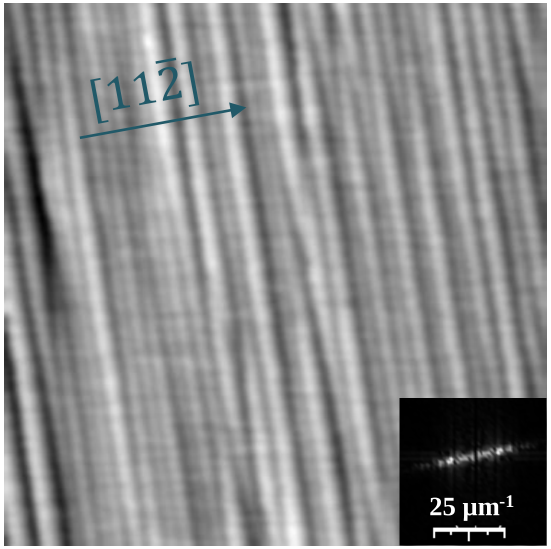

SiGe Nano-structures organization

Homoepitaxy on vicinal surfaces: Si/Si(111)-(11$\bar{2}$) vicinal

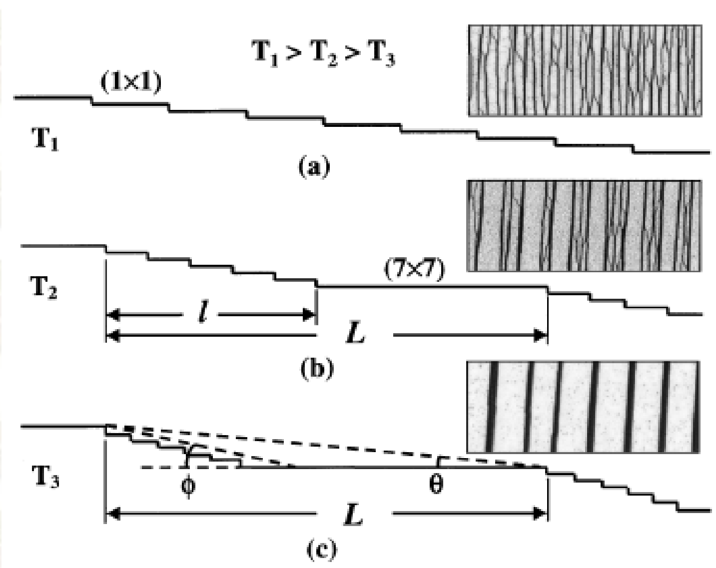

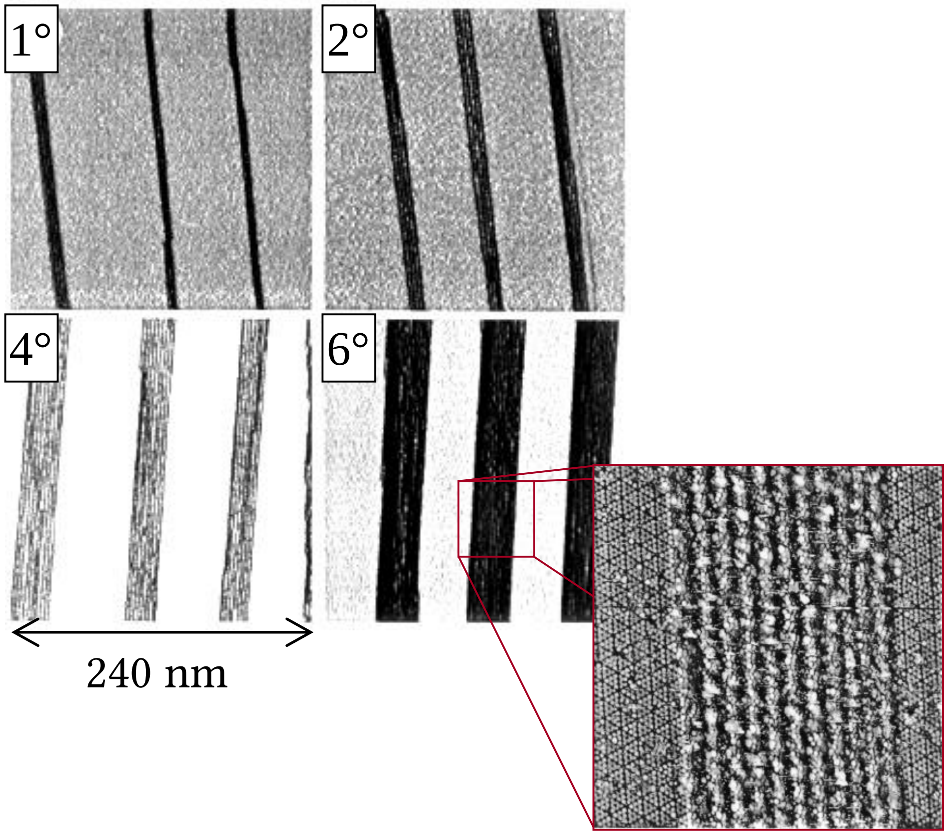

F. K. Men, *et al.*, Phys. Rev. Lett., **88** (2002)

SiGe Nano-structures organization

Homoepitaxy on vicinal surfaces: Si/Si(111)-(11$\bar{2}$) vicinal

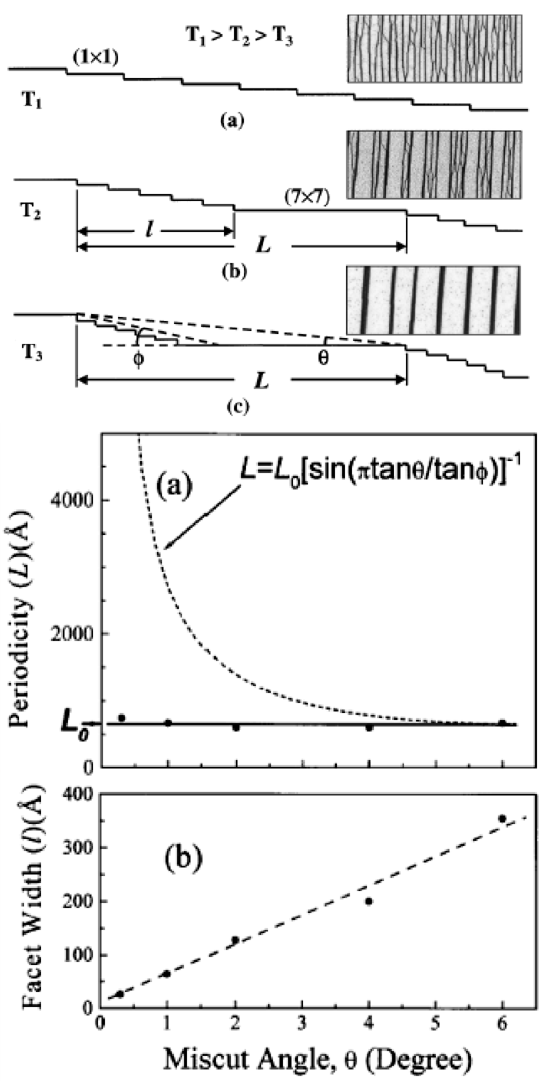

Two steps process:

- (elastic) free energy minimization

⇨ L tuning (L independent from miscut if l = L/2)

- facet free energy minimization

⇨ l tuning

$$\Delta f(T) = -\frac{\pi c}{L}\cot\left(\frac{l}{L}\pi\right)$$

$$L = \pi a_0 \left[\sin\left(\frac{l}{L}\right)\pi\right]^{-1}$$

SiGe Nano-structures organization

Homoepitaxy on vicinal surfaces: Si/Si(111)-$(11\bar{2})$ vicinal

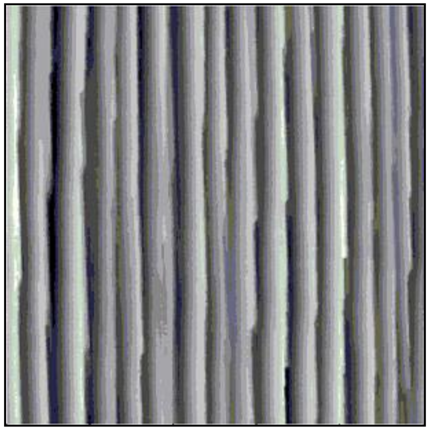

Si dots organisation

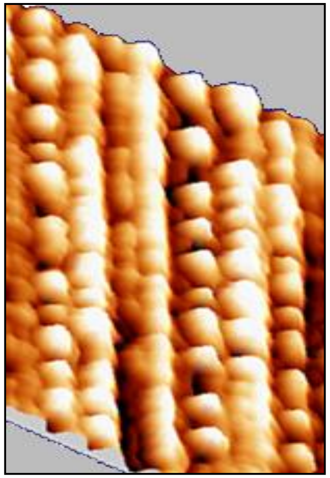

On steps bunching

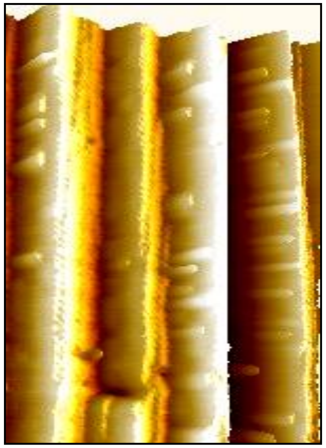

On (331) facets

SiGe Nano-structures organization

Heteroepitaxy on vicinal surfaces: SiGe/Si

TEM cross-section

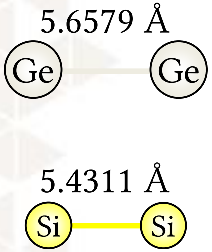

ε = 4.2 %

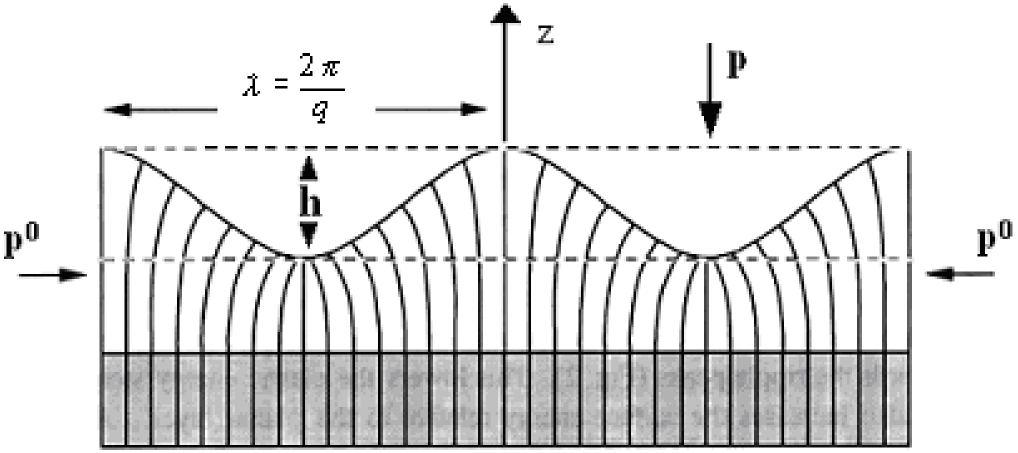

Stranski krastanov growth mode

SiGe Nano-structures organization

Heteroepitaxy on vicinal surfaces: SiGe/Si

Stransky Krastanov
first step: pseudomorphic epitaxy

x = 0.4
m = 1.6 %
h = 50 Å

Nominal (001)

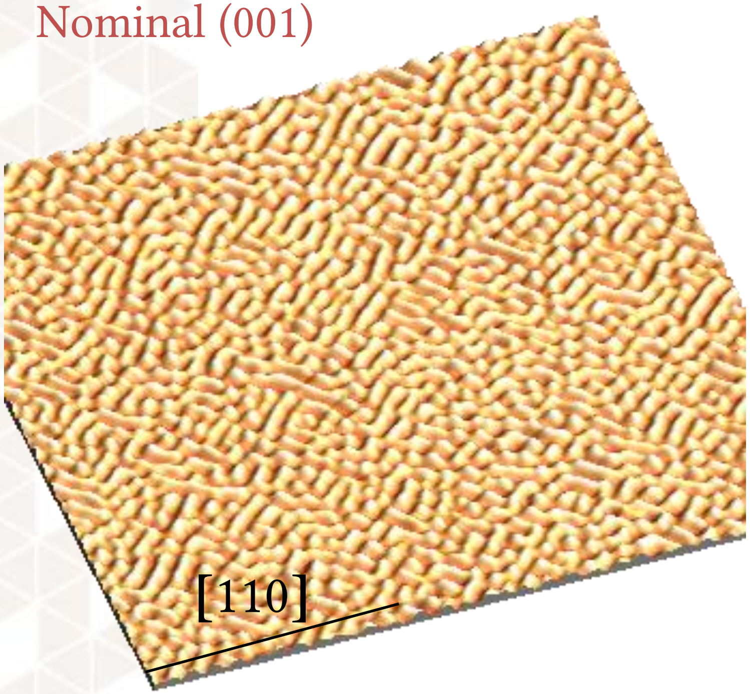

Si (001)

Vicinal (001)

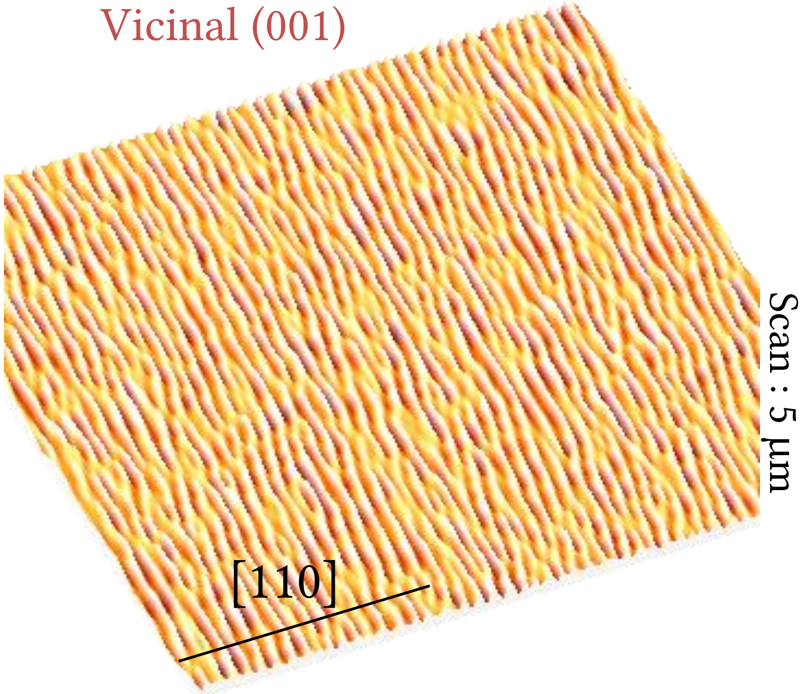

Si(118) = Si(001) 10° misoriented

P.D. Szkutnik, A. Sgarlata, A. Balzarotti, N. Motta, A. Ronda, I. Berbezier, PRB, 2006

SiGe Nano-structures organization

Heteroepitaxy on vicinal surfaces: Ge/Si

Stransky Krastanov
Second step: dots nucleation

x = 0.4
m = 1.6 %
h = 50 Å

Nominal (001)

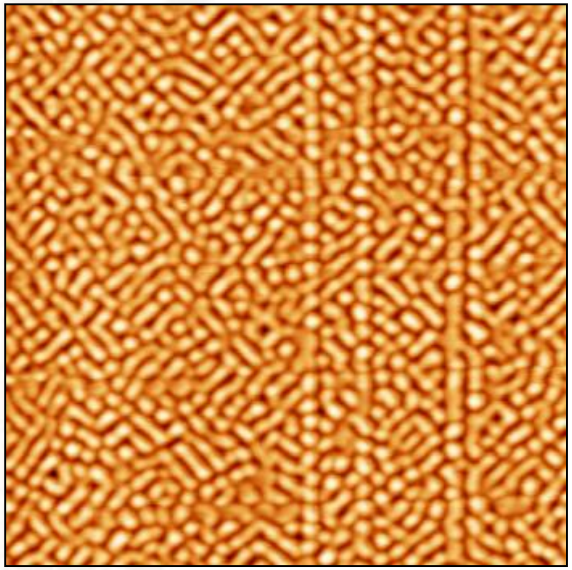

On top of undulations

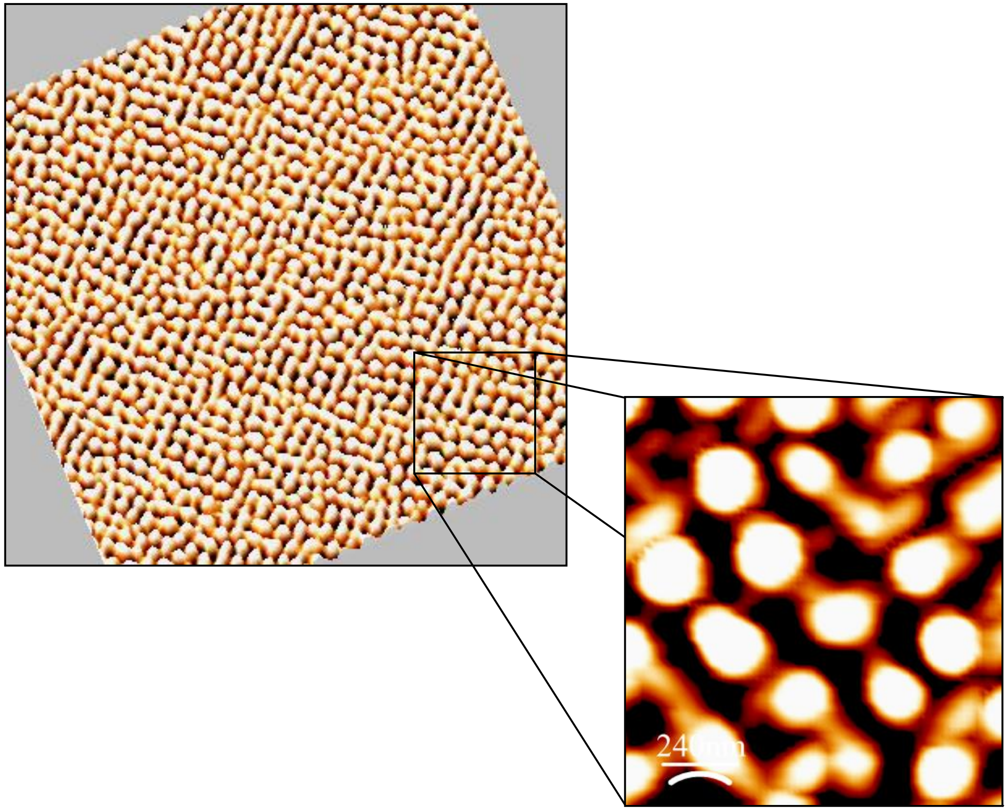

SiGe Nano-structures organization

Heteroepitaxy on vicinal surfaces: Ge/Si

$x = 0.4$
$m = 1.6\ \%$
$h = 50$ Å

Stransky Krastanov
Second step: dots nucleation

Vicinal (001)

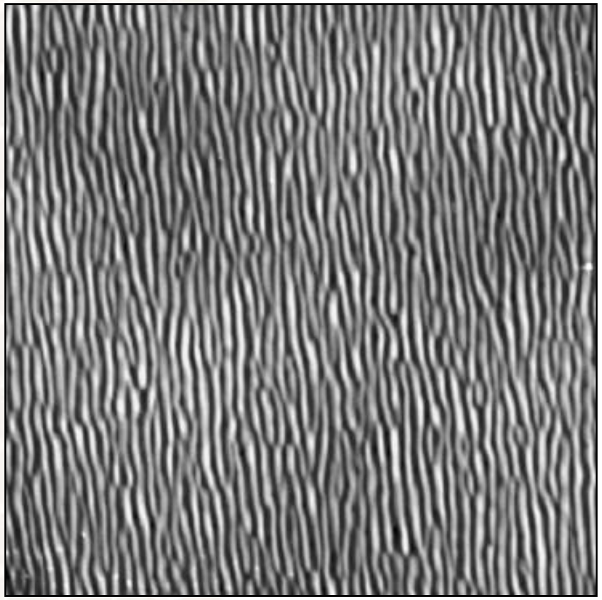

On top of undulations

$2{\cdot}10^{11}$ dots / cm^2

with surfactant:

On top and bottom of undulations

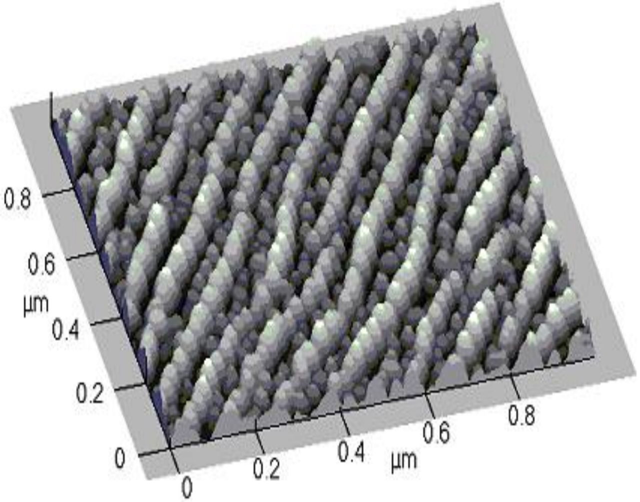

Chemical influence on surface energy

Misoriented substrates and strain instability leads to self-organization

Bad control of size distribution and fixed periodicity

Berbezier *et al.*, Appl. Phys. Lett., **83** (2004)

SiGe Nano-structures organization

Heteroepitaxy on Very High Index vicinal surfaces: Ge/Si

Self-organized Ge nanowires formed on Si(173 100 373)

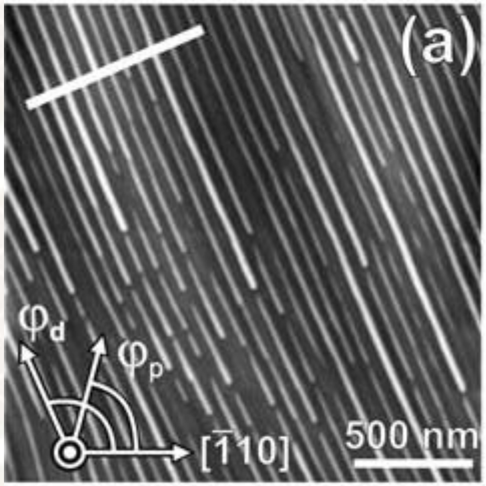

AFM image

2.0 x 2.0 μm^2

altitude angle $\theta = 28.21$

azimuthal direction $\varphi_p = 75°$

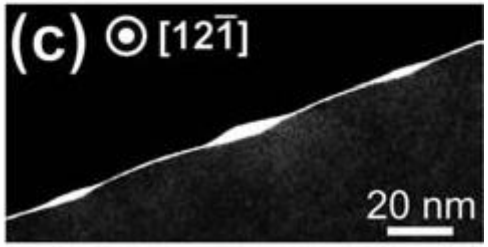

HADF STEM

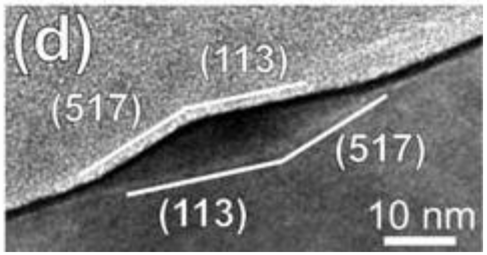

HRTEM

$[12\bar{1}]$ zone-axis

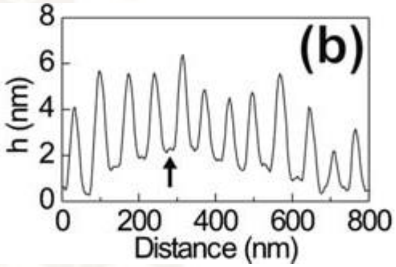

Height *h* as a function of the position along the white line in (a)

K. Ohmori, *et al.*, Nano Lett., **5**, 369–372 (2005)

Synopsis

Introduction

- Usual Si cleaning process
- Bottom-up is not, yet, efficient

Ion beam lithography

- Fast review of lithography technics
- Focused Ion Beam principles
- High resolution
- Limits: surface and volume defects

Using Focus Ion Beam for surface preparation

- Gold dewetting
- Au dots
- Silicon dewetting

Conclusion

Lithography technics

Development of new technologies: working at nanoscale

Top-Down lithography techniques

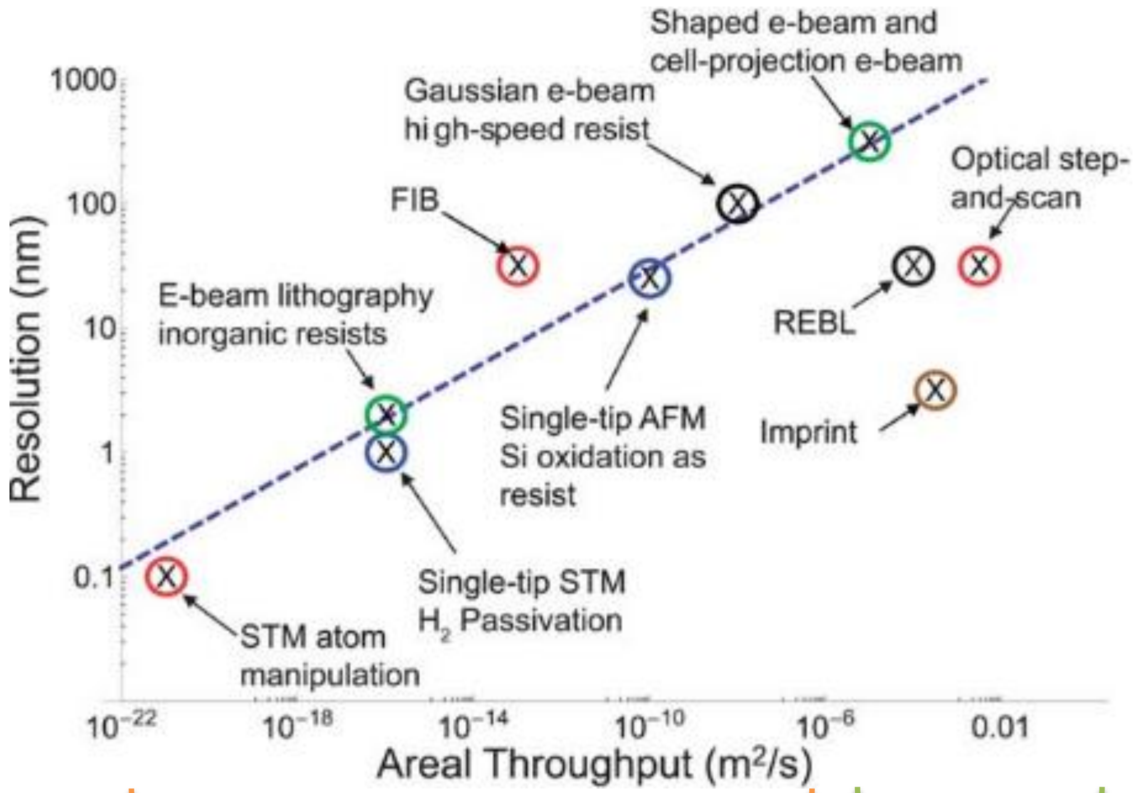

Sequential writing process

Parallel writing process

Industrial productivity: 10^{-4} m^2/s

J. A. Liddle, G. M. Gallatin, Nanoscale **3**, 2679–2688 [2011]

Wet etching

Development of new technologies

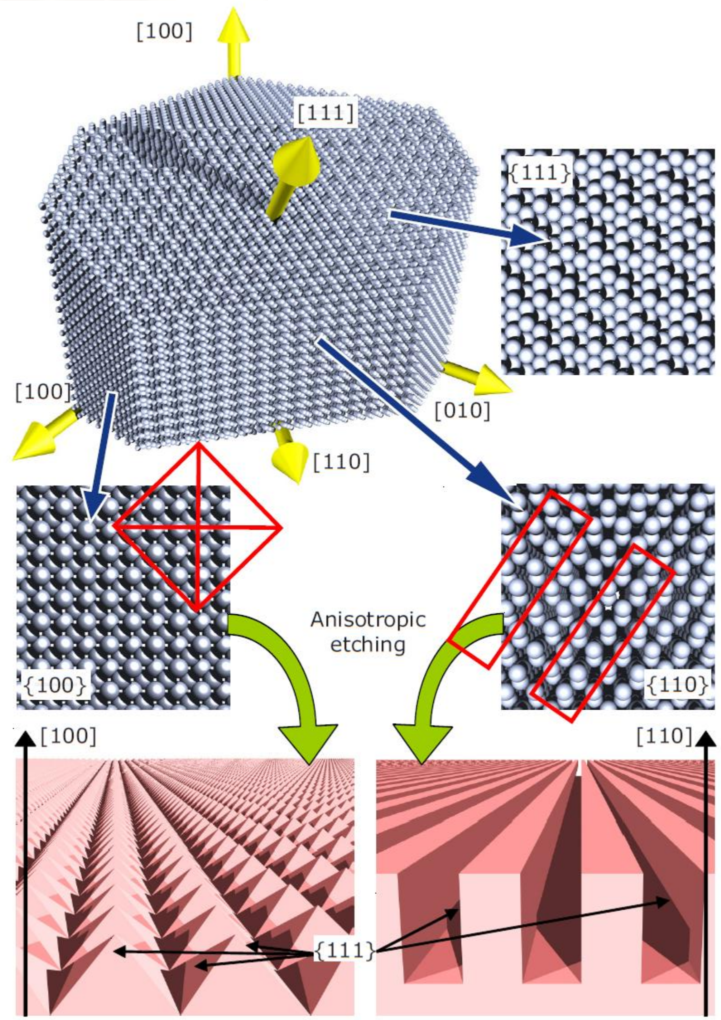

Etchant	Etch rate ratio		Etch rate (absolute)			Advantages (+) Disadvantages (-)
	(100)/(111)	(110)/(111)	(100)	Si_3N_4	SiO_2	
KOH (44%, 85°C)	**300**	**600**	1.4 mm/min	<1 Å/min	14 Å/min	(-) Metal ion containing (+) Strongly anisotropic
TMAH (25%, 80°C)	**37**	**68**	0.3-1 mm/min	<1 Å/min	2 Å/min	(-) Weak anisotropy (+) Metal ion free
EDP (115°C)	**20**	**10**	1.25 mm/min	1 Å/min	2 Å/min	(-) Weak anisotropy , toxic (+) Metal ion free, metallic hard masks possible

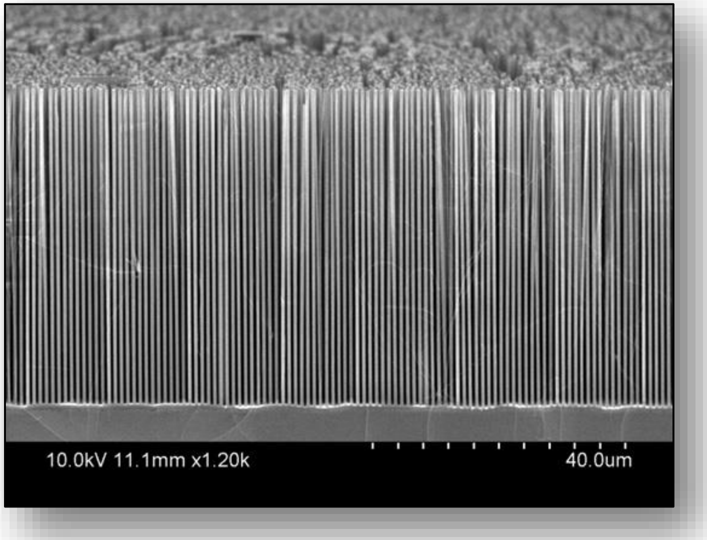

Si nanowires with diameter of 550 nm, height of 51 μm, thus an aspect ratio of ≈93, produced through Au-MacEtch with Au mesh film patterned using soft lithography on p+ Si

e-beam lithography

CVD deposition on e-beam patterns

Ge nanodots growth on patterned oxide layer

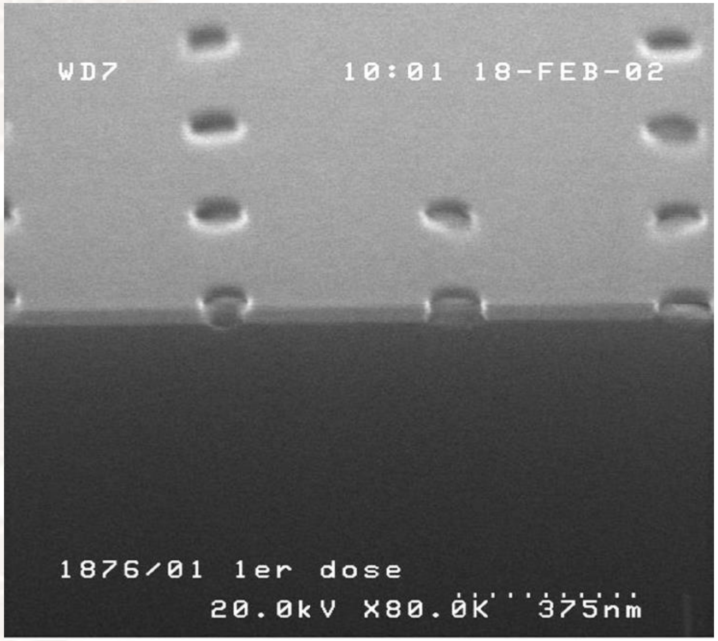

e- beam patterning

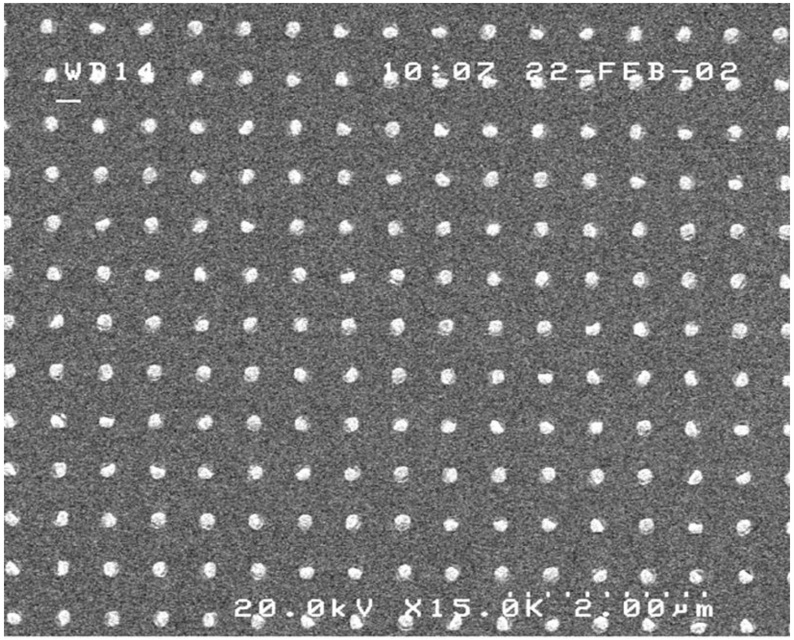

Selective CVD Ge growth

Size > 80 nm

Density ≈ $10^{10}/\text{cm}^2$

O. Kermarrec, Y. Campidelli, D. Bensahel, STMicroelectronics

Ion-beam lithography

Silicon substrate FIB patterning

Pitch	24 nm
Pattern diameter	15 nm

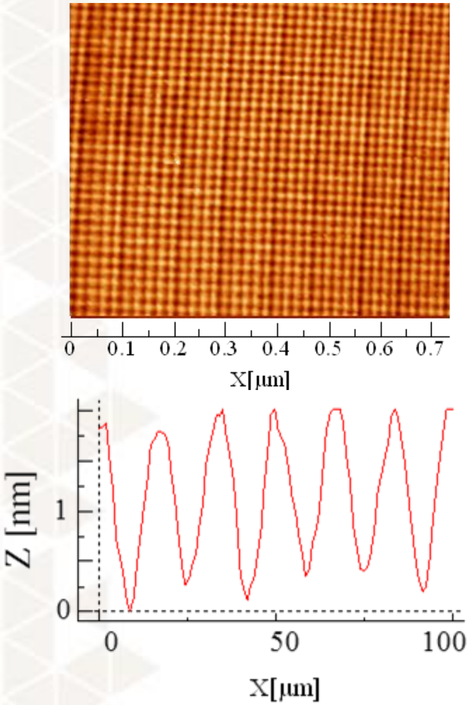

High resolution

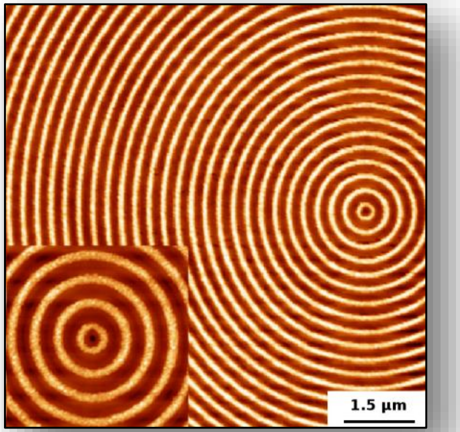

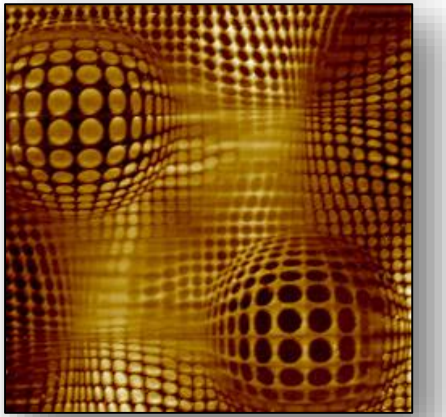

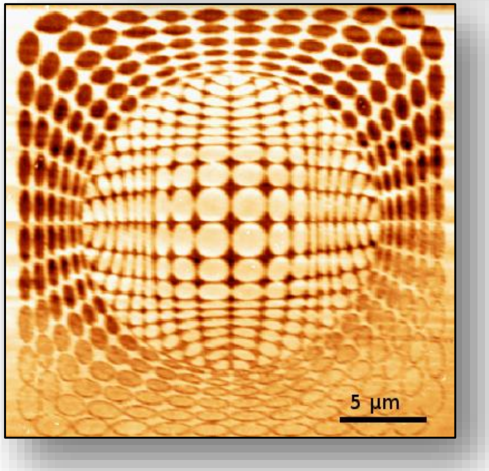

Pattern flexibility

Ion-beam lithography

FIB use

Failure analysis

Cross-section tool

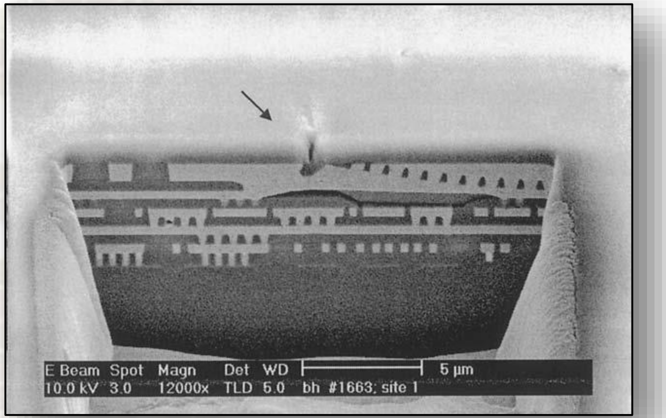

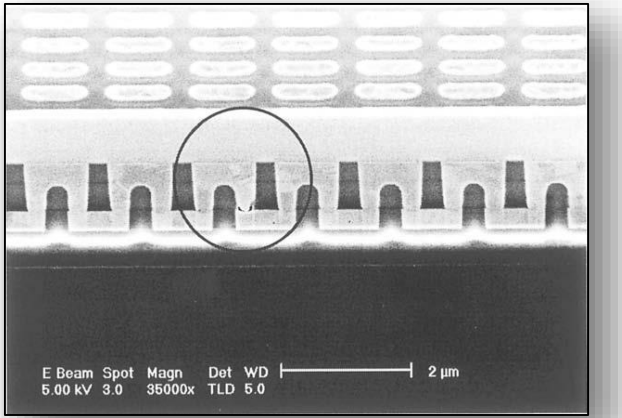

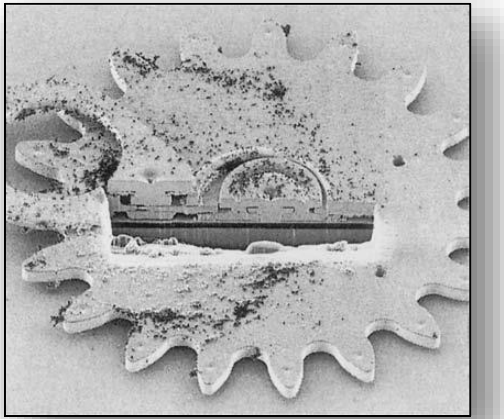

Microelectronic

Mechanic

Ion-beam lithography

FIB use

Failure analysis

Z contrast

Channeling effect

Secondary Electron (SE)

Si device (static random access memory)

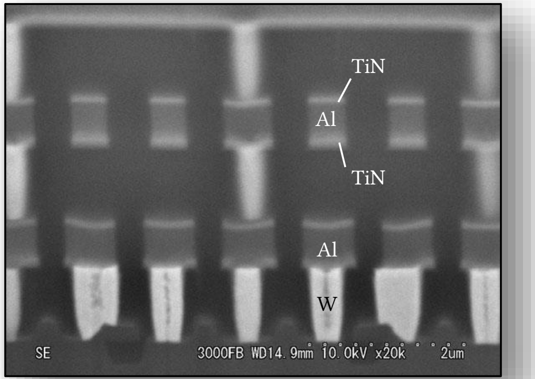

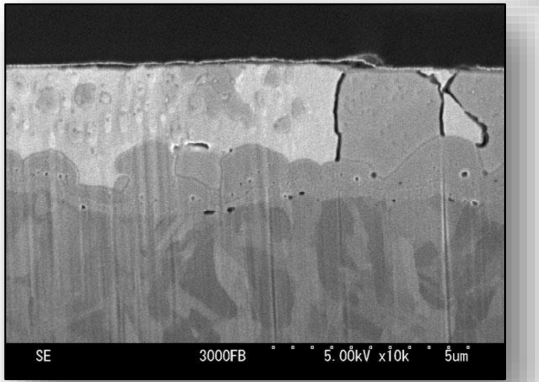

Solder (Pb-Sn)

Cu

Ion-induced Secondary Electron (ISE)

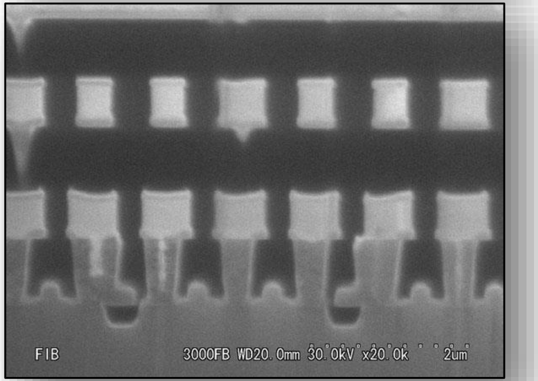

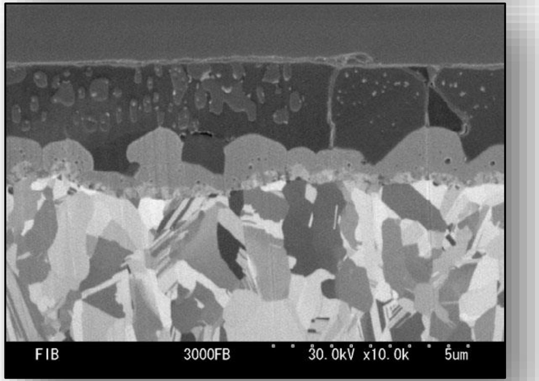

Ion-beam lithography

FIB use

TEM lamella preparation

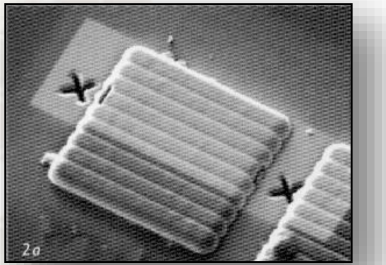

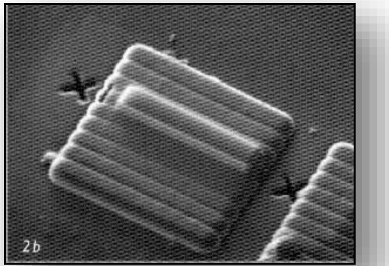

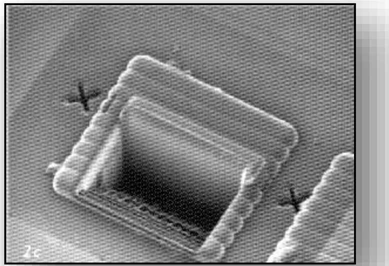

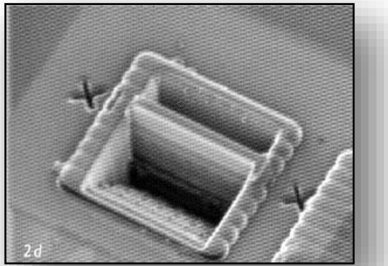

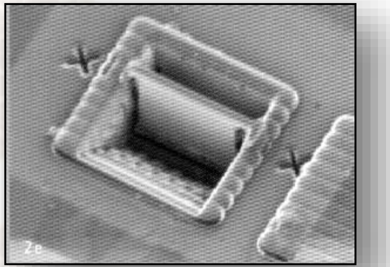

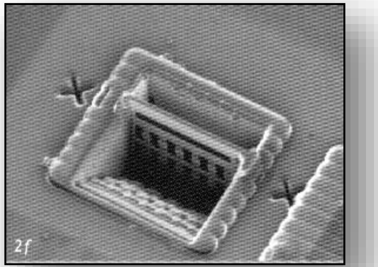

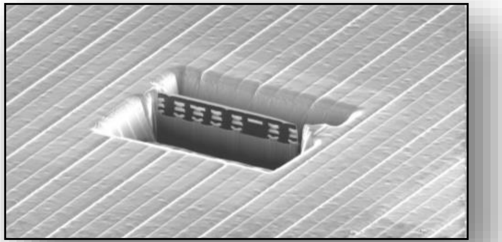

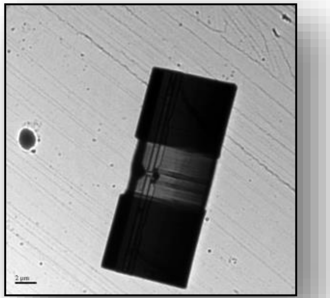

Ion-beam lithography

FIB use

Gas Injection System

Selective/enhanced etching

Deposition (W, Pt, SiO_2, ...)

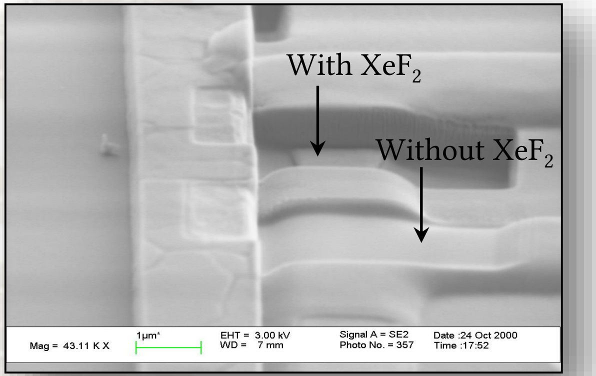

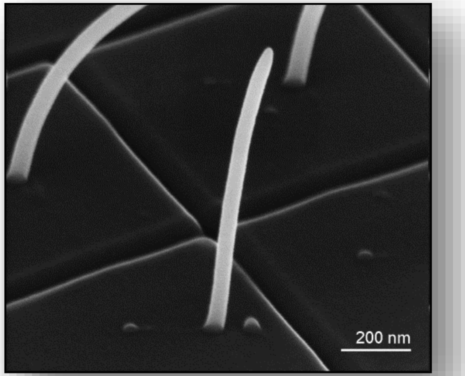

GIS deposition of 50 nm thin,
1 µm tall, Pt nanowires

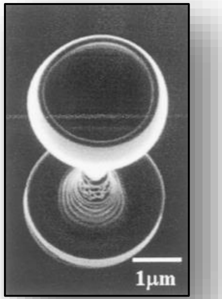

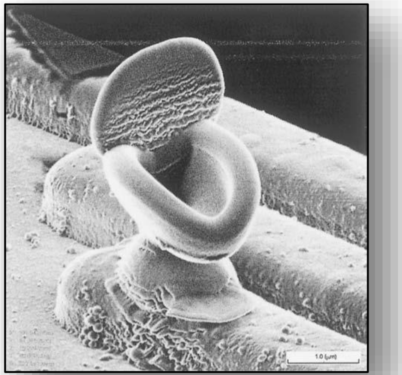

Courtesy of Orsay Physics

Ion-beam lithography

Ion column with mass filter

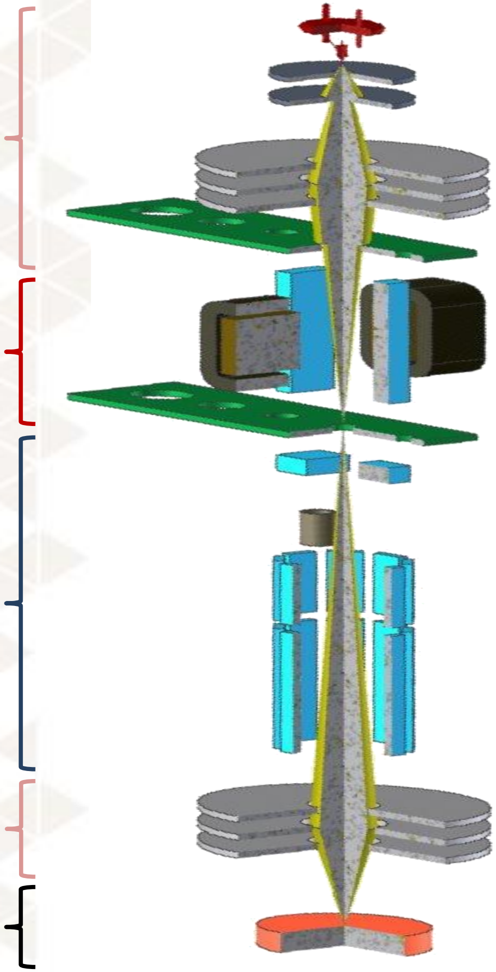

Ion gun
- LMIS source
- Extraction electrodes
- Condenser lens (electrostatic)
- Ion current selection aperture

Mass filter
- Wien mass filter
- Ion mass selection aperture

Scanning system
- Blanking deflectors
- Faraday cup (current measurement)
- Octupole (scanning and stigmation)

Objective
- Objective lens (electrostatic)

Chamber
- Sample stage

Orsay Physics LMIS:

Ga

Au-Si

Working voltage: 30 kV

Intensity (Source)	10^6 A/cm^2
Source size	50 nm
Energetic dispersion	5-10 eV
Species	Ga, Au, Si, Ge, …

Sputtering rate: Ga^+ 30 kV: 2.2 atoms/ion (0.26 mm^3/nA.s)

Courtesy of Orsay Physics

Ion-beam lithography

Mass filter

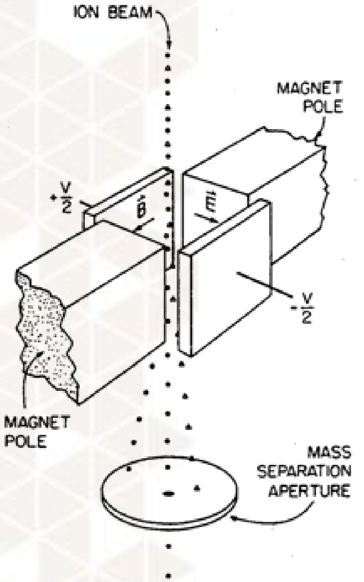

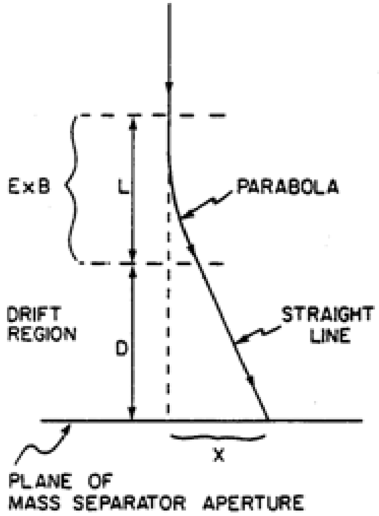

Straight trajectory condition: $m = m_0$

Forces equilibrium condition: $E = v \times B$

$$v = \frac{E}{B} = \frac{V}{dB} \Leftrightarrow \sqrt{\frac{2qV_0}{m_0}} = \frac{V}{dB}$$

Deflection: $m = m_0 + \Delta m$

$$x = \frac{1}{4}\frac{V}{V_0}\frac{L}{d}\left(\frac{L}{2} + D\right)\frac{\Delta m}{m}$$

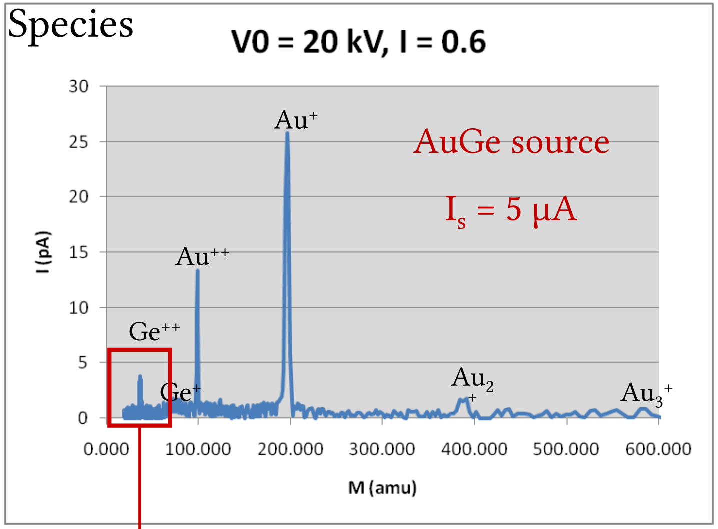

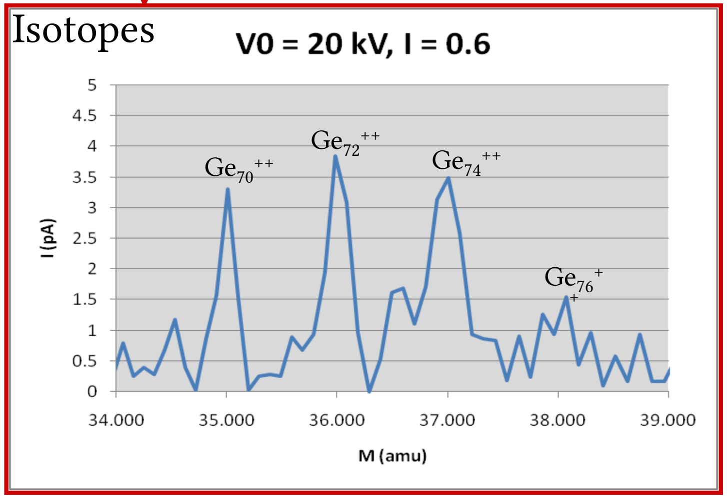

Mass resolution: Au: $r_m < 4\%$ Ga: $r_m < 2\%$

Ion-beam lithography

Performances: lateral resolution

Resolution with mass filtered COBRA-FIB for AuSi source:

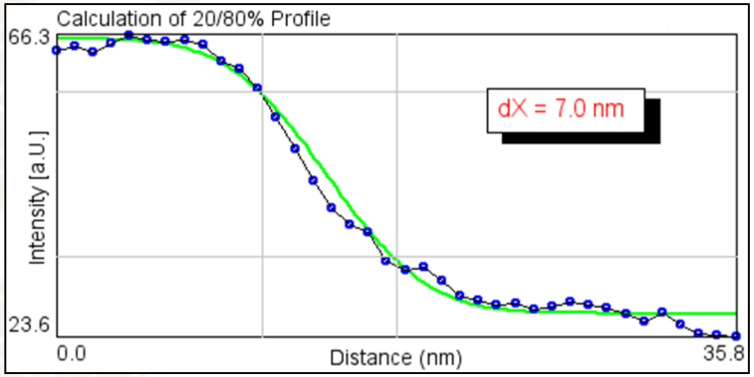

for I ≈ 10 pA (20-80%)

⇒ Si beam < 10 nm

⇒ Au beam < 10 nm

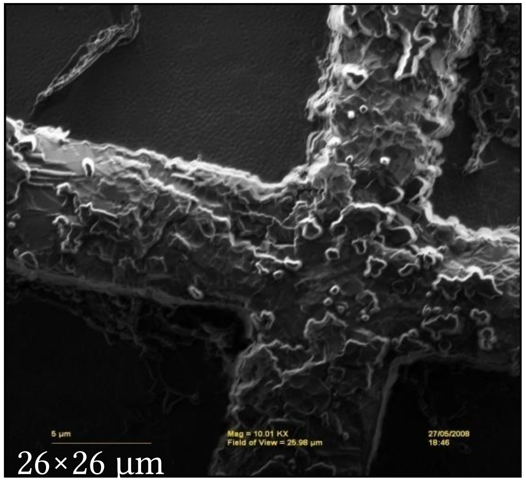

Resolution with new COBRA-FIB for Ga source:

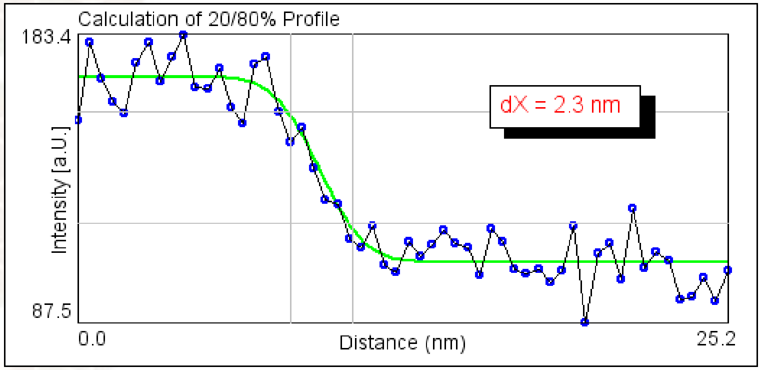

1.7 nm resolution has been performed at 20-80 with Cobra-FIB

for I ≈ 1 pA (20-80%)

⇒ Ga beam < 2.5 nm

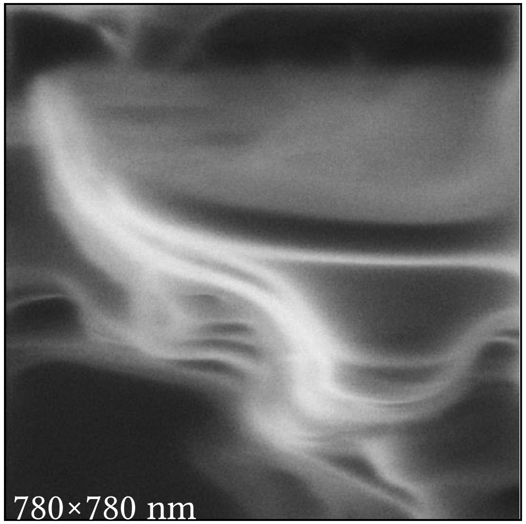

Ion-beam lithography

Lithographic process

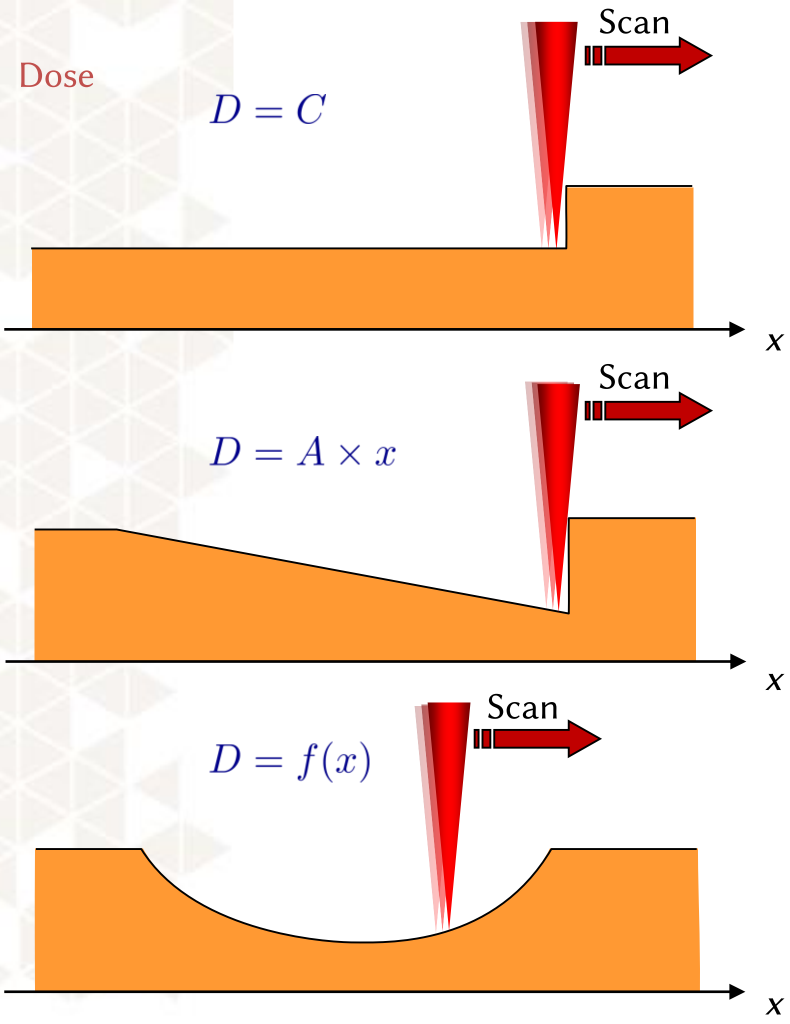

$D = C$

$D = A \times x$

$D = f(x)$

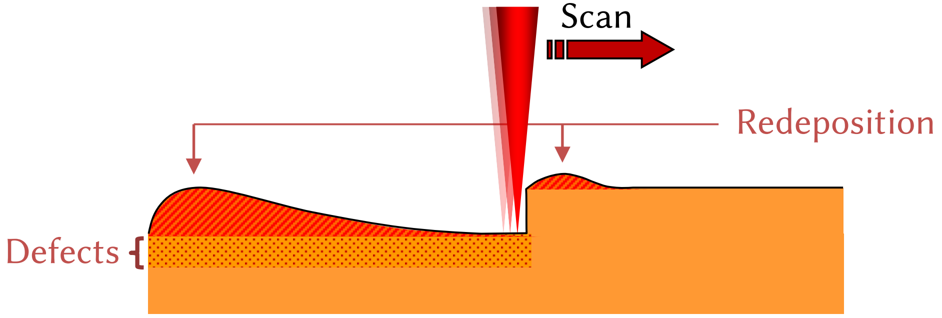

Si Substrate
30keV Ga$^+$·$D = 1.9 \times 10^{18}$ ions/cm^2

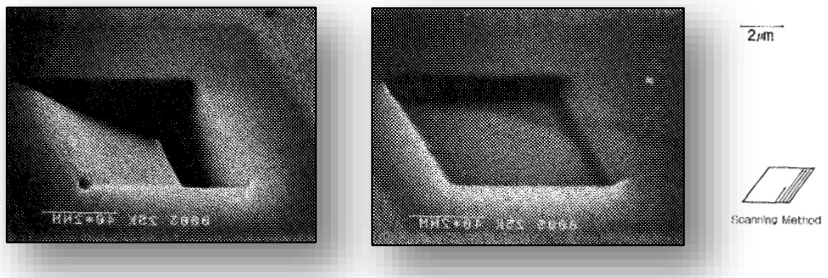

300 scan lines
***single* pass**
(2 s/line)

300 scan lines
200 *repetitive* passes
(10 ms/line)

Yamaguchi *et al.*, J. Vac. Sci. Technol. B, **3**, 71 (1985)

Ion-beam lithography

Ion/Matter interaction

Ion-induced secondary electron image

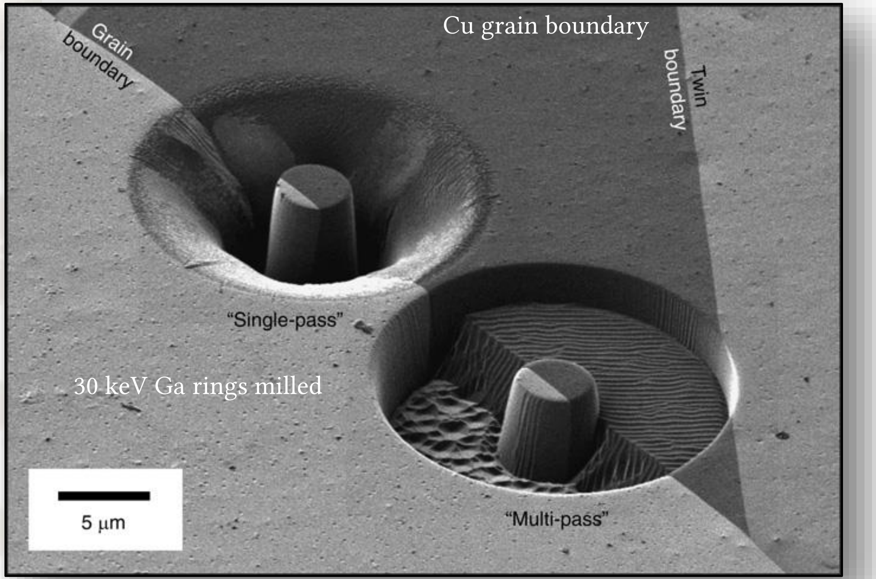

Single-pass ring:
- enhanced sputtering yield (deeper trough)
- redeposition (sloped, thicker sidewalls)

Multi-pass ring:
- channeling effects
- surface roughening

C.A.Volkert and A.M.Minor, MRS Bull., **32**, 389 (2007)

Advantages
- Local nanopatterning
- High resolution
- Maskless and resistless process
- (Specific nonpolluting ion sources)

Drawbacks
- Swelling
- Amorphisation
- Redeposition
- Defects (vacancies, interstitials)
- (Implantation)

Ion-beam lithography

FIB patterning: dose

Ions	Ga$^+$
Acceleration voltage	30 kV
Beam current	2.4 µA
Probe current	1-500 pA

Dose: 0.05×10^{15} ions/cm²

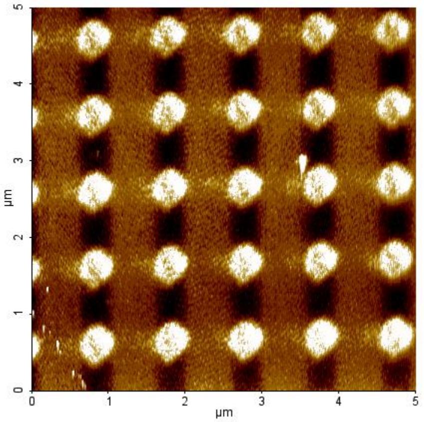

- Implantation
- Amorphization

Swelling

Dose: 4.09×10^{15} ions/cm²

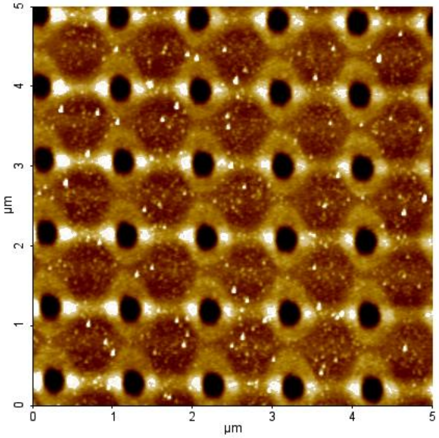

- Implantation
- Amorphization
- Sputtering

Excavation

Si wafer (001)

Chemical cleaning:

1. HNO_3 (65%) / 70°C / 5 min
2. H_2O (DI) / RT / 1 min
3. HF (49%) : H_2O (1:10) / RT / 30 s

COBRA-FIB from Orsay Physics system integrating SEM Tescan Lyra

Ion-beam lithography

FIB patterning: excavation rate

h: AFM measurement
r: SEM measurement

Ions	**Ga⁺**
Acceleration voltage	30 kV
Beam current	2.4 µA
Probe current	1-500 pA

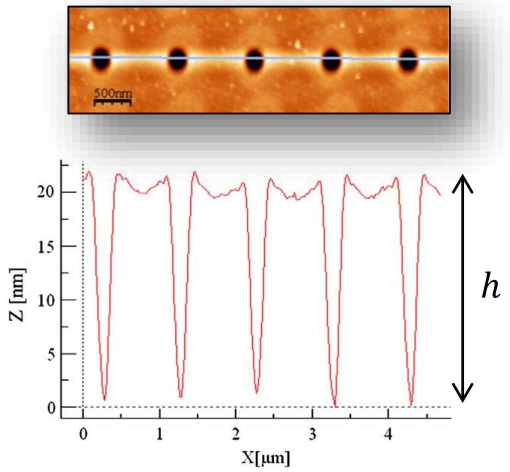

Holes:
conical shape

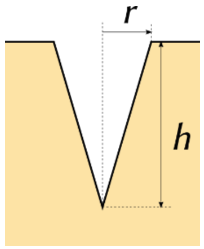

Excavated volume: $v = \frac{1}{3}\pi r^2 h$

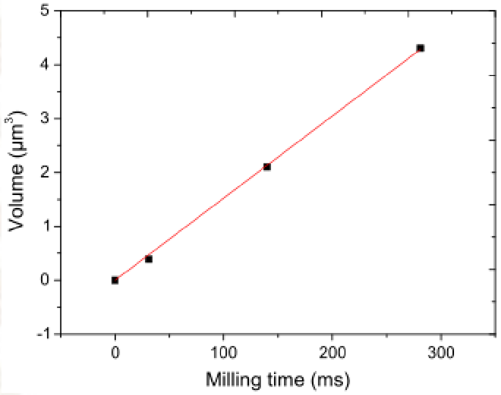

Excavated volume proportional to the time

$$\boxed{V_{\mathrm{Ga}} = K \cdot t}$$

with $K = 15.02\,\mu\mathrm{m}^3/\mathrm{ms}$

COBRA-FIB from Orsay Physics system integrated SEM Tescan Lyra

Ion-beam lithography

FIB patterning: excavation rate

Ga^{+}

Low current

High current

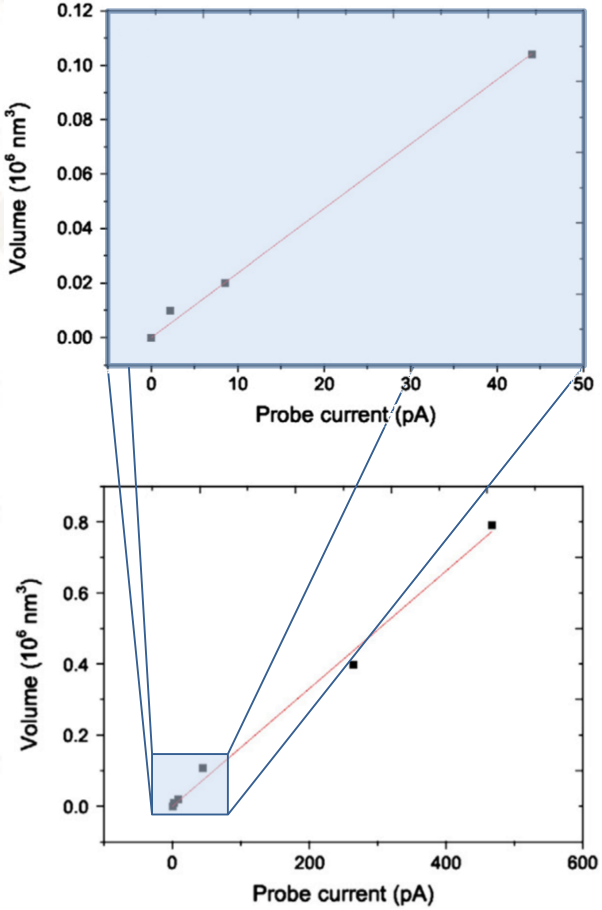

Au^{2+}

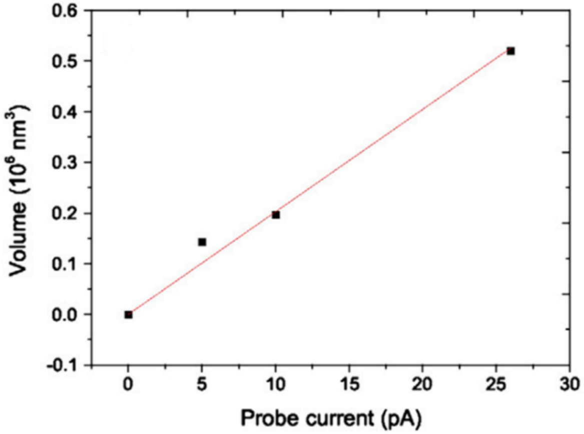

Excavated volume proportional to probe current

$$\boxed{v_{\mathrm{x}} = K_{\mathrm{x}} \cdot i_{\mathrm{p}}}$$

$$K_{\mathrm{Ga}^{+}} = 2.37 \cdot 10^{3}\,\mathrm{nm}^{3}/\mathrm{pA}$$

$$K_{\mathrm{Au}^{2+}} = 19.7 \cdot 10^{3}\,\mathrm{nm}^{3}/\mathrm{pA}$$

Au cross-section > Ga cross-section

Ion-beam lithography

FIB patterning: focus

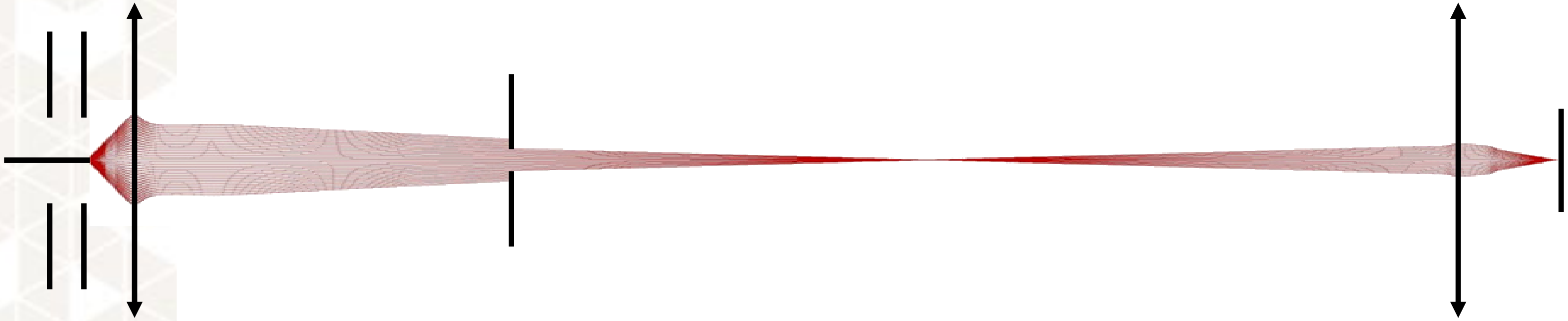

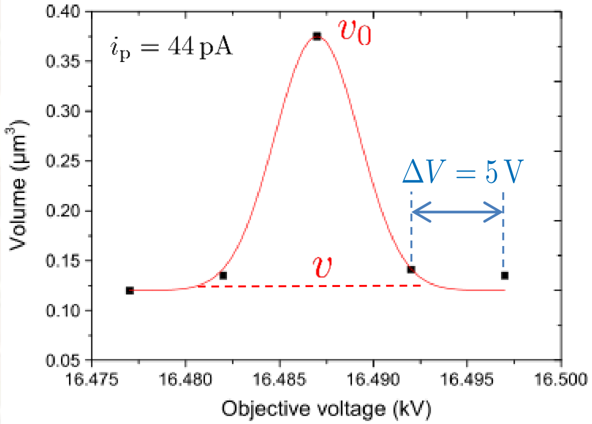

$$\frac{v_0}{v} = 3$$

Collective ions interaction during milling process

By defocusing, local dose decrease:
amorphization and swelling before excavation

Ion-beam lithography

Ion lithography optimized parameter

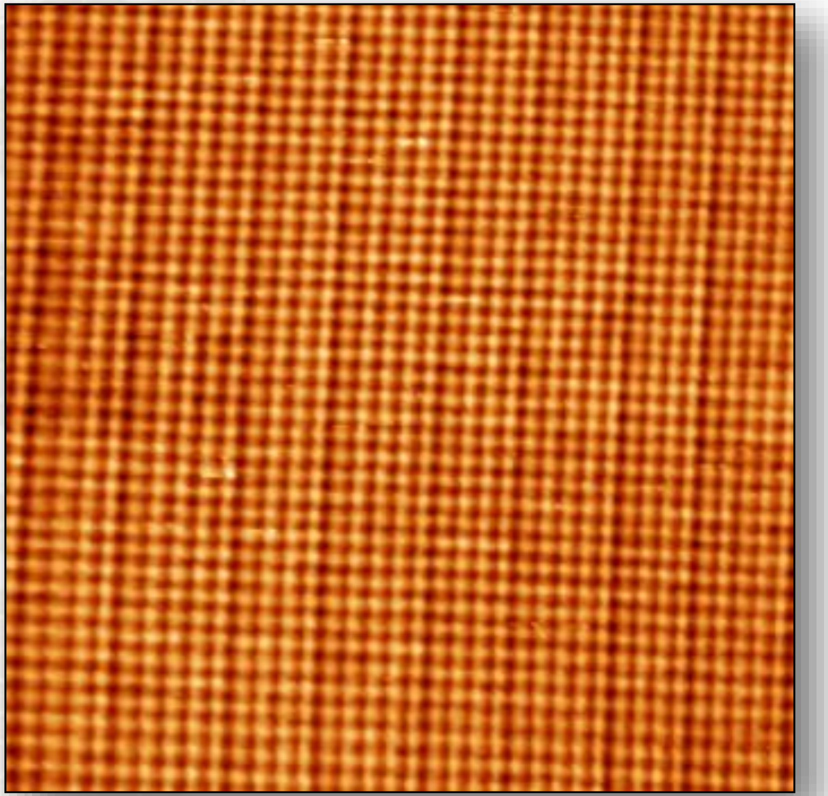

Using optimized experimental parameters:

- λ = 24 nm
- Ø = 15 nm
- D ≈ $2 \cdot 10^{11}$ cm^{-2}

Ga^{+} or Au^{2+}:
Ultimate hole diameter: 15 nm

Ion-beam lithography

Ultimate FIB patterning: sacrificial ultra-thin oxide film

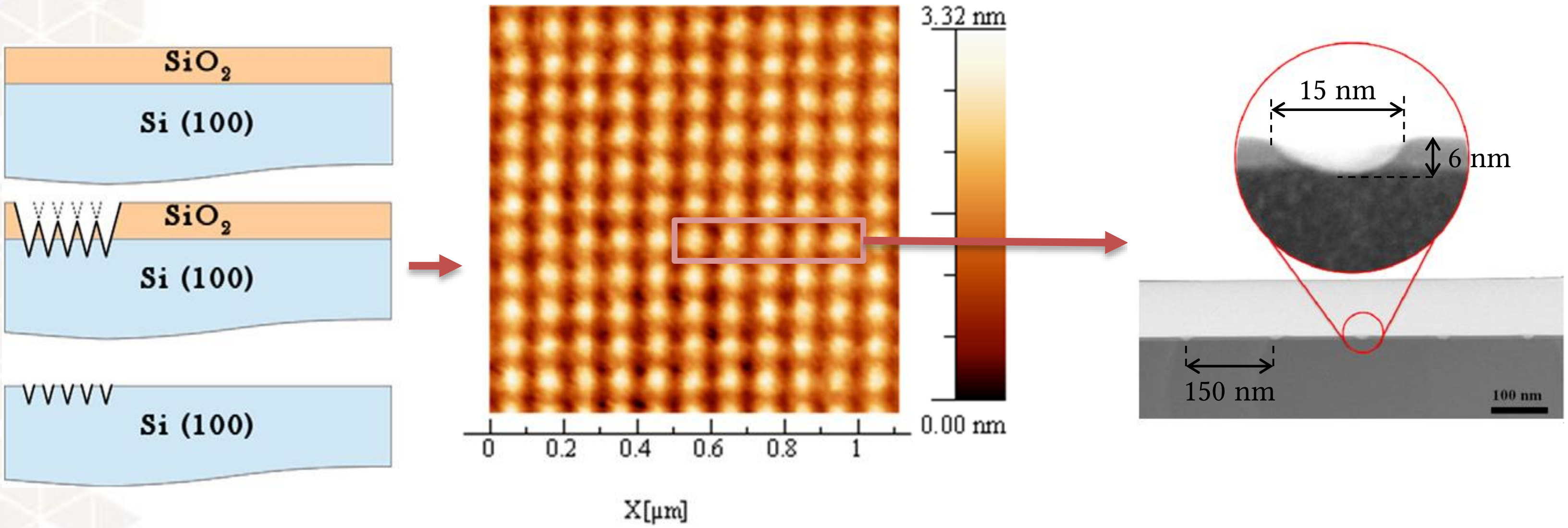

Ions	Ga$^+$
Acceleration voltage	30 kV
Beam current	2.4 µA
Probe current	1-6 pA

Reproducible depth penetration of 1 nm

Ion-beam lithography

FIB patterning: creating structures smaller than 5 nm

FIB processing method for ultra-thin membrane processing

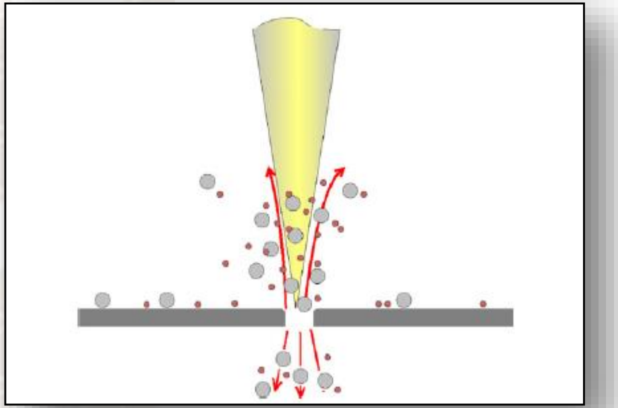

TRIM simulations

35 keV Ga$^+$

SiC membranes

Membrane thicknesses

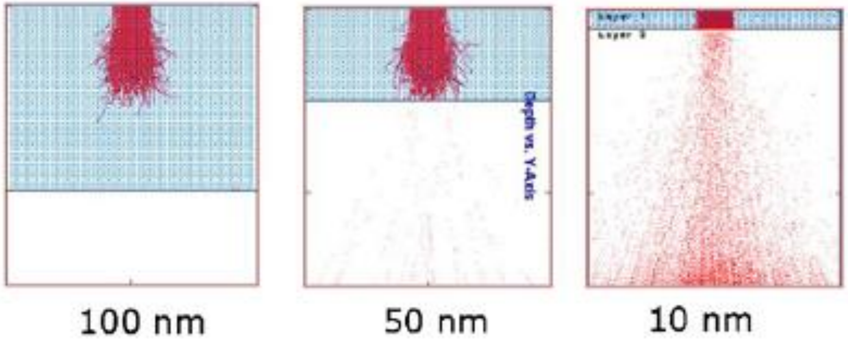

20 nm thick membrane

dose 10^6 ions

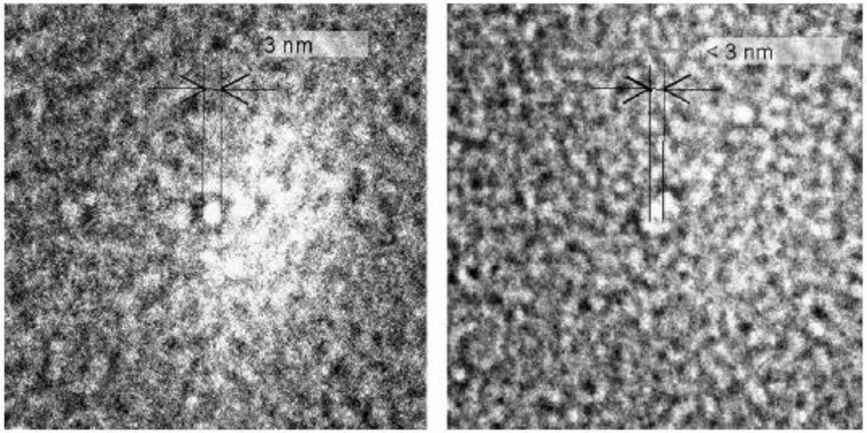

50 x 50 nm TEM images

Ion-beam lithography

Ion/Matter interactions

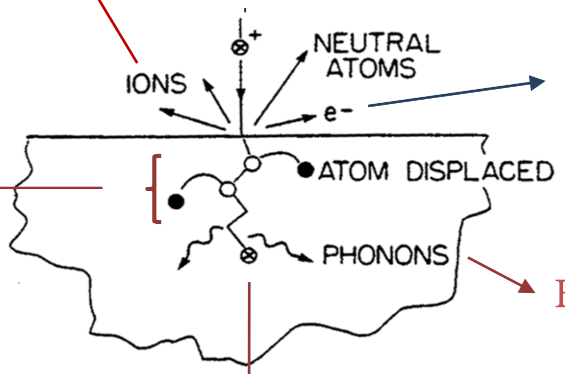

- Lithography
- Analysis (SIMS)

Defects:

- Amorphisation
- Interstitials
- Vacancies

Imagery

Heat

Implantation/contamination

Ion cross section > e^- cross section → Low ion diffusion

Probe size: Ion lithography < e^- lithography

Ion-beam lithography

Limiting FIB milling : MEB coupling

Dual-Beam

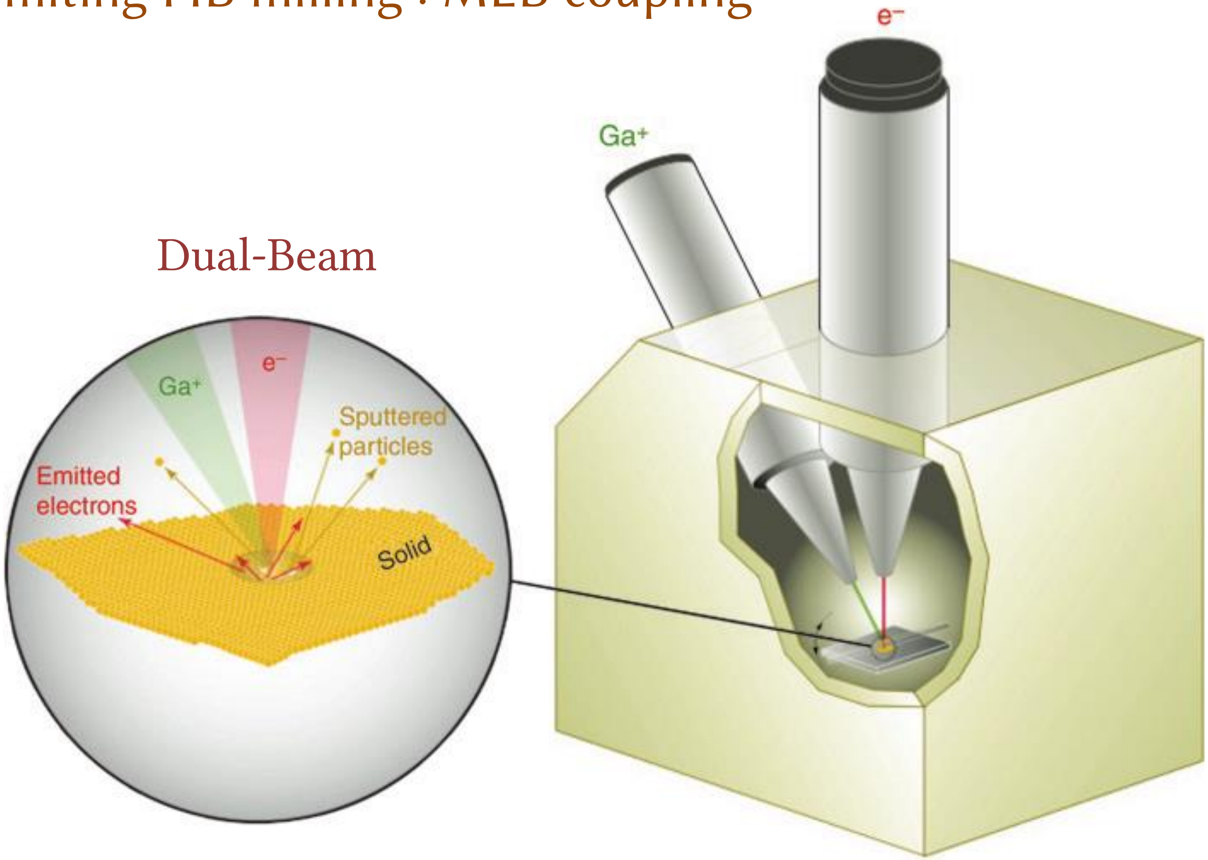

C.A.Volkert and A.M.Minor, MRS Bull., **32**, 389 (2007)

Imaging without milling: dual beam

Ion-beam lithography

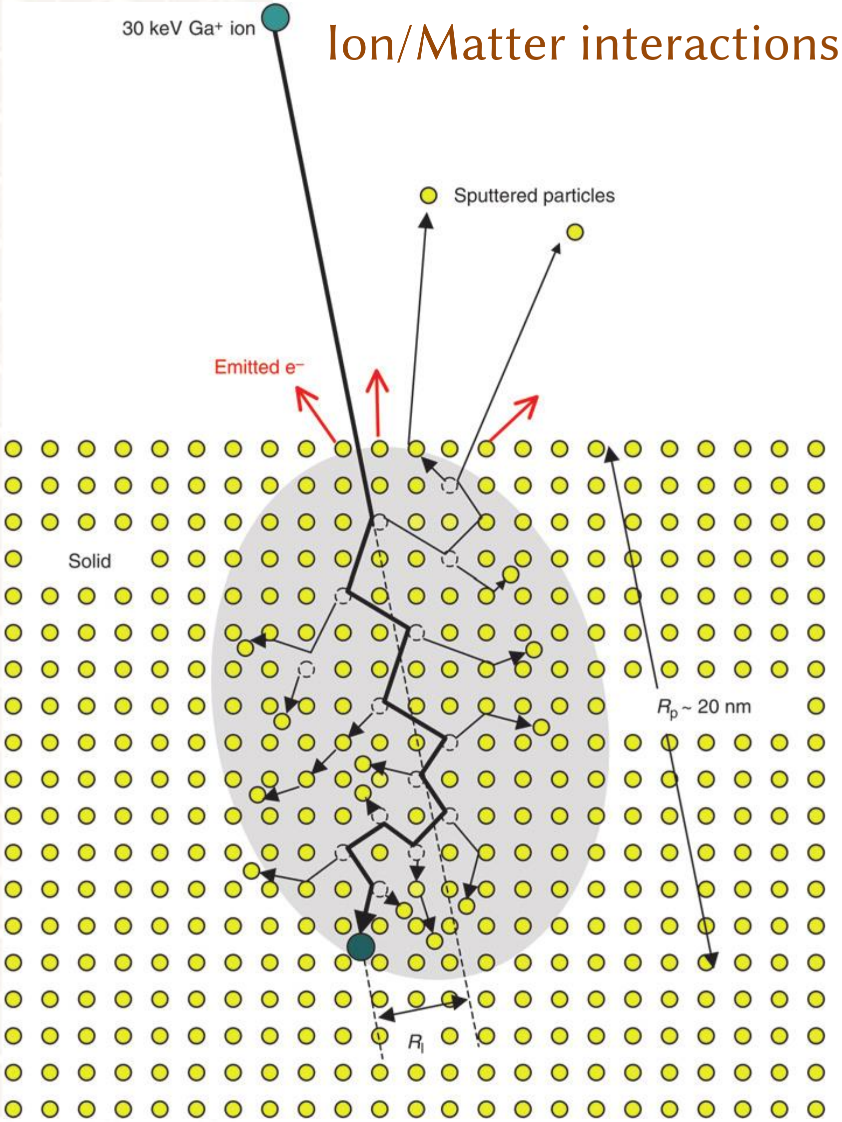

C.A.Volkert and A.M.Minor, *MRS Bull.*, **32**, 389 (2007)

Ion/Matter interactions: 3 regimes

Main parameters:

- incident ion energy (E_0)
- atomic masses (M1 and M2)
- atomic numbers (Z1 and Z2)

(1): ion, (2) target atoms

- **Regime I (knock-on regime)**:

$M_1 << M_2$ or E_0 is low, minimum sputtering

- **Regime II (linear cascade regime)**, where FIB operates:

$M_1 \sim M_2$, E_0 is moderate, governed by nuclear effects

- **Regime III (spike-on regime)**:

$M_1 > M_2$ and/or E_0 is high, majority of atoms move in collision cascade

For typical FIB usage:

$$R = \frac{6E_0(\mathrm{keV})}{\rho(\mathrm{g\,cm^{-3}})}\frac{M_2}{Z_2}\frac{M_1+M_2}{M_1}\frac{Z_1^{\frac{2}{3}}+Z_2^{\frac{2}{3}}}{Z_1}$$

Ion-beam lithography

Ion/Matter interactions

On first approximation

$$\nu(E) = \begin{cases} 0 & E < E_d \\ 1 & E_d \leqslant E < 2,5E_d \\ \dfrac{k(E)E_a}{2E_d} & 2,5E_d \leqslant E \end{cases}$$

E: Primary Knock-on Atom (PKA)

$\nu(E)$: atomic displacements

$\kappa(E) \approx 0.8$

E_d: displacement energy

E_a: damage energy

Energy loss from electronic and nuclear stopping as a function of energy

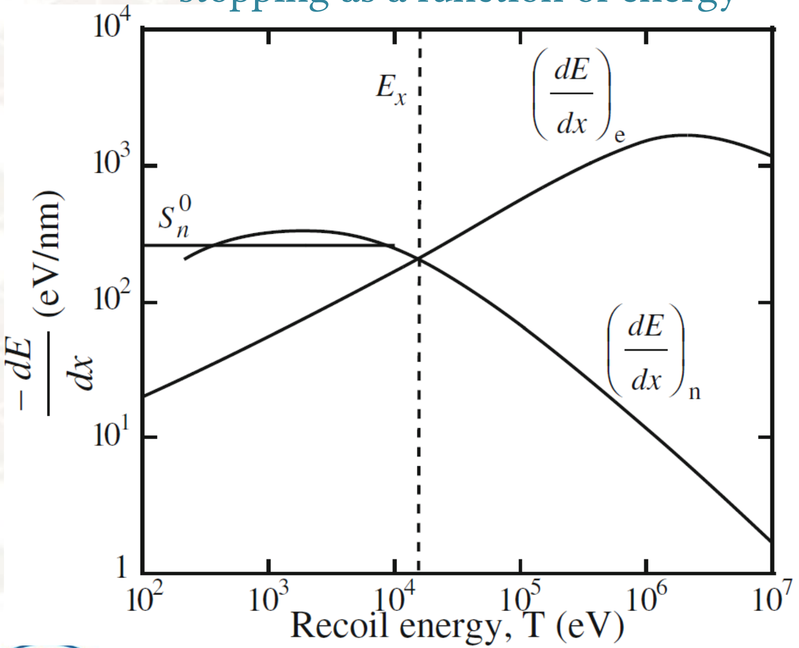

Dominant mechanism for FIB process (1-50 keV):
Nuclear stopping

G.H. Kinchin and R.S. Pease,
``The Displacement of Atoms in Solids by Radiation,''
Reports on Progress in Physics, vol. 18, pp. 1-51, 1955.

Ion-beam lithography

Ion/Matter interactions

Stopping power

$$S(E) = 2\pi \frac{4M_1M_2}{(M_1+M_2)^2} E_0 \int_0^{p_{\max}} \sin^2 \frac{\theta}{2} p dp$$

Number of silicon vacancies and interstitials generated by the primary recoil

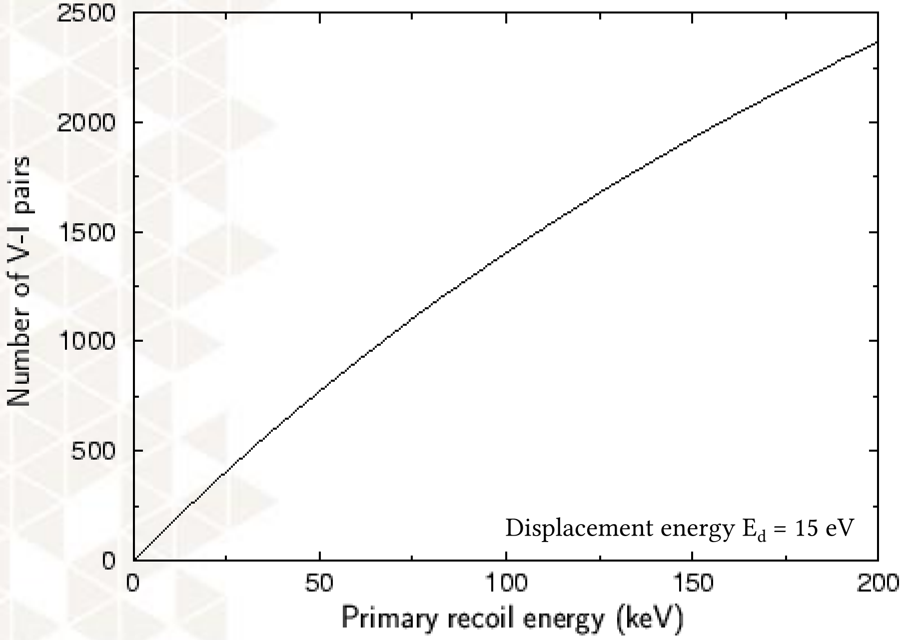

M. T. Robinson, *Defects and radiation damage in metals.*, Cambridge University Press, Cambridge (1969)

Sputtering yield

$$Y(E_0) \approx \frac{1}{4}\Gamma_m \frac{\alpha N S_n(E)\Delta x_n}{E_0}$$

Sputtering yields for typical FIB energies

$$10^{-1} < Y < 10^2$$

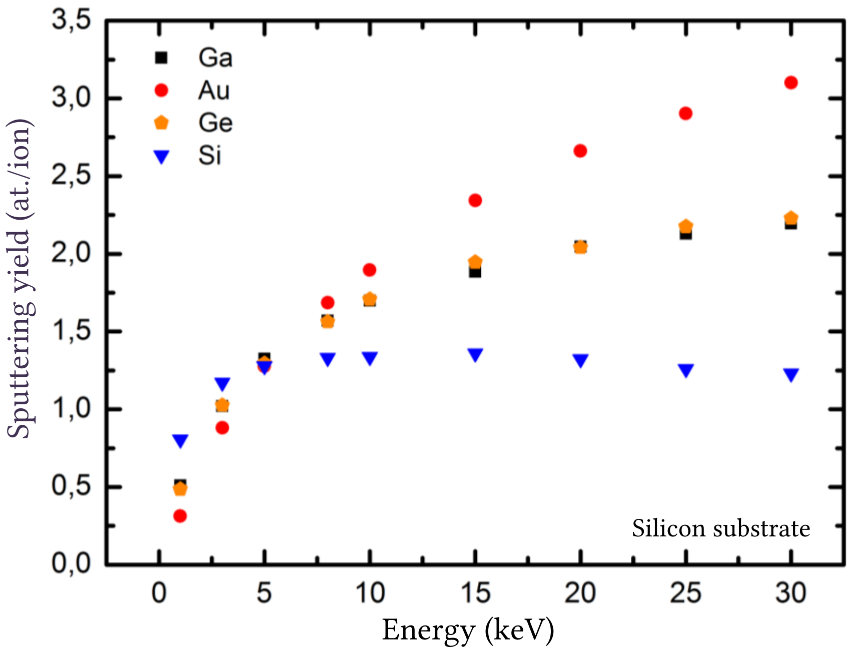

Ion-beam lithography

Ion/Matter interactions

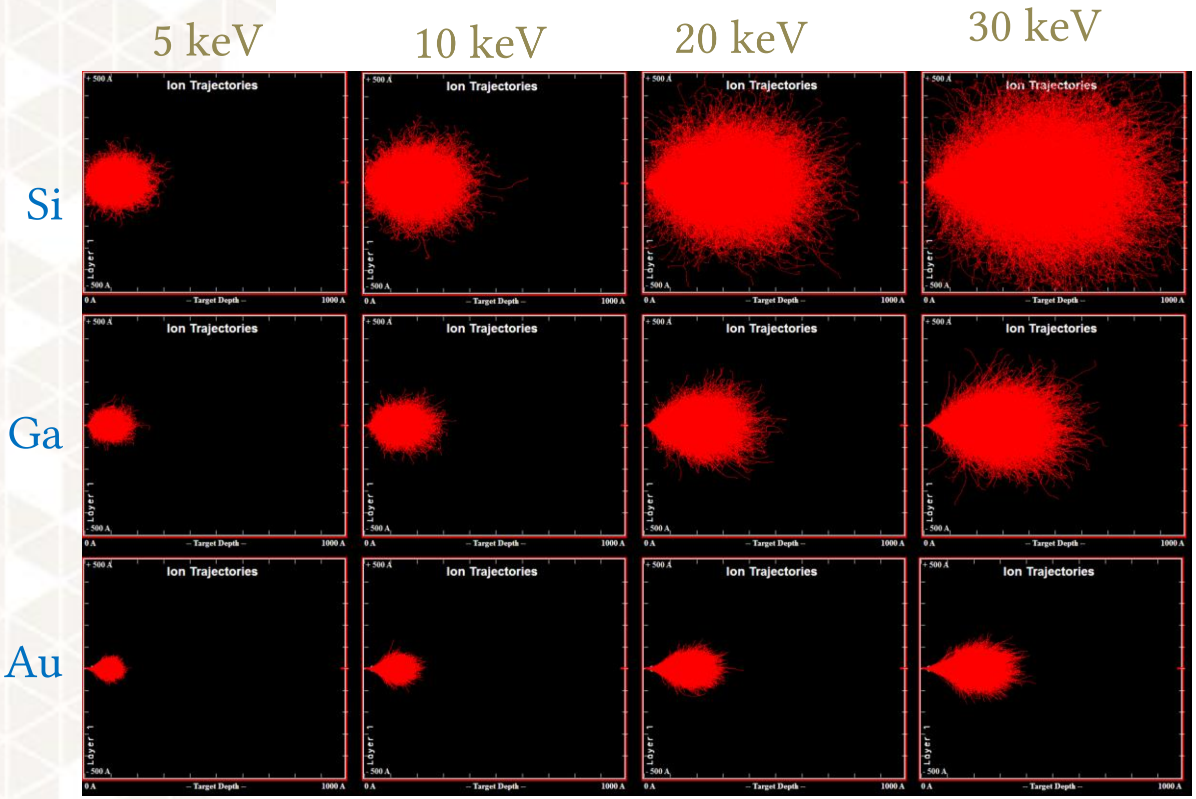

Box: 100 x 100 nm

Ion	Max. depth (nm)	Max. width (nm)
Si	90	70
Ga	60	36
Au	40	20

Ion energy: 30 keV

Ion-beam lithography

Ion/Matter interactions

SRIM - Ga$^+$ - 30 kV

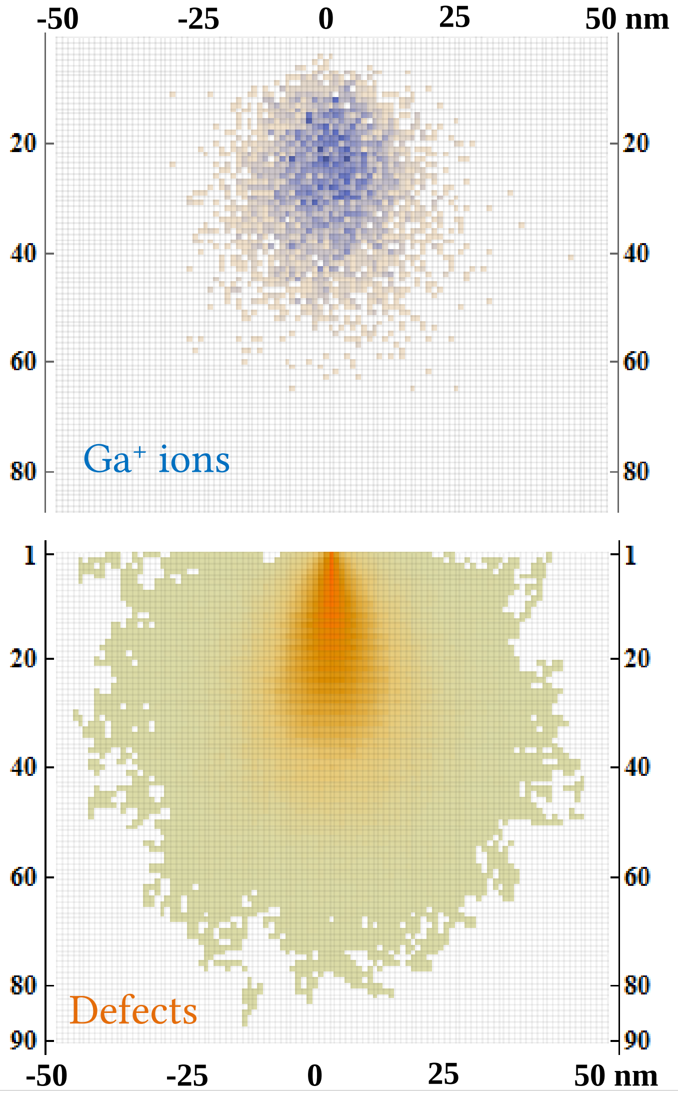

Principles

Monte Carlo simulations:

- Incident ion trajectories
- Recoil atoms trajectories
- Phonons
- Nuclear and electronic energy loss

Drawbacks

- No crystalline orientation (channeling)
- No defects accumulation
- Punctual probe

Ion-beam lithography

Ion/Matter interactions

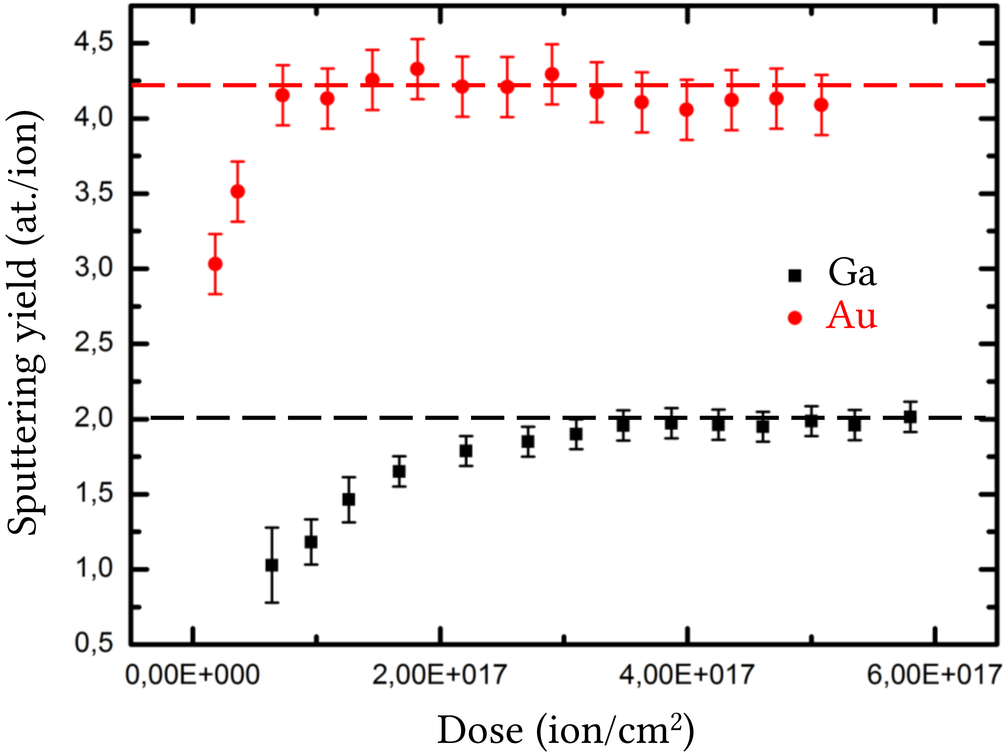

Ion	Simulations (at./ion)	Experiments (at./ion)
Ga^+	2,2	2
Au^+	3,1	4,2

Ion-beam lithography

Ion/Matter interactions

- **Amorphization** of sample surface
- Ion Implantation: incident atoms remain in the sample target
  - **Dopping** effect
  - May reach critical composition for **second phase formation**
- Lattice defects
  - **Vacancies** – displaced or “missing” atoms from their equilibrium lattice positions
  - **Interstitials** – atoms which are positioned in between equilibrium lattice positions
  - **Dislocations** – a missing “half-plane” of atoms
- **Local heating** due to large displacement of atoms that may occur within the collision cascade (10’s of nanometers from surface)

Example: Ga^+ ion lithography

- Concentration of primary defects (knock-outs from lattice sites): average 1000 defects per ion
- Ga in most semiconductors is acceptor, affecting electronic, optical, magnetic and thermal properties
- Concentration of Ga in the irradiated zone can be given by: $C_{Ga} = 1/(1+\gamma)$, where γ is sputter yield

Ion-beam lithography

Square patterns: Ga$^+$ (30 keV) on Si substrate

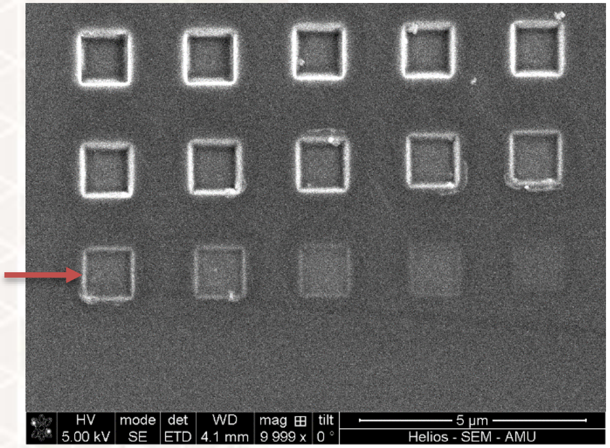

D = $3 \cdot 10^{16}$ - 5.10^{17} at./cm^2

D = $3 \cdot 10^{17}$ at./cm^2

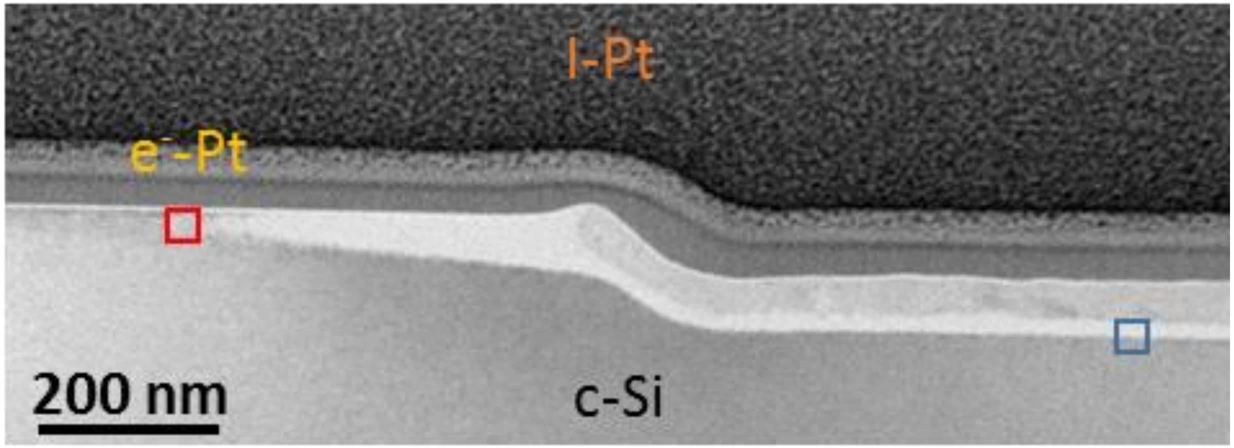

Structural characterization

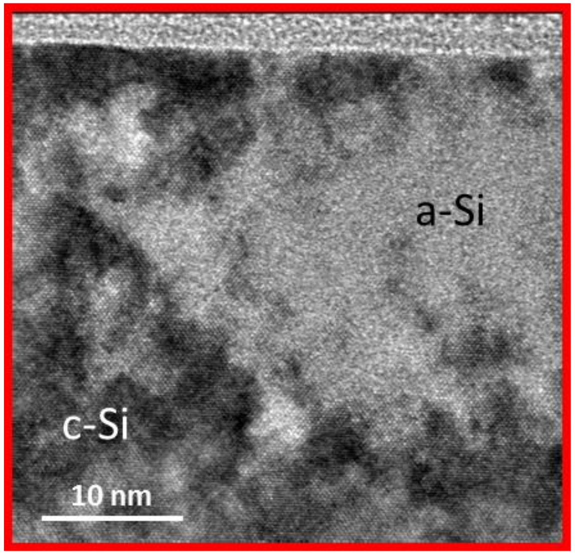

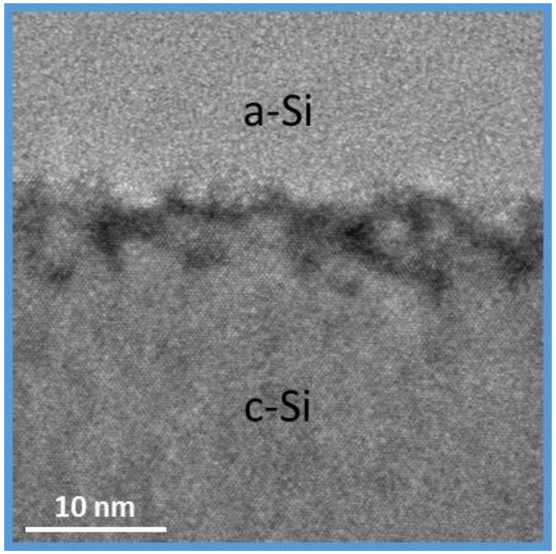

Ion-beam lithography

Square patterns: Ga$^+$ (30 keV) on Si substrate

D = $3 \cdot 10^{17}$ at./cm^2

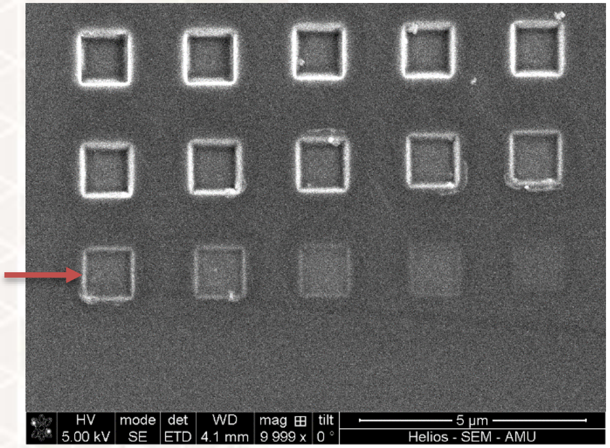

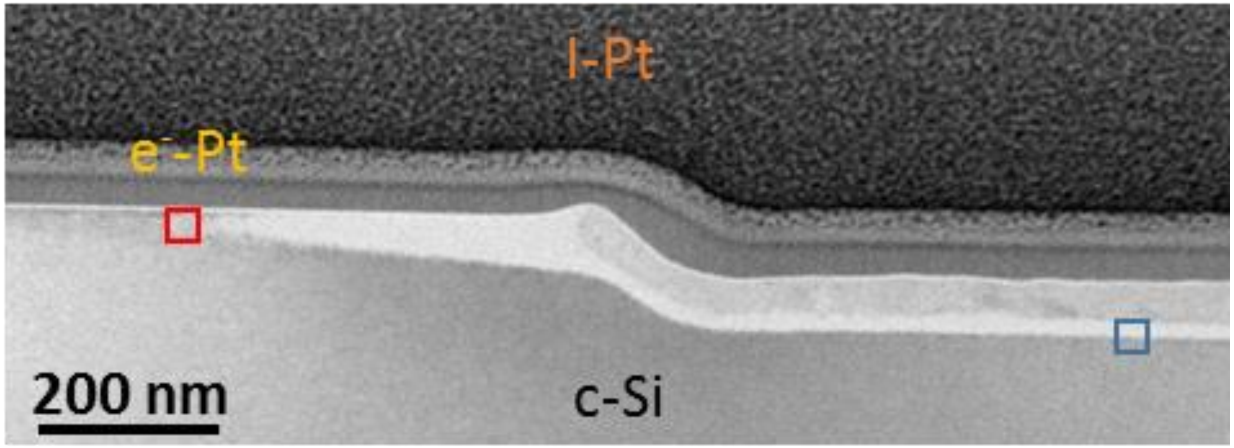

D = $3 \cdot 10^{16}$ - 5.10^{17} at./cm^2

Caractérisation chimique (EDX)

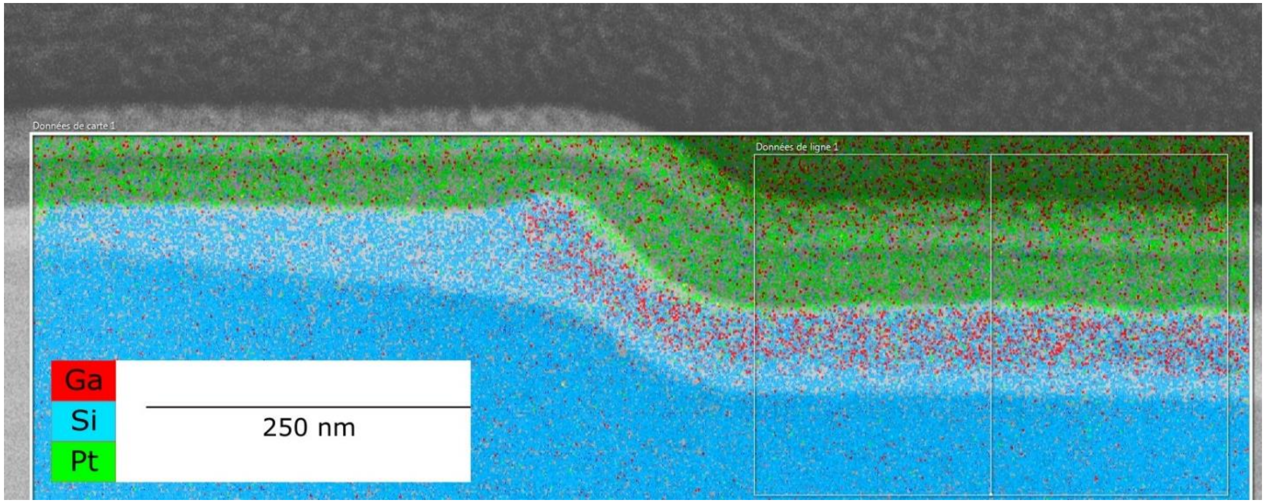

Ion-beam lithography

Ion/Matter interactions

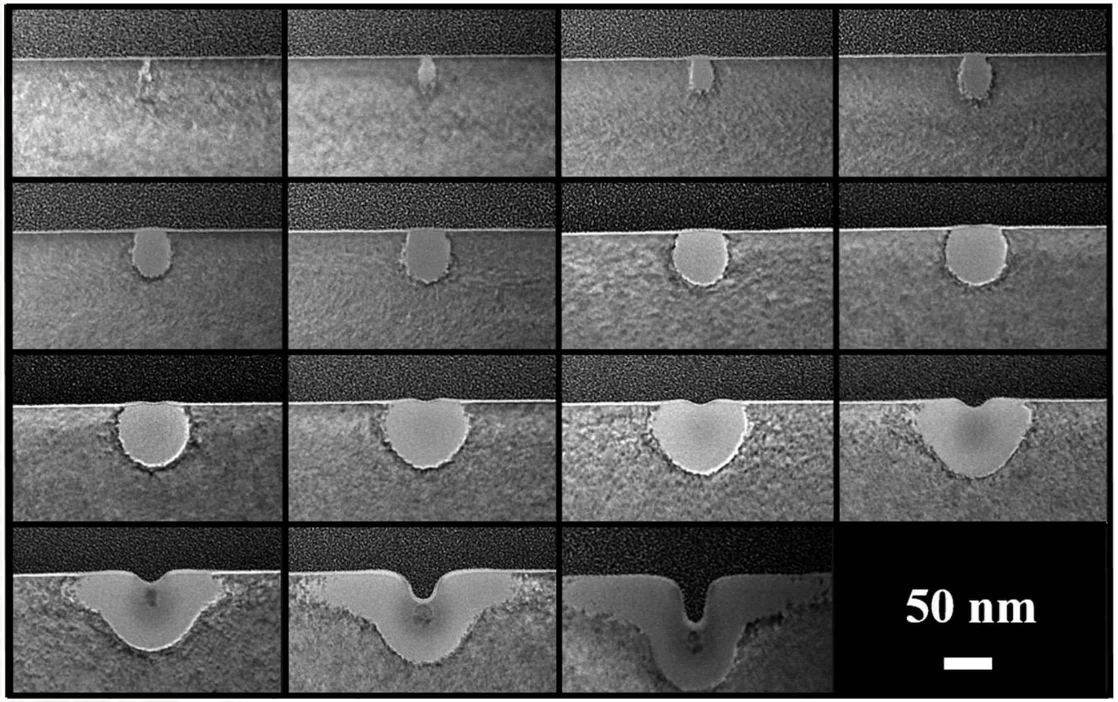

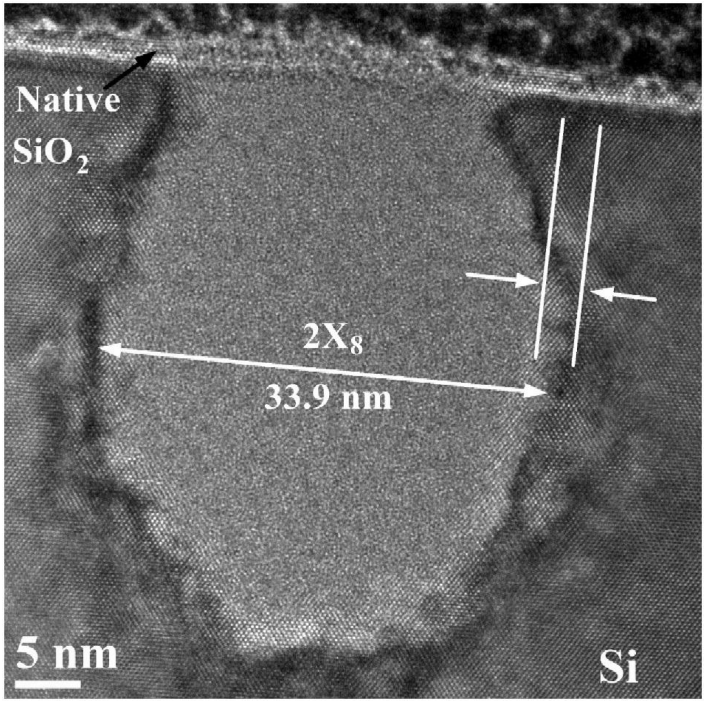

D = $1.1 \cdot 10^{-9}$ C/m to $1.8 \cdot 10^{-5}$ C/m

Y. Greenzweig *et al.*, Microelectronic Engineering, 155, 19 (2016)

Ion-beam lithography

Ion/Matter interactions

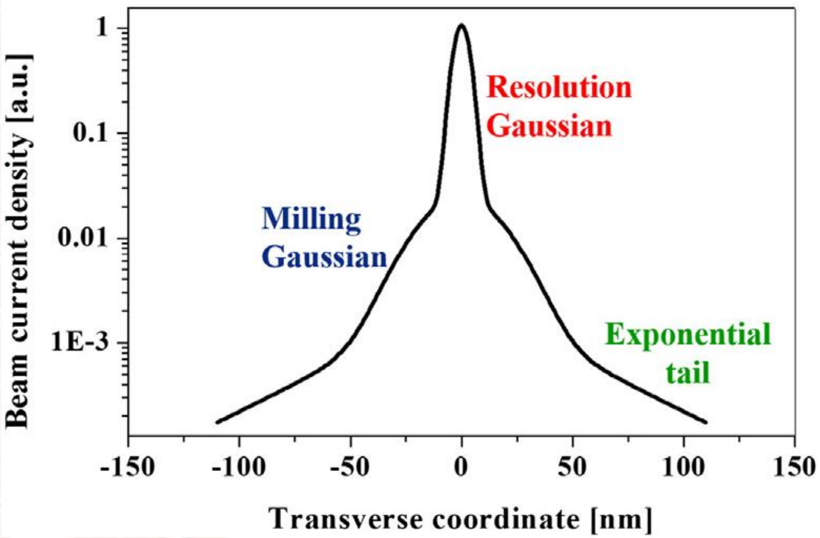

$$J_{B}(x) = \frac{I_1}{\sqrt{2\pi a_1^2}}\, exp\left(-\frac{x^2}{2a_1^2}\right) + \frac{I_2}{\sqrt{2\pi a_2^2}}\exp\left(-\frac{x^2}{2a_2^2}\right) + \frac{I_3}{2a_3}\, exp\left(-\frac{|x|}{a_3}\right)$$

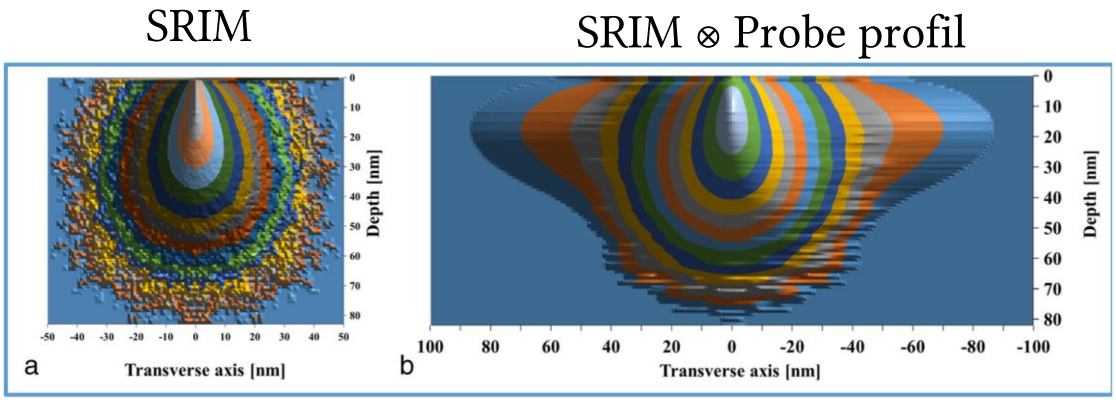
SRIM

SRIM ⊗ Probe profil

Y. Greenzweig *et al.*, Microelectronic Engineering, 155, 19 (2016)

Ion-beam lithography

Ion/Matter interactions

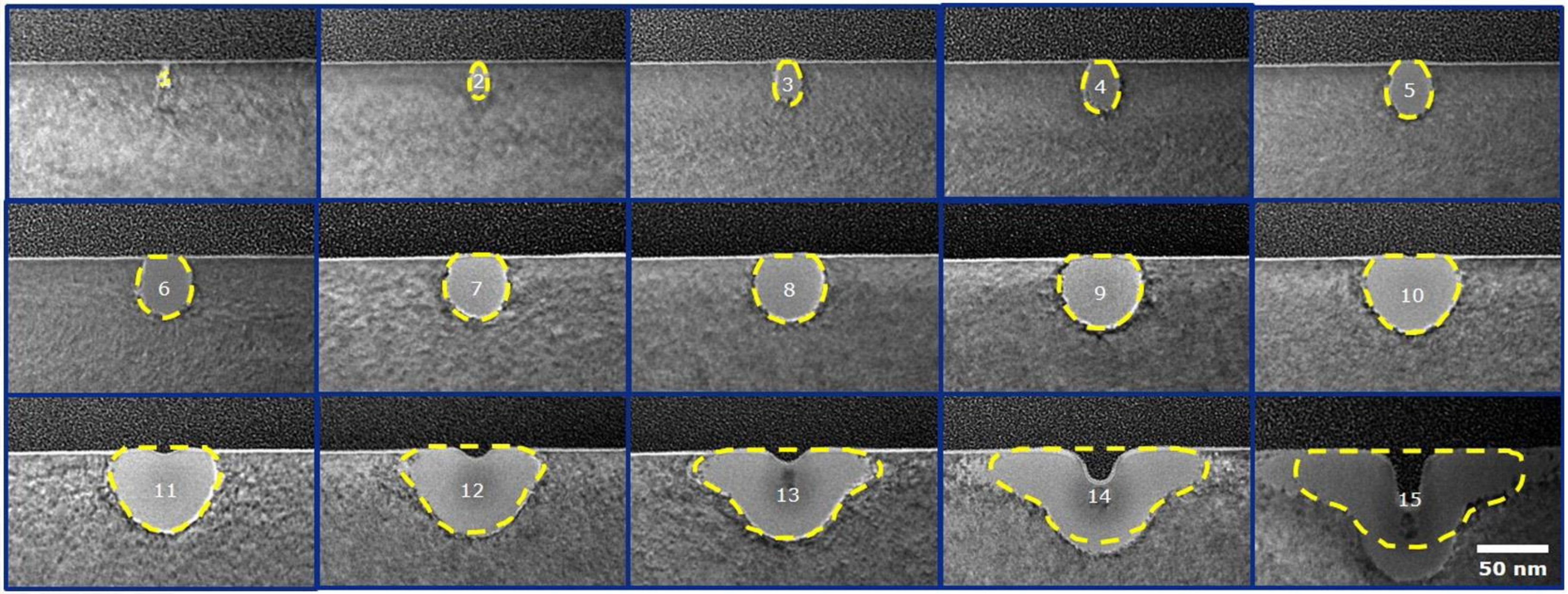

Y. Greenzweig et al., *Microelectronic Engineering*, 155, 19 (2016)

Ion-beam lithography

Square patterns: Ga$^+$ (30 keV) on Si substrate

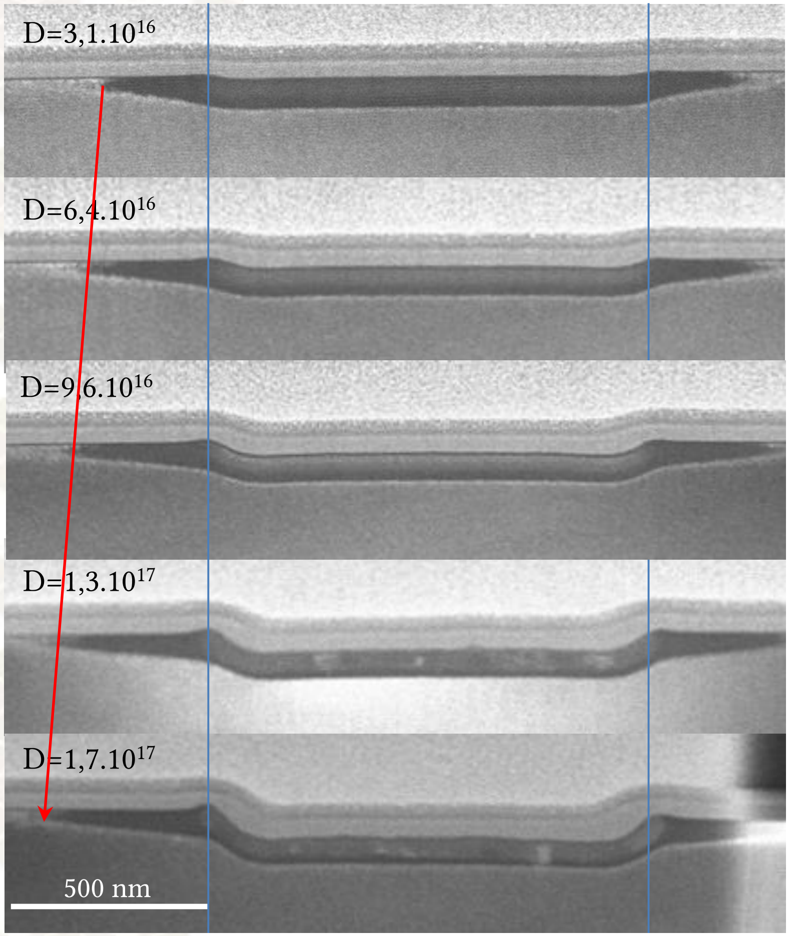

D = 3·10^{17} at./cm^2

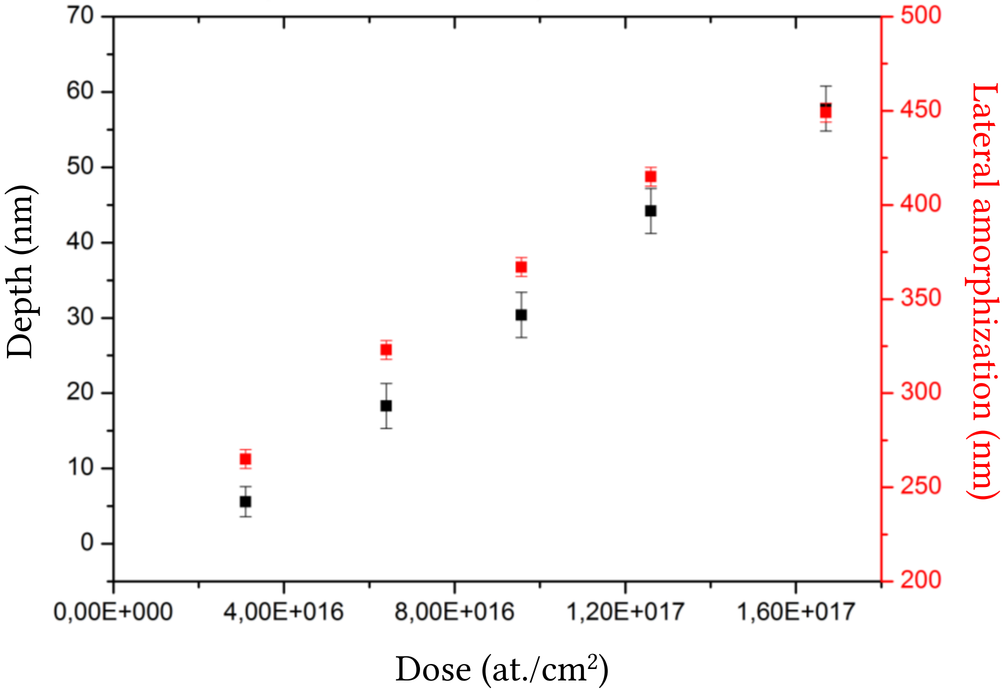

Depth and width of amorphized layer proportional to ion dose

Ion-beam lithography

Square patterns: Ga⁺ (8, 20 and 30 keV) on Si substrate

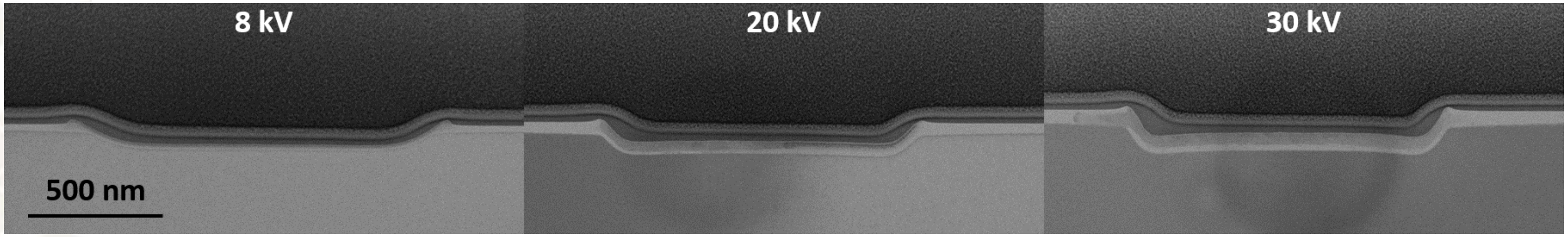

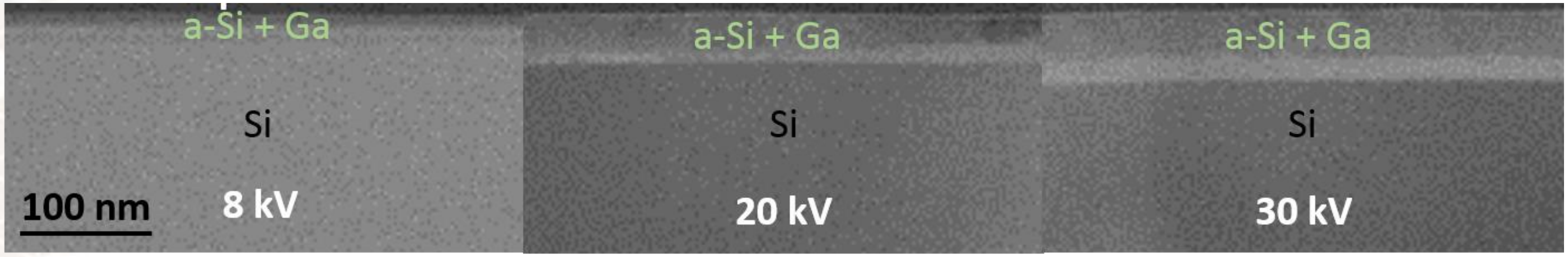

D = $3{\cdot}10^{17}$ at./cm^2

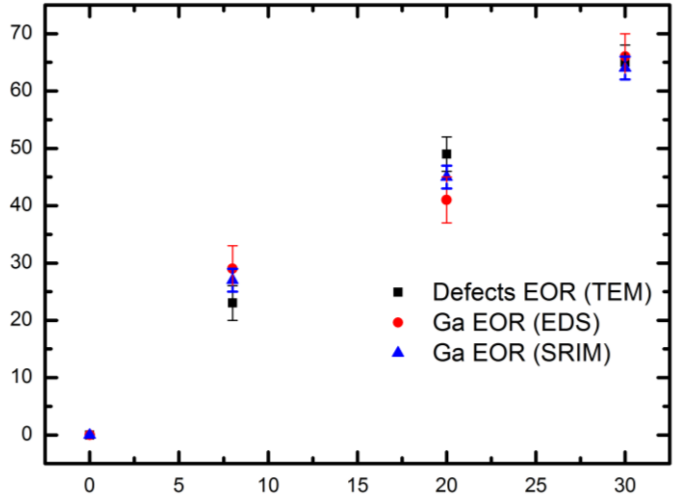

Working at low energy

Ion-beam lithography: defects healing

Square patterns: Ga$^+$ (8, 20 and 30 keV) on Si substrate

Defects healing by annealing

Before

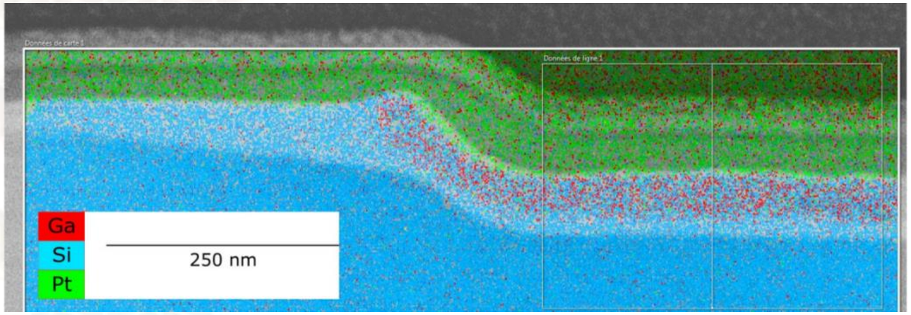

After

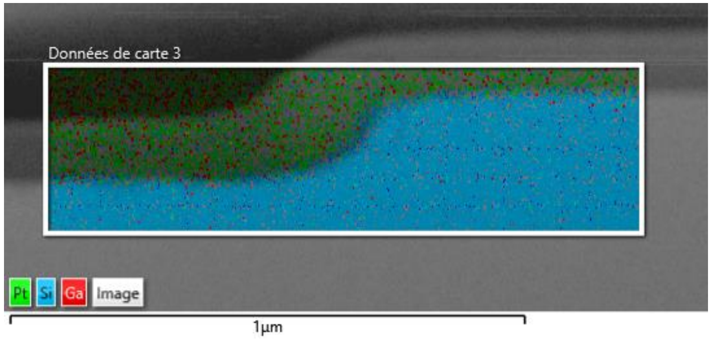

600°C / 10 min. then 850°C / 5 min

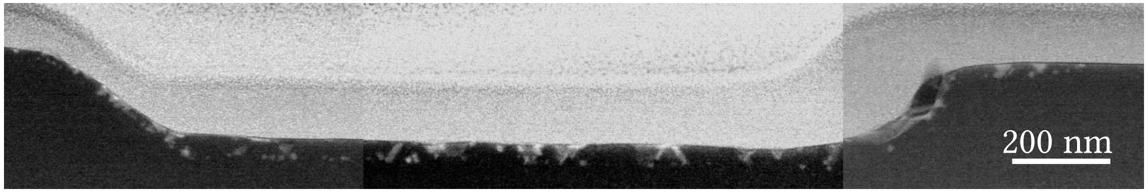

No gallium contamination detectable: Ga diffusion

Lot of structural defects: stacking faults, dislocations

Ion-beam lithography: defects healing

Square patterns: Au$^+$ (8, 20 and 30 keV) on Si substrate

Defects healing by annealing

Before annealing

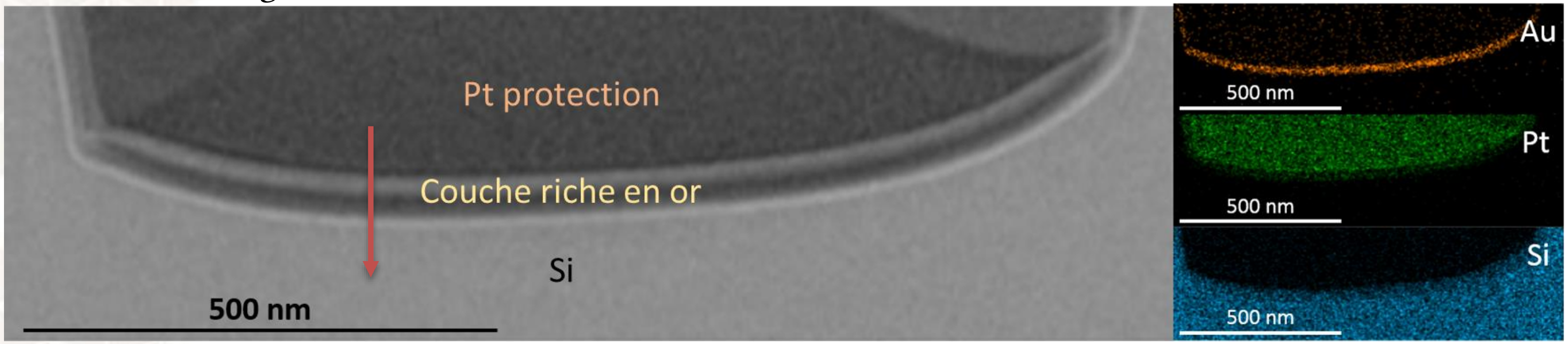

EDX line profile

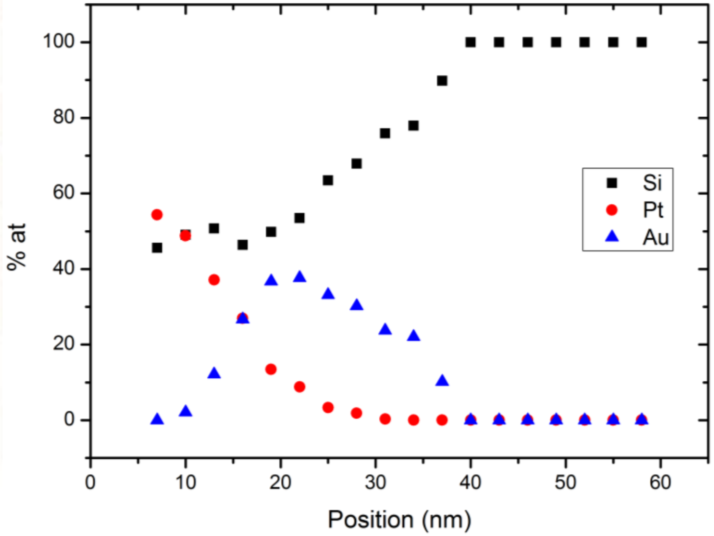

Gold-silicon alloy layer

Ion-beam lithography: defects healing

Square patterns: Au$^+$ (8, 20 and 30 keV) on Si substrate

Defects healing by annealing

After annealing

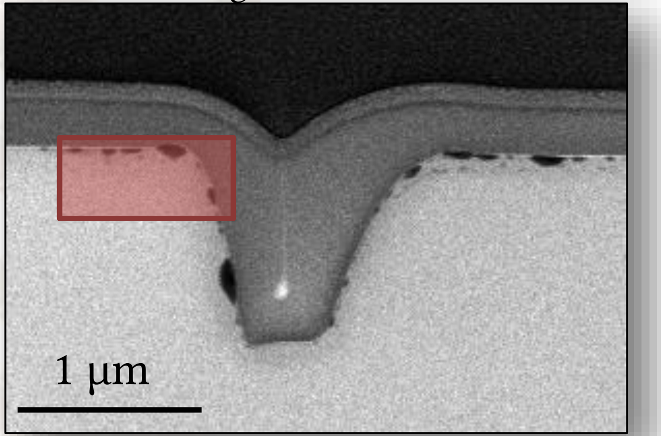

600°C / 10 min. then 850°C / 5 min

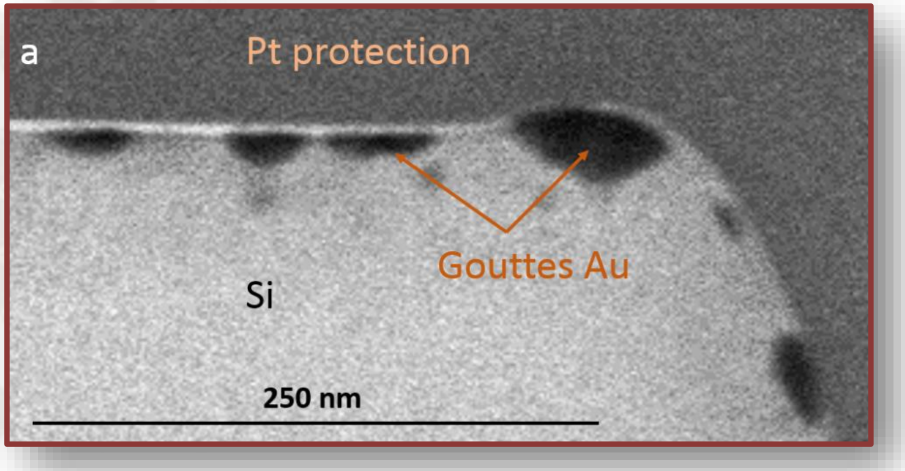

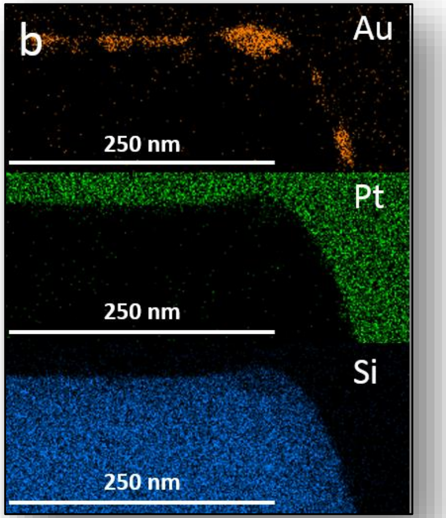

Gold segregation

Ion-beam lithography: defects healing

Square patterns: Si$^+$ (8, 20 and 30 keV) on Si substrate

Defects healing by annealing

After annealing

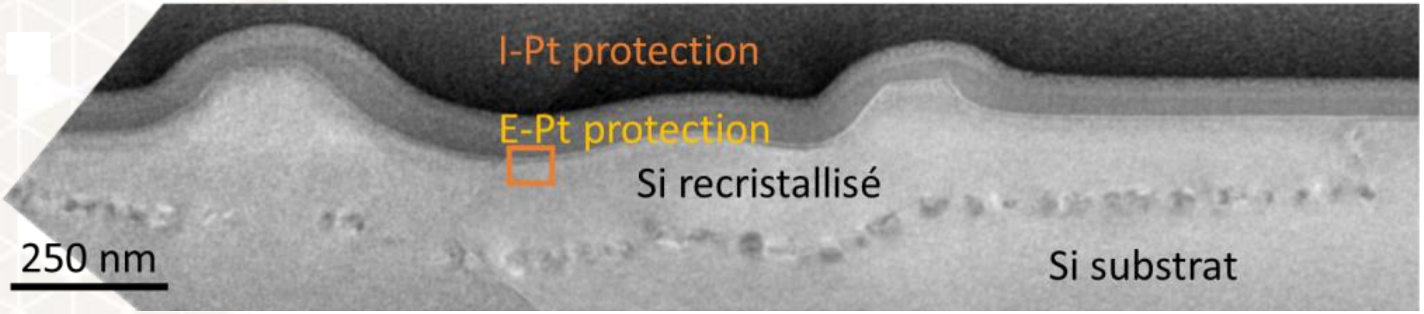

600°C / 10 min. then 850°C / 5 min

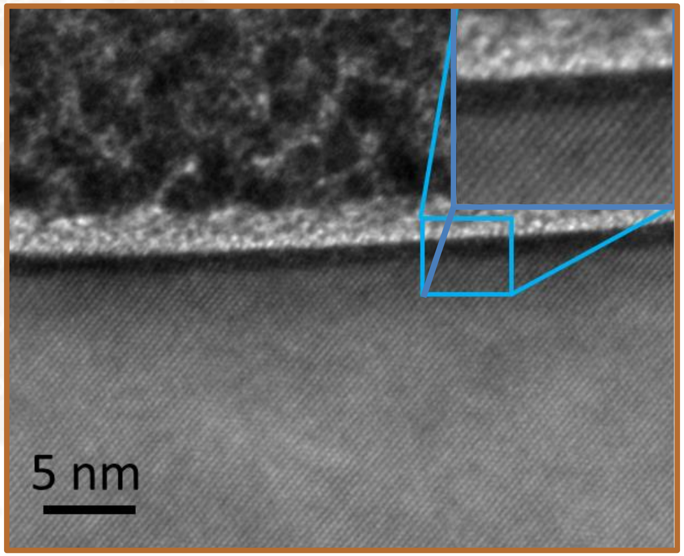

Si in Si: no contamination

Fully recrystallized lattice

End of Range defects (interstitials atoms): thickness 40-70 nm

Ion-beam lithography: defects healing

Square patterns: Si^+ (8, 20 and 30 keV) on Si substrate

Defects healing by annealing

Previous recipe	600°C / 10 min. then 850°C / 5 min
New recipe	700°C / 30 min

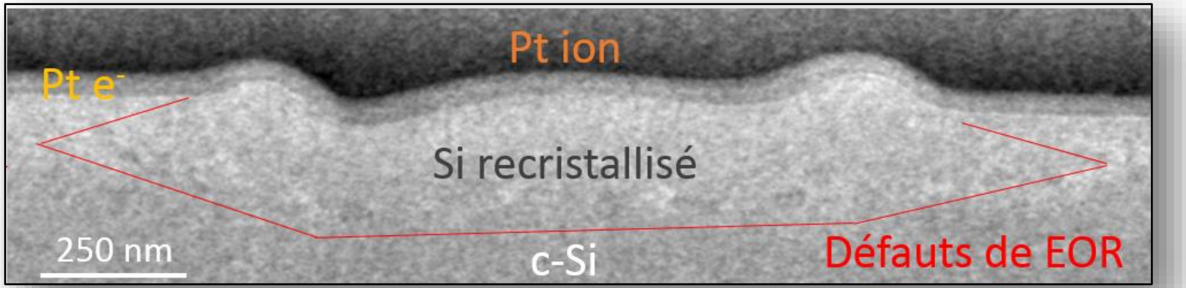

Reduction of End of Range defects (thickness 10-20 nm)

Synopsis

Introduction

- Usual Si cleaning process
- Bottom-up is not, yet, efficient

Ion beam lithography

- Fast review of lithography technics
- Focused Ion Beam principles
- High resolution
- Limits: surface and volume defects

Using Focus Ion Beam for surface preparation

- Gold dewetting
- Au dots
- Silicon dewetting

Conclusion

Ion-beam lithography: Ge dots

8 Ge monolayers growth on FIB patterned Si(100) substrate

550°C: metastable state

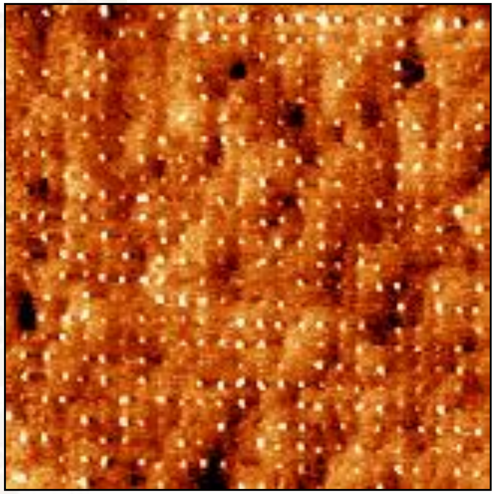

d = 50 nm

D = $4\cdot10^{10}$/cm^2

750°C: stable state

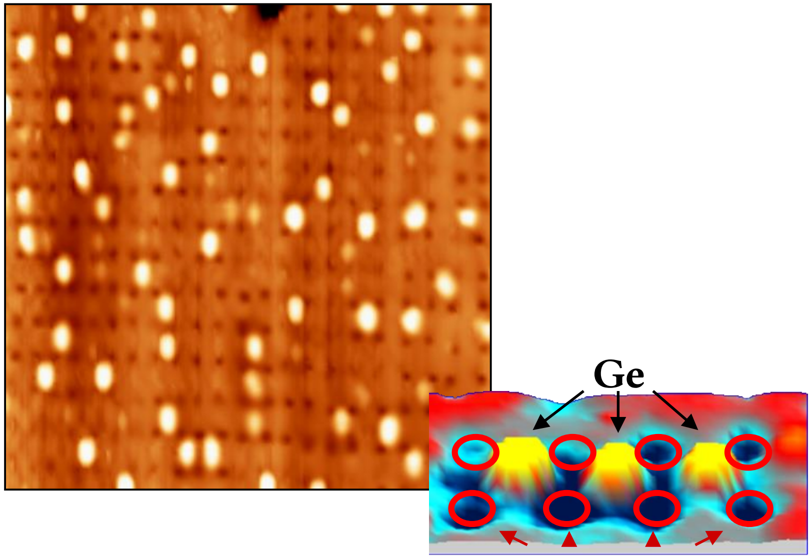

⇨ Scattering controlled diffusion

$$k(E,T) = k_0 \exp\left(-\frac{E}{k_B T}\right)$$

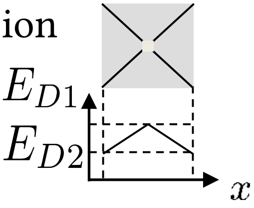

$$E = E_D(x,y) + nE_N \qquad E_{D1}(x,y) > E_{D2}(x,y)$$

Scattering barrier higher inside holes (E_{D1}) than on terrace (E_{D2})

⇨ Preferential nucleation inside patterned holes

$$k_1(E_1,T) = k_2(E_2,T)\exp\left(-\frac{E_{D1}-E_{D2}}{k_B T}\right)$$

Scattering barriers negligible at high temperature

⇨ Nucleation controlled by elastic energy

⇨ Preferential nucleation on terraces

Pascale *et al.* Phys. Rev. B 77, 075311 (2008)

Ion-beam lithography: gold dewetting

Gold Dewetting process

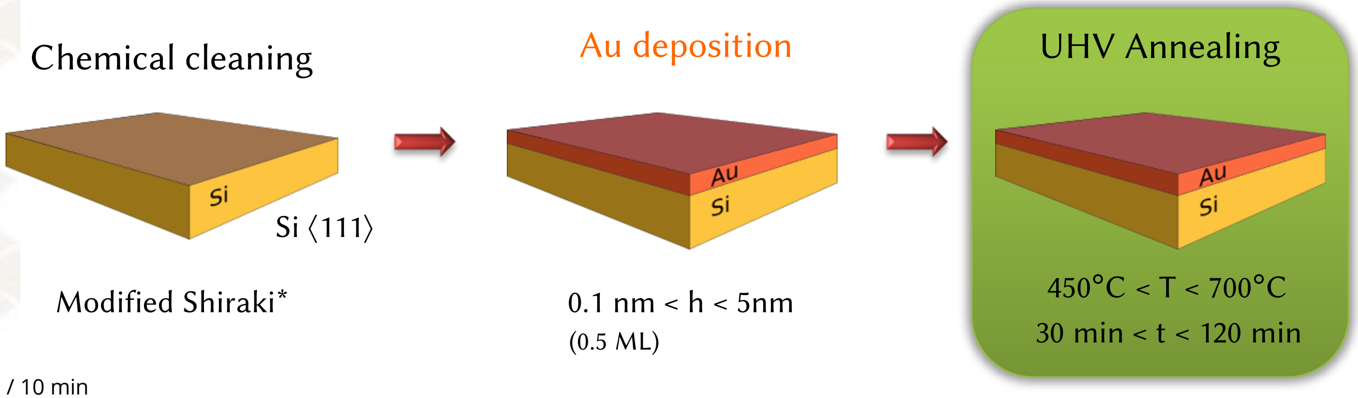

Chemical cleaning

Si ⟨111⟩

Modified Shiraki*

Au deposition

0.1 nm < h < 5nm

(0.5 ML)

UHV Annealing

450°C < T < 700°C

30 min < t < 120 min

* Modified Shiraki:

1. HNO_3(65%) / 70°C / 10 min
2. H_2O (DI) / RT / 1 min
3. HF(49%) : H_2O (1:10) / RT / 30 s

Dewetting process depends on Au layer thickness *h*

I. $h_{\mathrm{Au}} \leq 0.4$ nm

II. $0.4 \leq h_{\mathrm{Au}} \leq 5$ nm

III. $h \geq 5$ nm

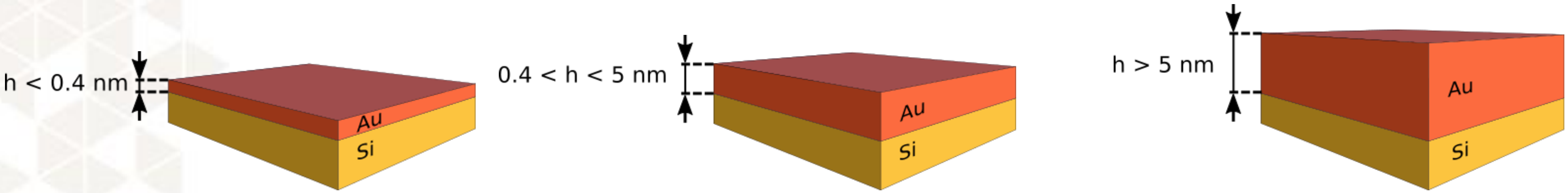

Ion-beam lithography: gold dewetting

Gold dewetting regimes

I. $h_{Au} \leq 0.4$ nm

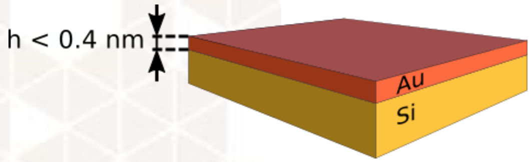

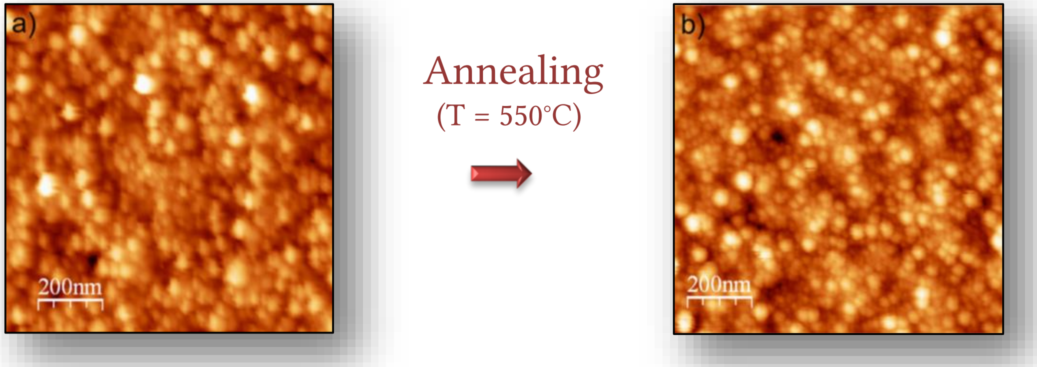

Annealing
(T = 550°C)

- Same RMS roughness: 0.5 nm
- Close Au nanocrystalline mean grains size

no significant difference

Consistent with the standard morphology of ultra-thin Au films on Si(111): nanocrystalline grains on top of 2D sub-ML structures

Ion-beam lithography: gold dewetting

Gold dewetting regimes

II. $0.4 \leq h_{\mathrm{Au}} \leq 5$ nm

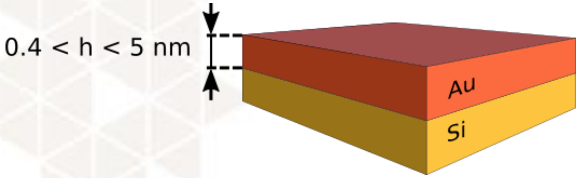

$h_{\mathrm{Au}} = 1$ nm

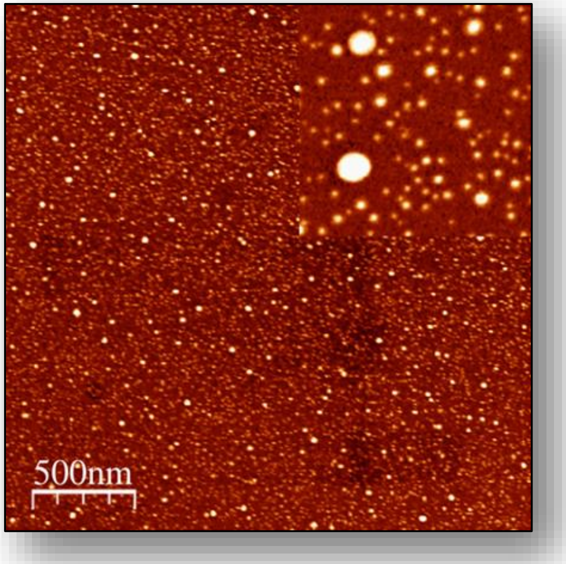

$h_{\mathrm{Au}} = 5$ nm

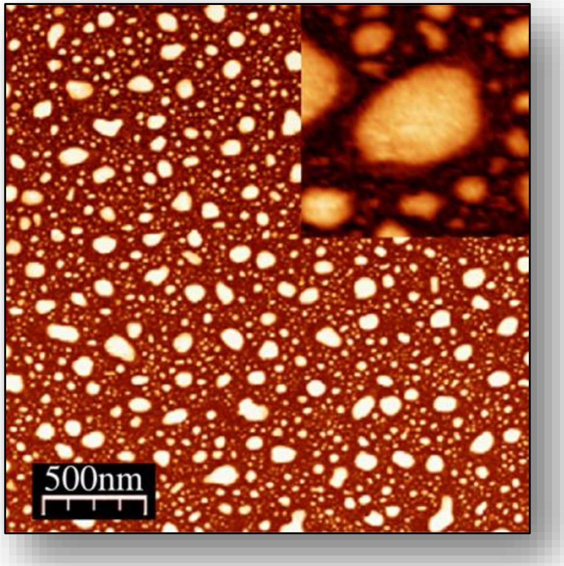

- Au droplets formation
- Bimodal distribution

Ion-beam lithography

Gold dewetting regimes

II. $0.4 \leq h_{Au} \leq 5$ nm

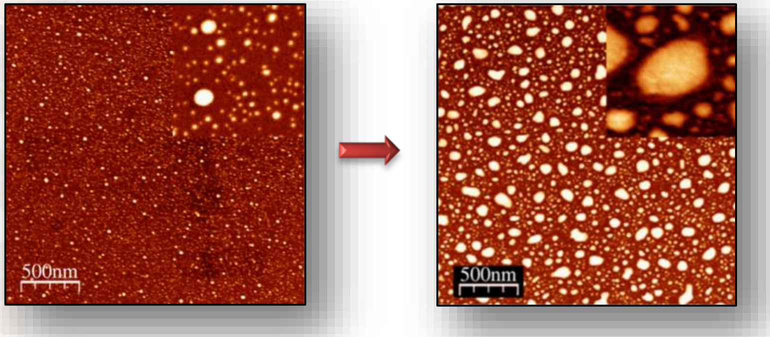

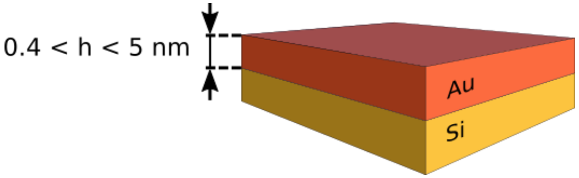

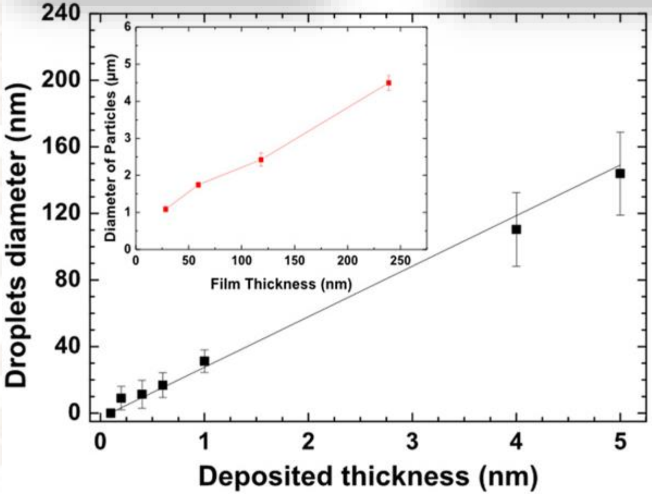

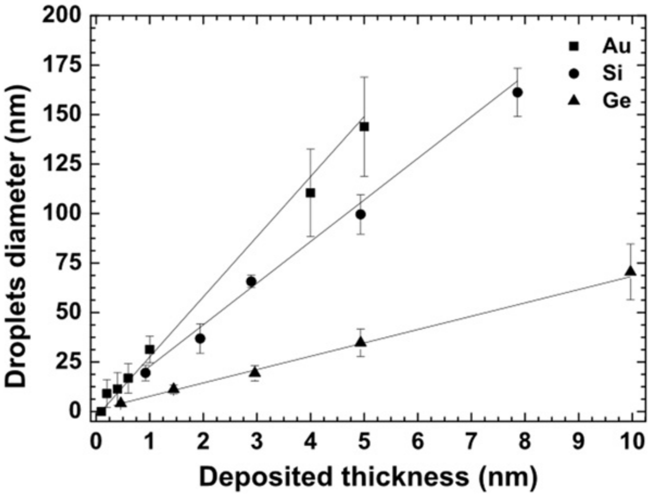

Linear size evolution: $D \approx 30 \times h$

Characteristic of dewetting process

Ion-beam lithography: gold dewetting

Gold dewetting regimes

II. $0.4 \leq h_{\mathrm{Au}} \leq 5$ nm

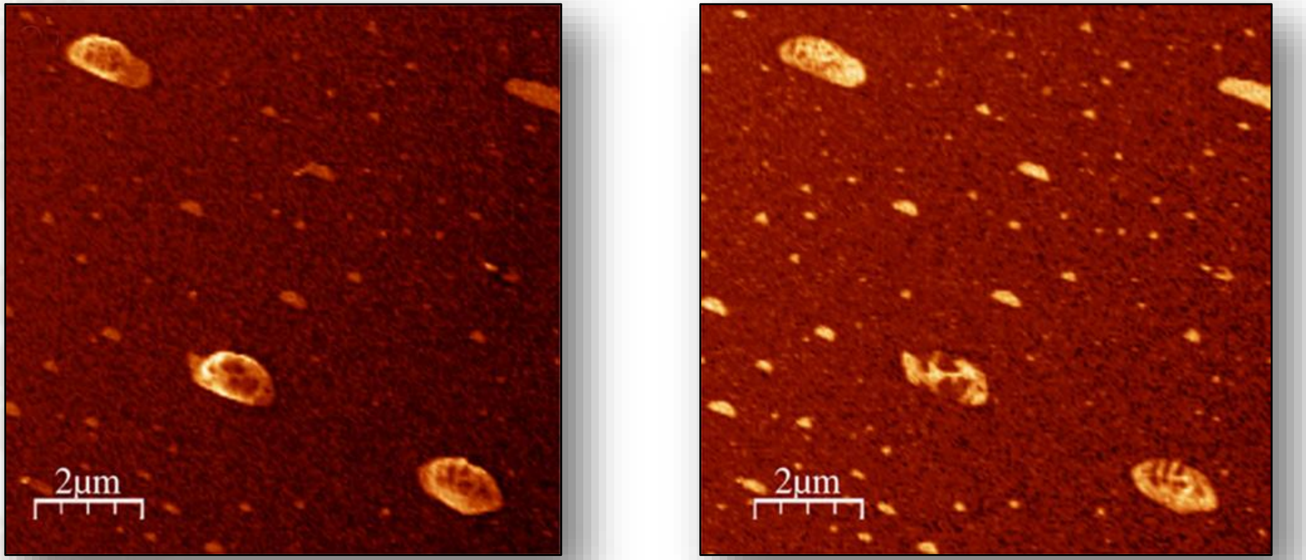

SE SEM BSE

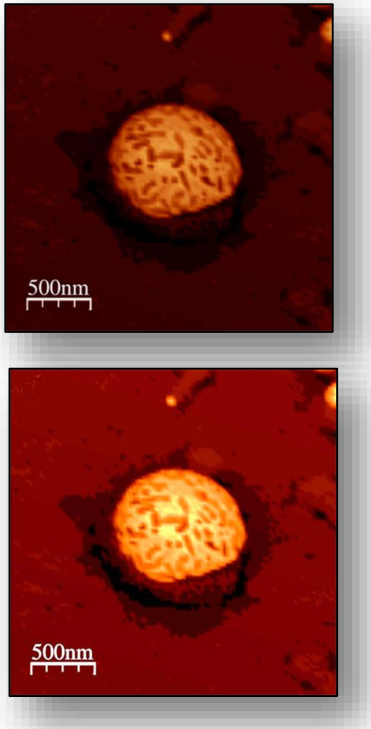

SE

Silicon channels into droplets: phase separation of the binary alloy during cooling

Si-Au intermixing results in pinning of the droplets

Ion-beam lithography: gold dewetting

Gold dewetting regimes

III. $h \geq 5$ nm

Annealing (30 min)

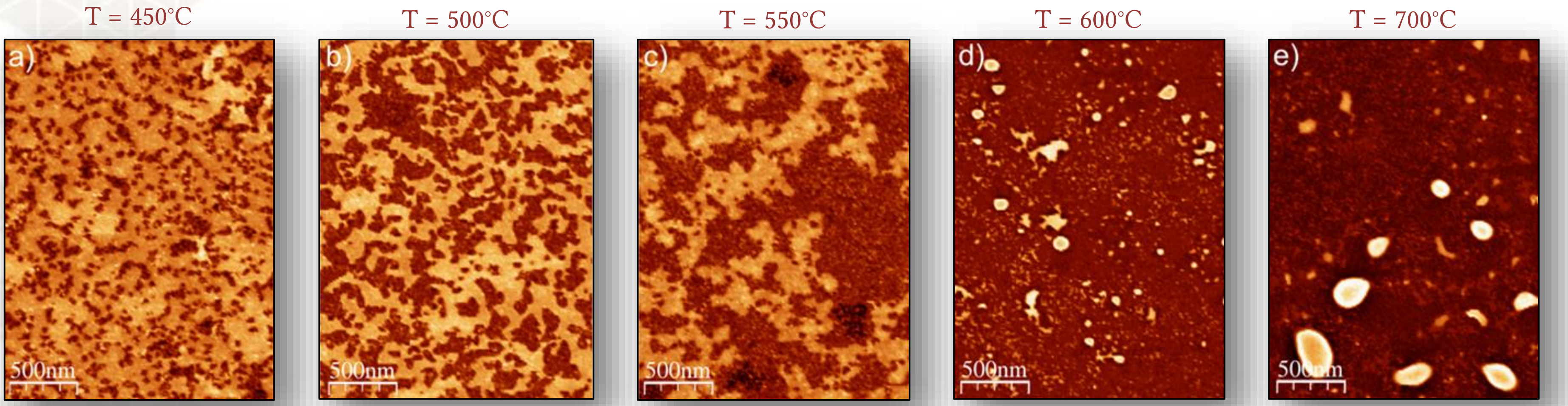

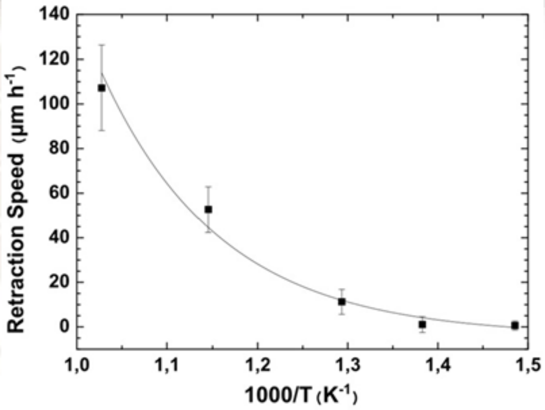

- Diffusion activation energy: $E = 0.6$ eV

Gold self diffusion

Hard Au diffusion control

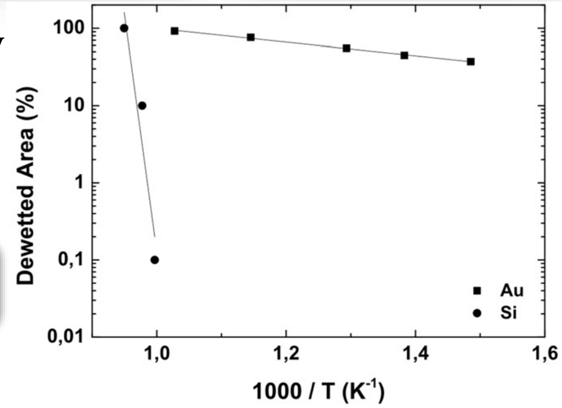

Ion-beam lithography: gold dewetting

Gold dewetting regimes

III. $h \geq 5$ nm

No Si channels into droplets... unless additional supply of Si atoms

MBE deposition:
350 nm Si upon
6 nm Au layer

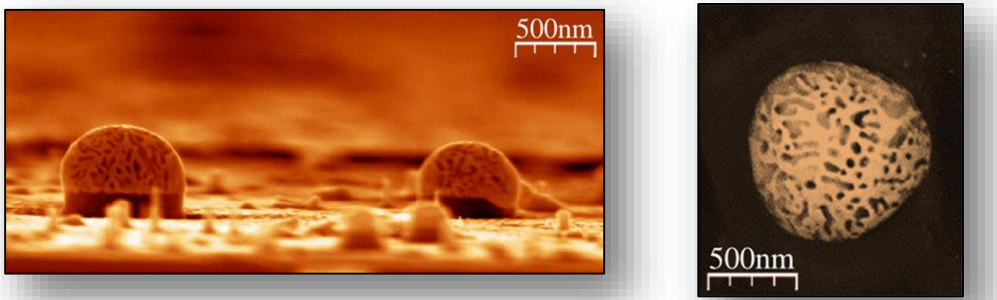

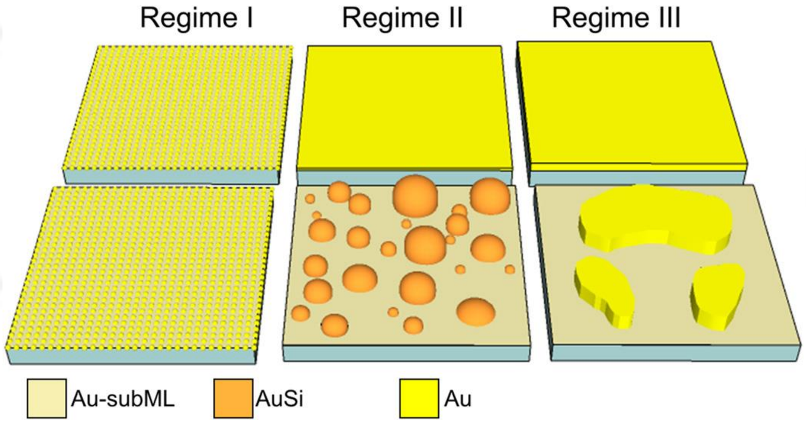

Summary

Ion-beam lithography: gold dewetting

Au layer FIB patterning

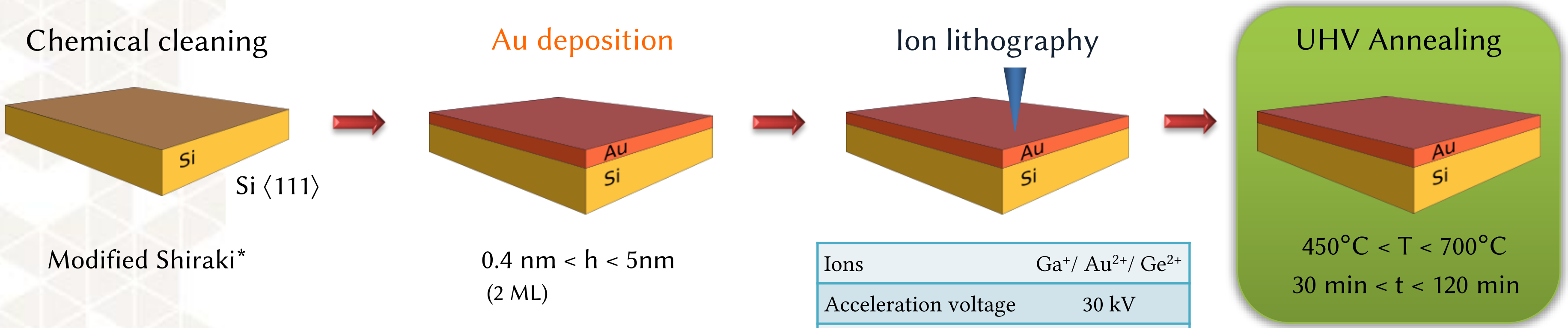

Modified Shiraki*

0.4 nm < h < 5nm
(2 ML)

Ions	Ga^+/ Au^{2+}/ Ge^{2+}
Acceleration voltage	30 kV
Probe current	10-100 pA

450°C < T < 700°C
30 min < t < 120 min

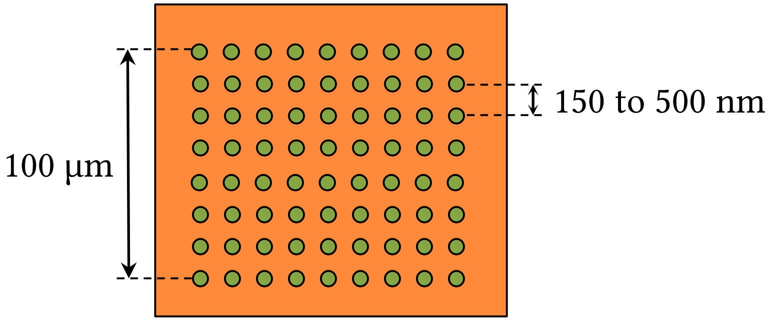

---

* Modified Shiraki:

1. HNO_3(65%) / 70°C / 10 min
2. H_2O (DI) / RT / 1 min
3. HF(49%) : H_2O (1:10) / RT / 30 s

Ion-beam lithography: gold dewetting

Gold dewetting regimes

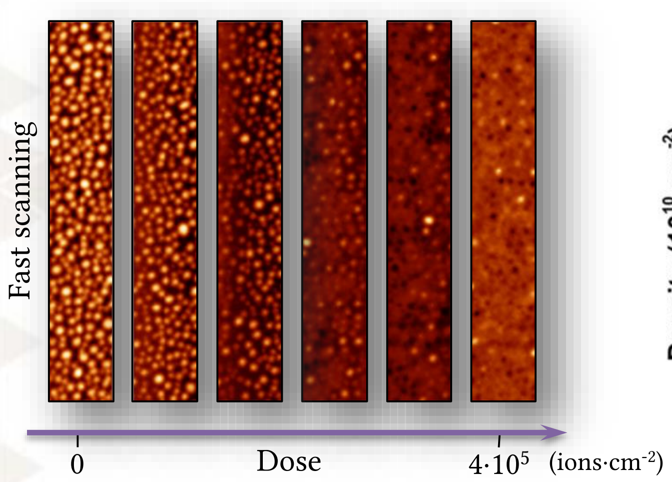

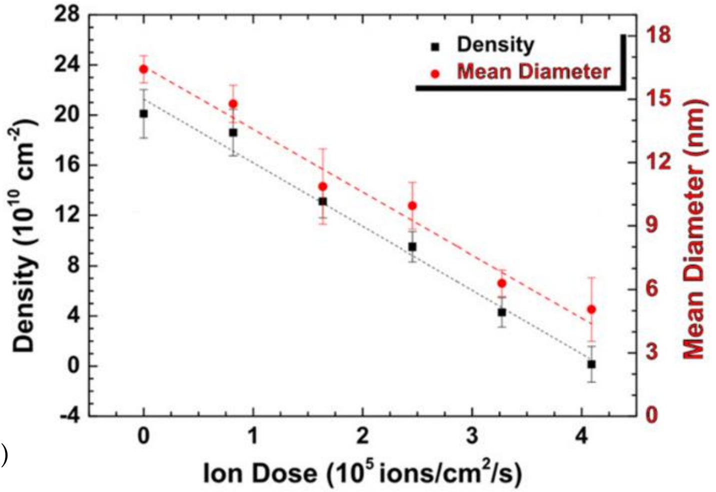

Au droplets formation reduced by FIB erosion

Ion-beam lithography: gold dewetting

Dewetting: temperature influence

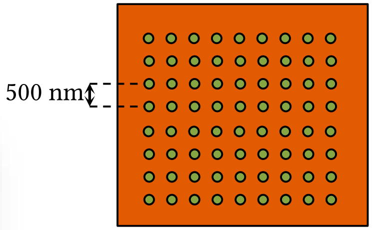

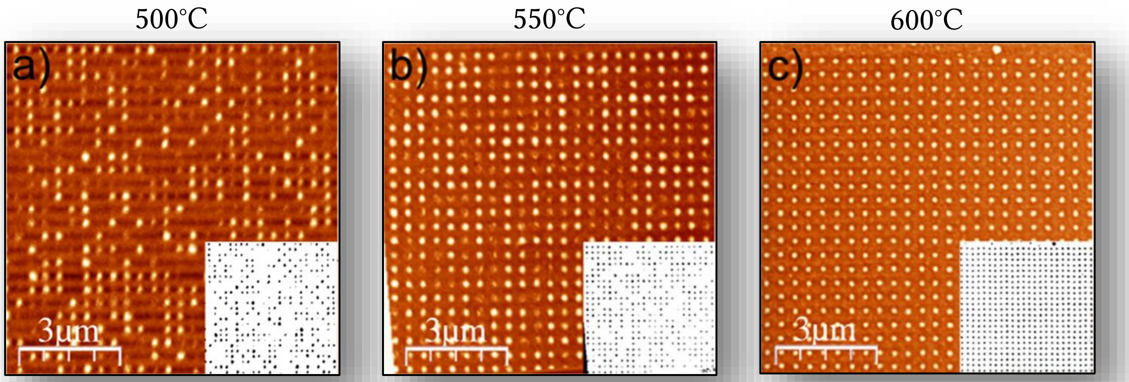

Occupancy < 30 % 50 % 100 %

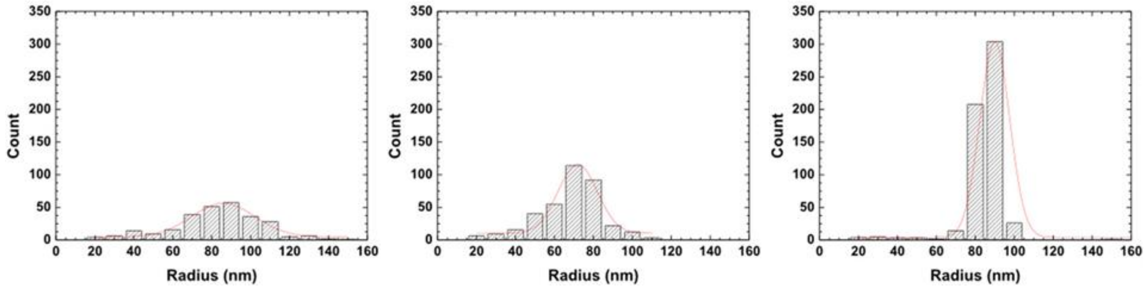

Au – Si interdiffusion induced in FIB patterns ⇒ droplets formation

Au diffusion promoted by the temperature

Ion-beam lithography: gold dewetting

FIB patterning: pitch limit

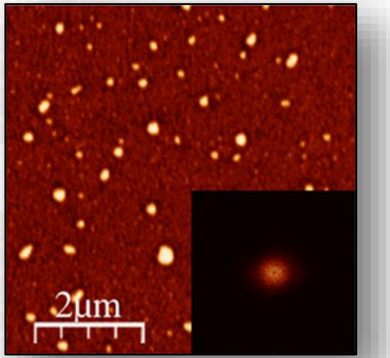
Unpattern

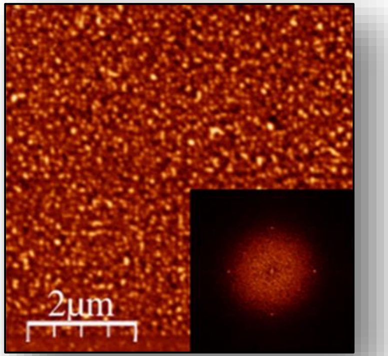
Pitch = 100 nm

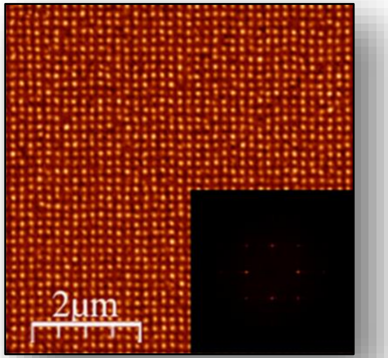
Pitch = 250 nm

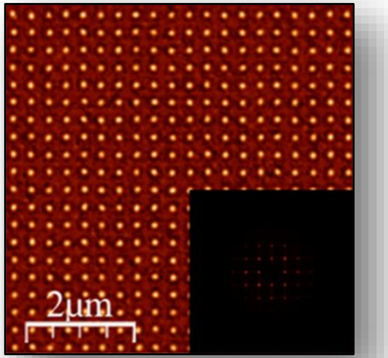
Pitch = 500 nm

Superimposition of the patterned areas:
extended tail of the ion beam

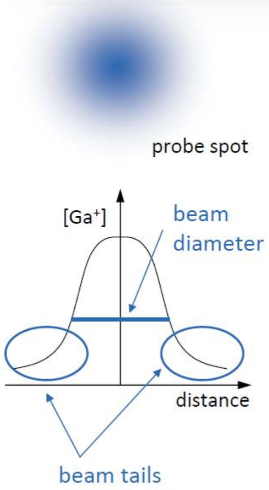

Optimizing FIB pattern

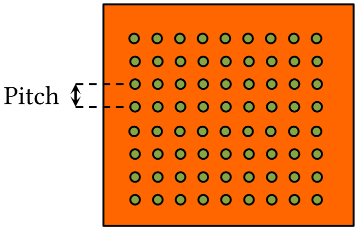

Ion-beam lithography: Au dots

Au patterning + Ge deposition on Si(100)

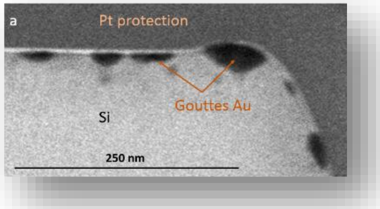

Fabrication process :

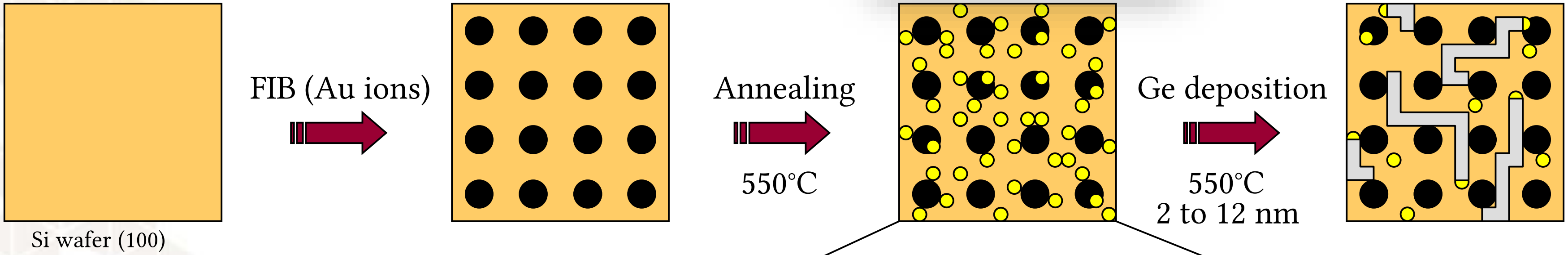

FIB (Au ions)

Annealing
550°C

Ge deposition
550°C
2 to 12 nm

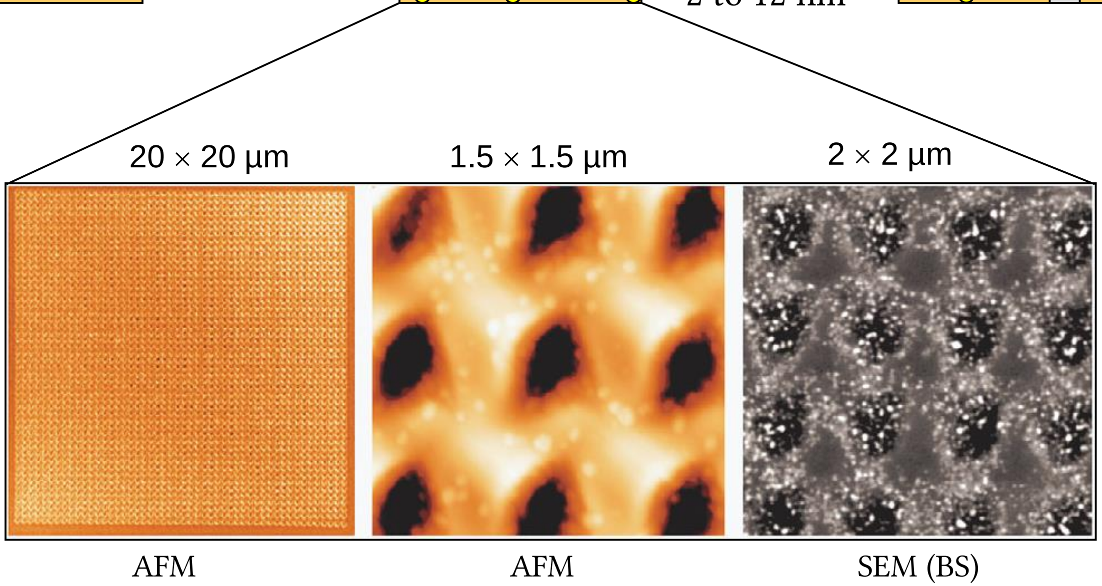

Au lithography + annealing

Formation of Au dots

I. C. Marcus *et al.* Cryst. Growth Des. (2011)

Ion-beam lithography: Au dots

Au patterning + Ge deposition on Si(100)

Unpatterned surface

FIB Patterned surface
⇒ in plane nanowires growth

Bimodal distribution :
- huts
- domes

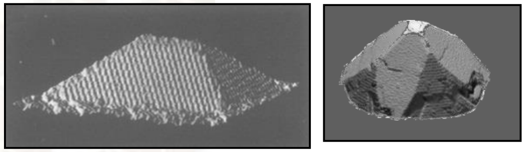

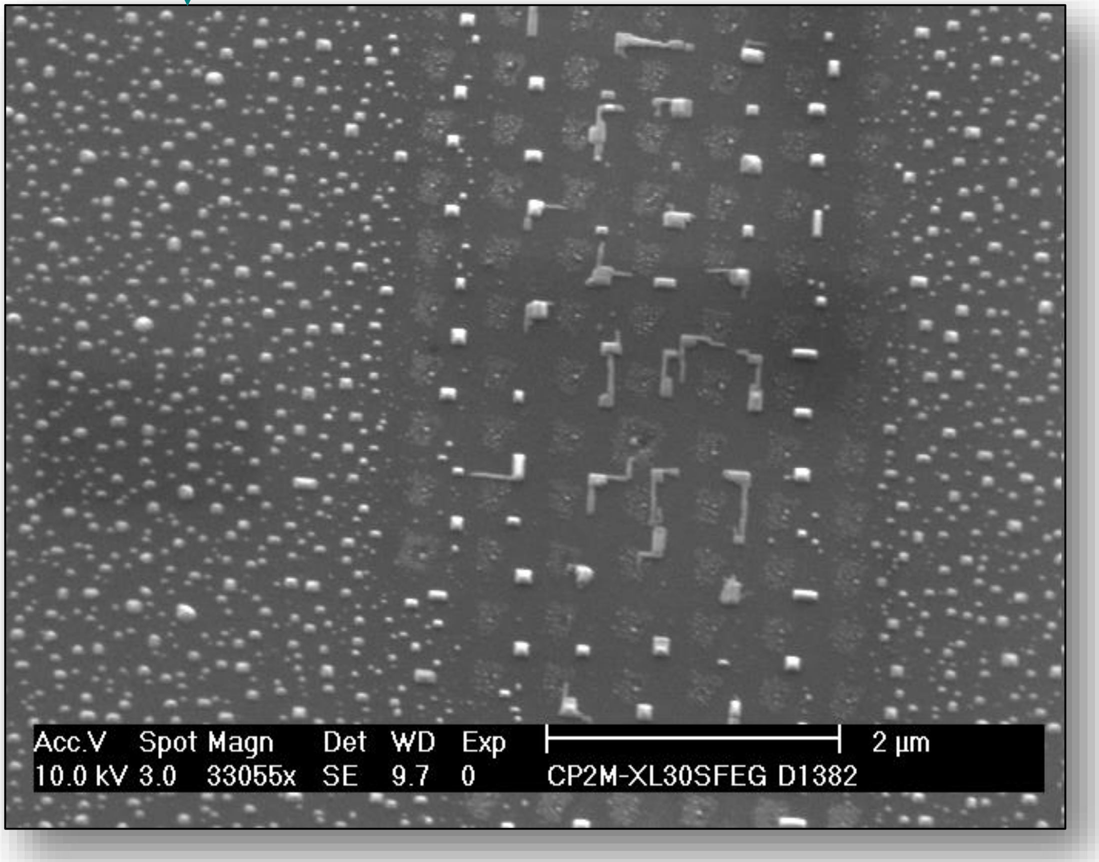

Nanowire growth speed:

$$\nu_s = \alpha_{ls}\left(\mu_l - \mu_s\right)$$

I. C. Marcus *et al.* Cryst. Growth Des. (2011)

Ion-beam lithography: Au dots

Au patterning + Ge deposition on Si(100)

FIB pattern

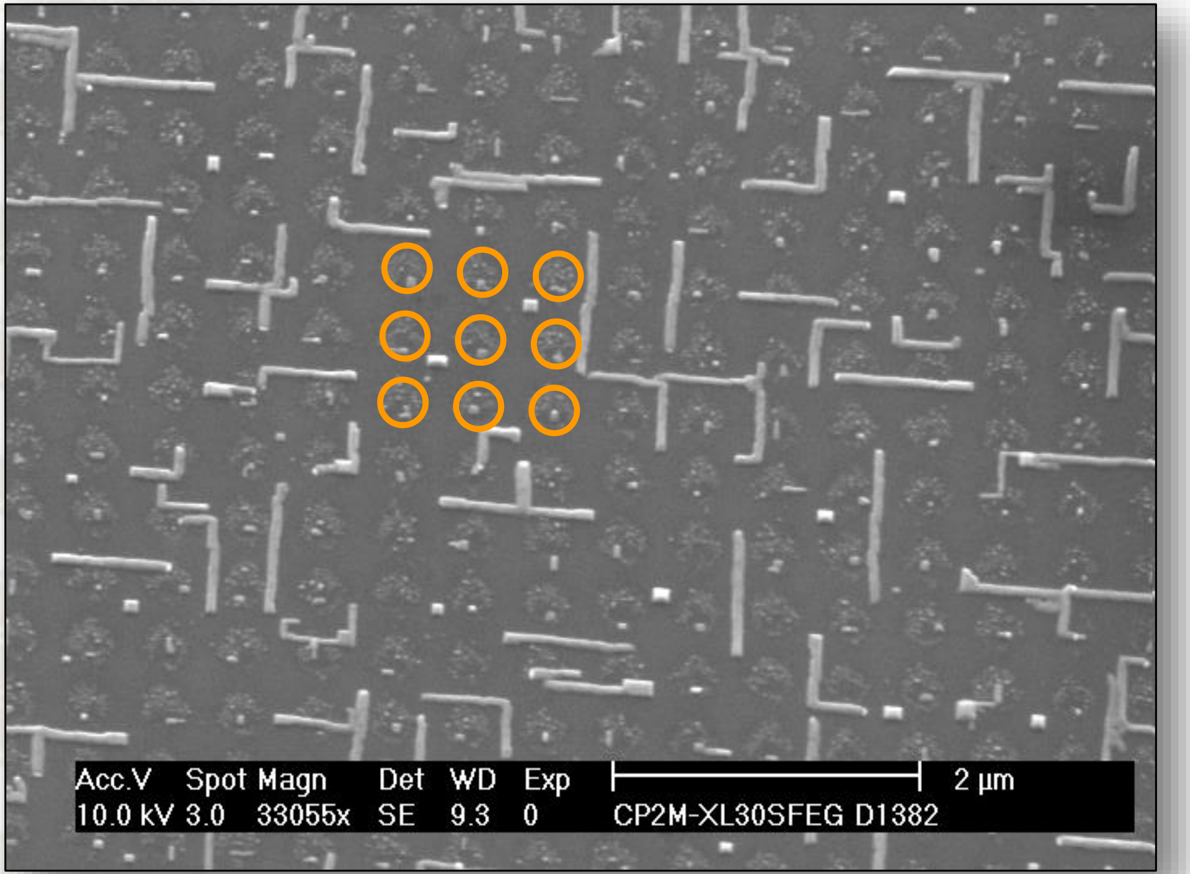

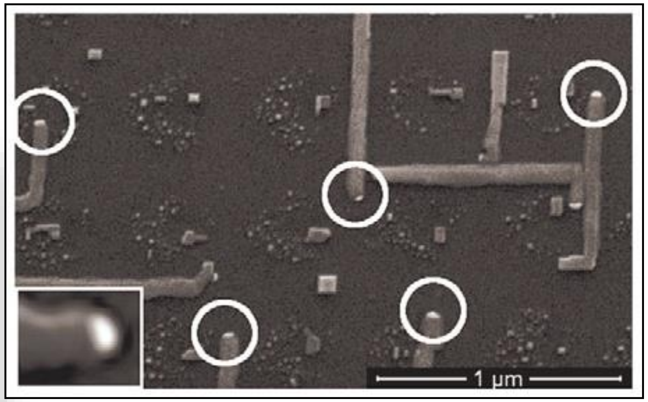

Au catalyst droplets

Ge nanowires :
- Trapezoidal section
- Section square root: 50 nm
- Length: 1000 nm

$\Rightarrow$ aspect ratio = 0.05

I. C. Marcus *et al.* Cryst. Growth Des. (2011)

Ion-beam lithography: Au dots

Au patterning + Ge deposition on Si(100)

Influence of ion dose (a. u.)

1

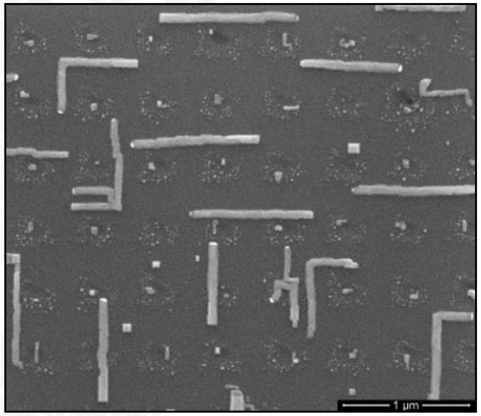

2

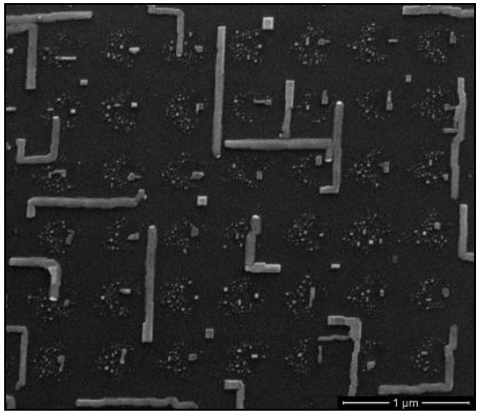

2.5

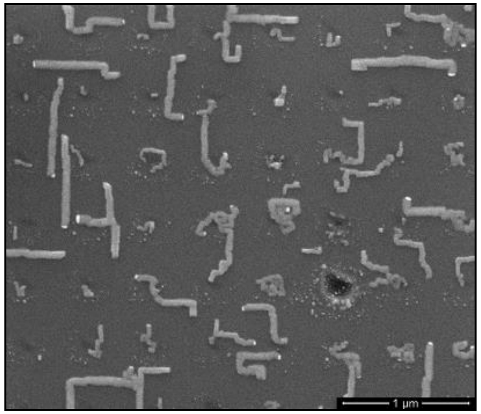

3

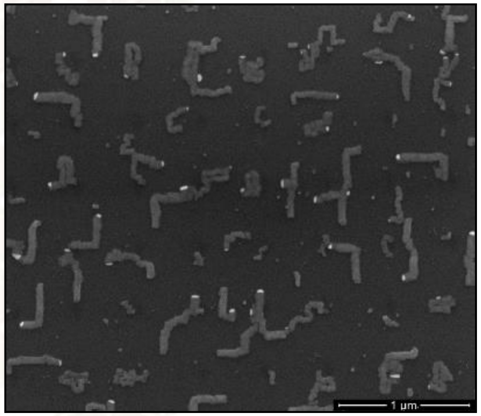

3.5

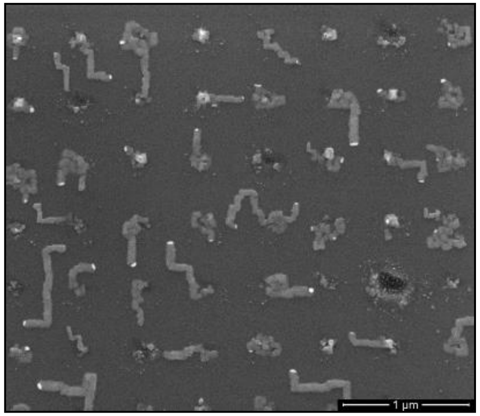

4

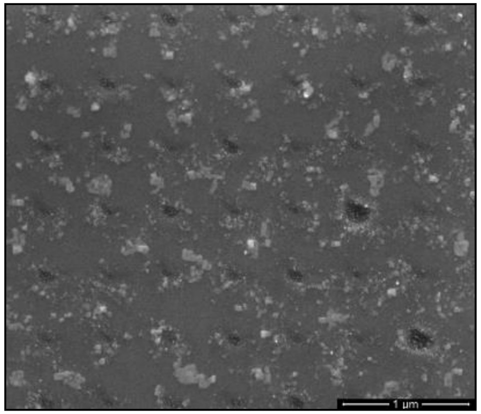

- Growth along <110> directions
- Surface roughness acts as a diffusion barrier: waviness growth, almost hindered for higher doses

I. C. Marcus *et al.* Cryst. Growth Des. (2011)

Ion-beam lithography: Au dots

Organised Ge dots on Si(100) using “FIB single” process

Principle: do a single image using Au ions FIB

Single image of the substrate surface

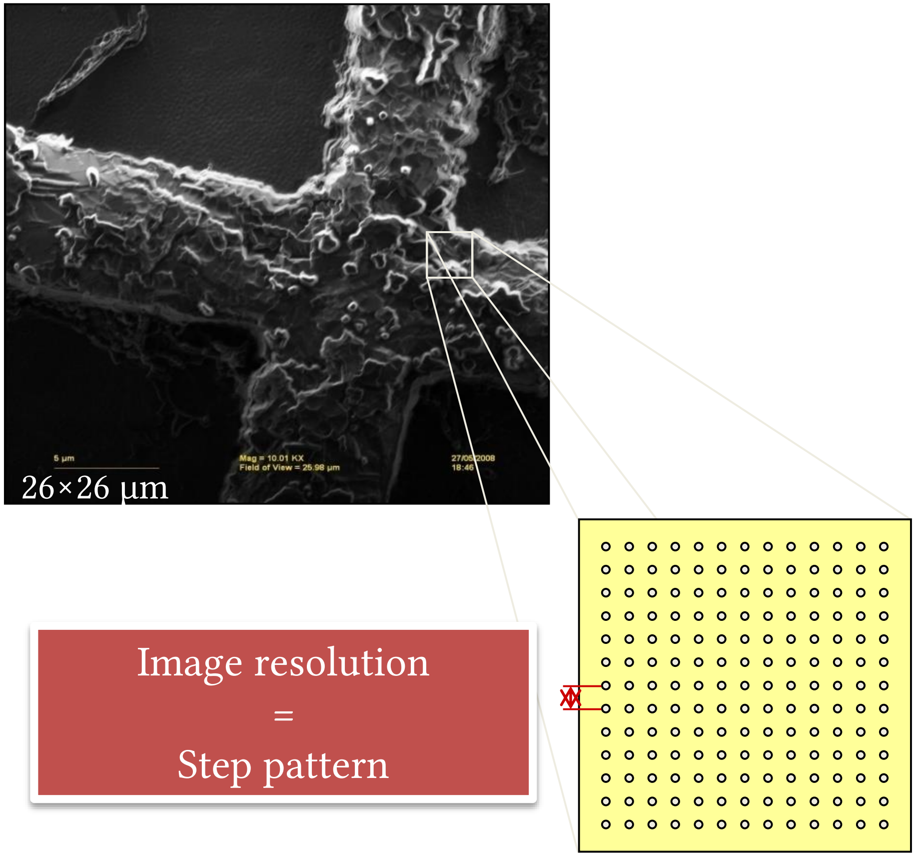

26×26 µm

Image resolution
=
Step pattern

Ion-beam lithography: Au dots

Organised Ge dots on Si(100) using "FIB single" process

Principle: do a single image using Au ions FIB

- Specific parameters: Au deposition
- Dots array: step = Magnification + resolution

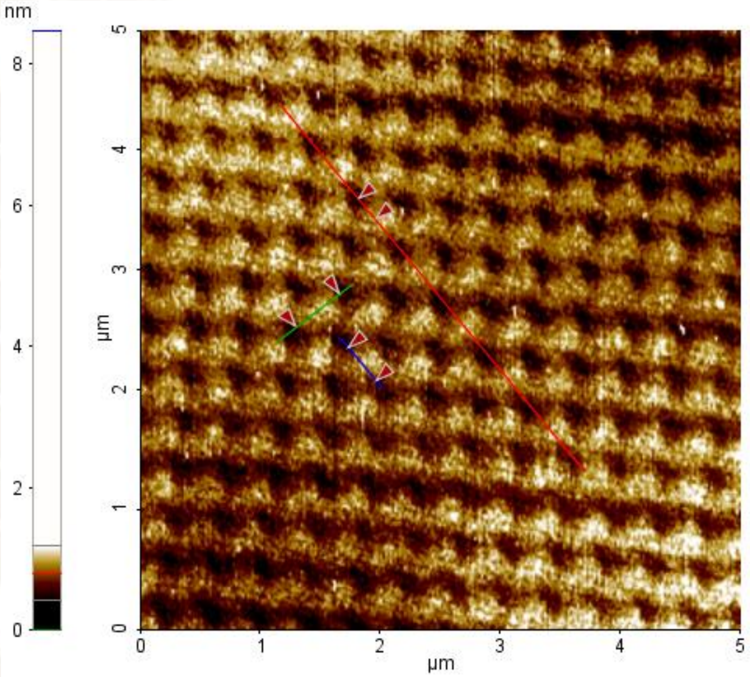

Line Profile: Red

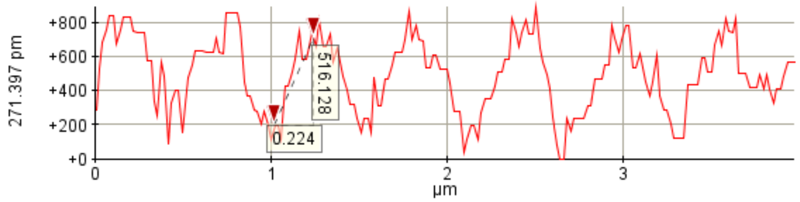

Line Profile: Green

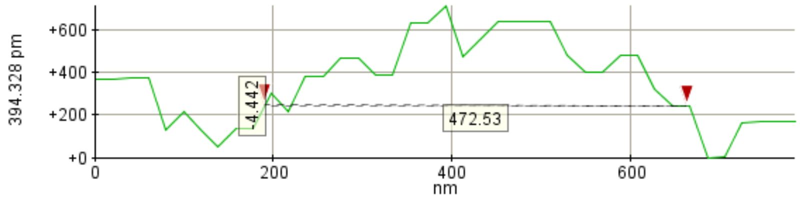

Line Profile: Blue

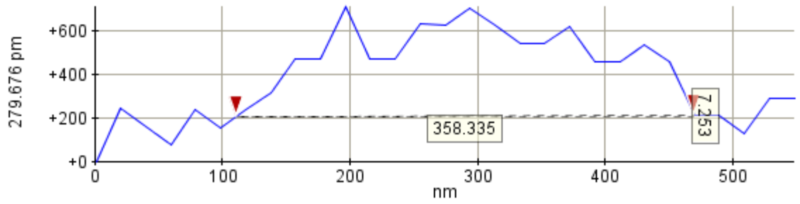

Large structure (≈ 450 nm) and weak height (0.5 nm)

Ion-beam lithography: Au dots

Organised Ge dots on Si(100) using “FIB single” process

Presence of gold on surface during Ge deposition:
- increase number of droplets nucleation centres
- reduce Ge scattering

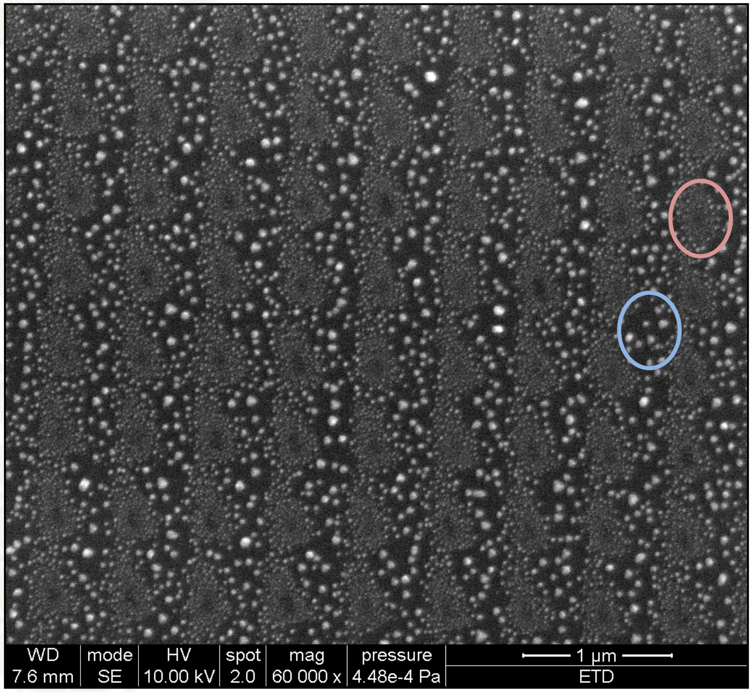

with gold

without gold

FIB step tuned

Step = 500 nm (768 × 768)

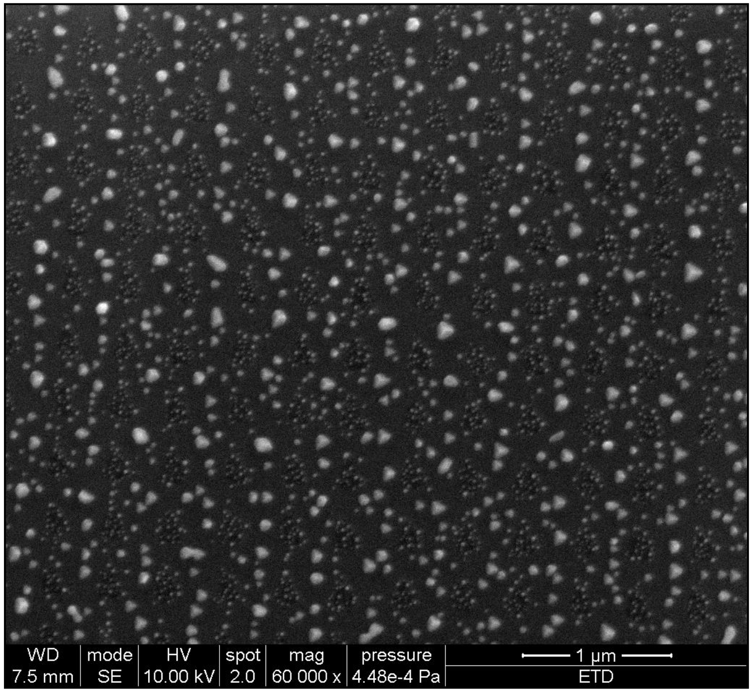

Step = 480 nm (1024 × 1024)

Array of Ge droplets

Ion-beam lithography: Au catalyst

Au dewetting + Si deposition on Si(111)

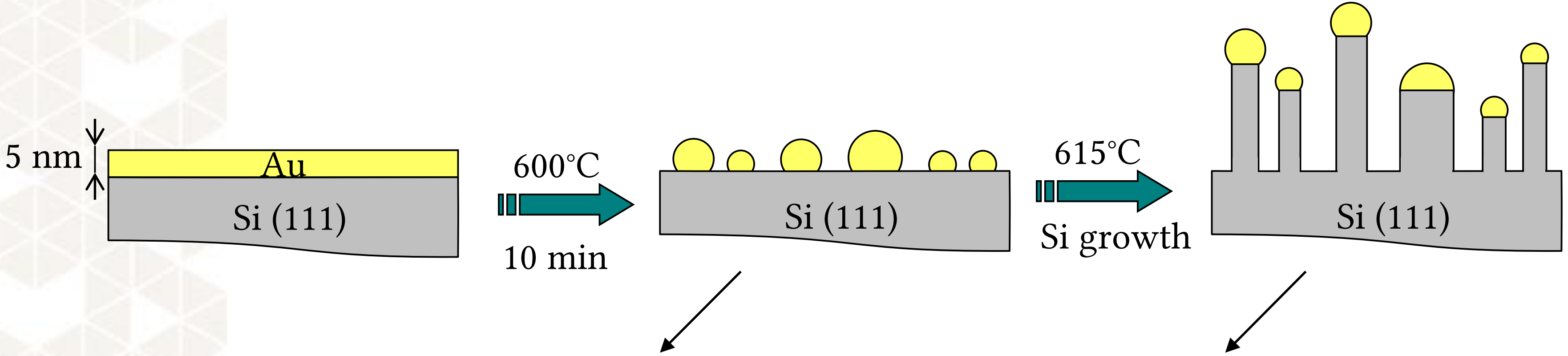

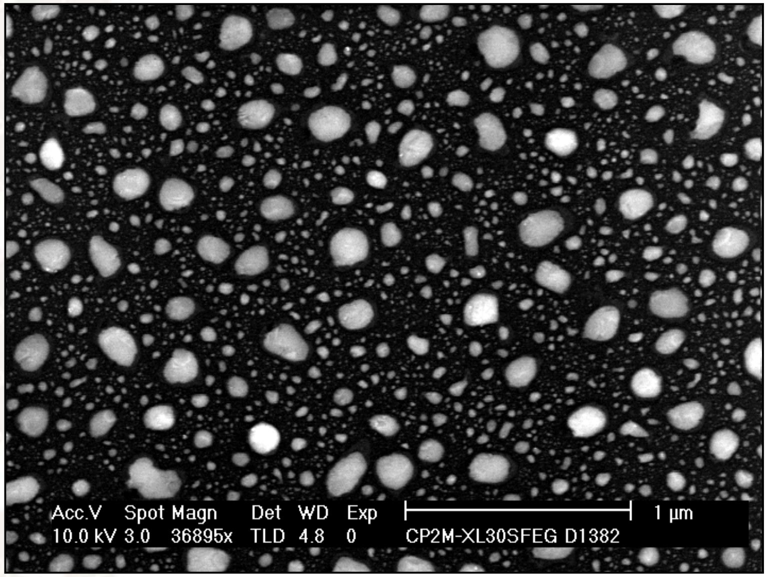

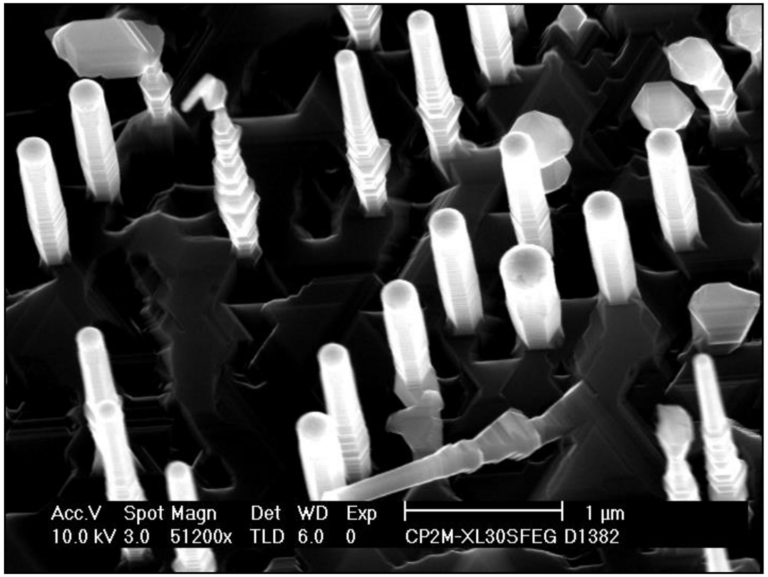

In collaboration with Prof. M. De Crescenzi and his team (University of Roma Tor Vergata, Italy)

Ion-beam lithography: Au catalyst

Au dewetting + Si deposition on Si(111)

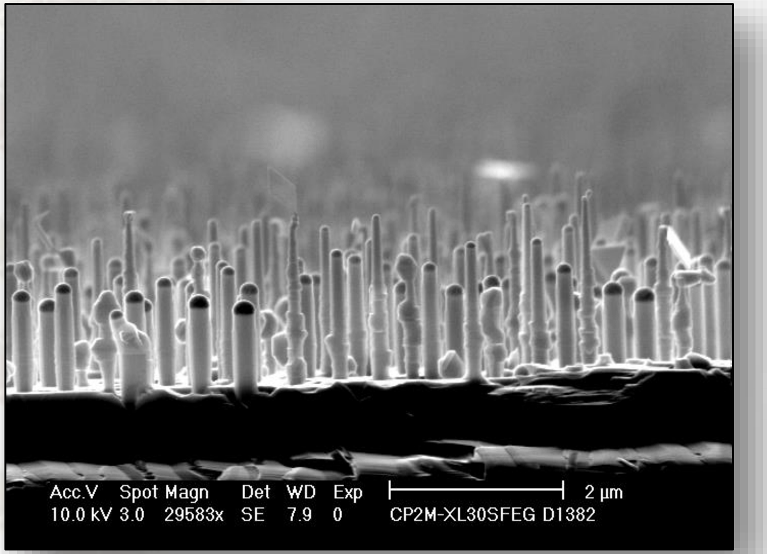

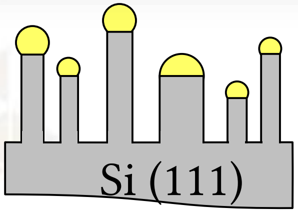

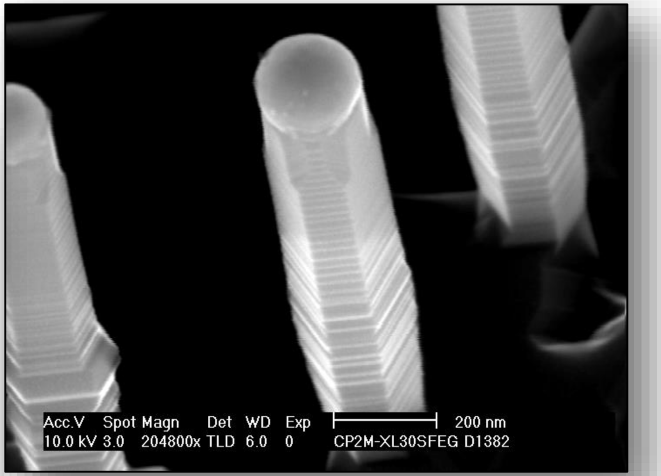

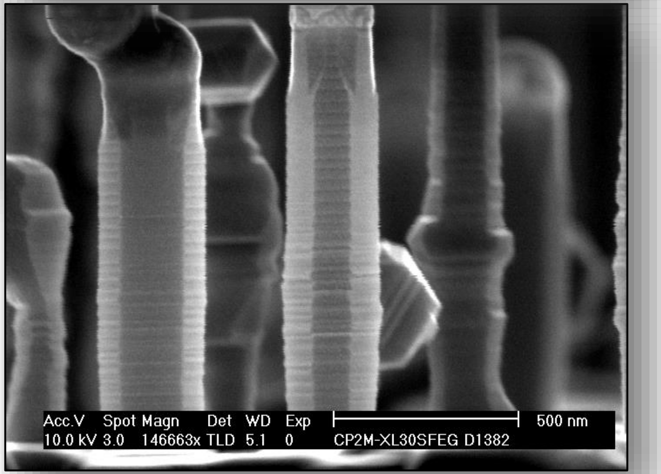

∅ ≈ 200 nm
h ≈ 1500 nm

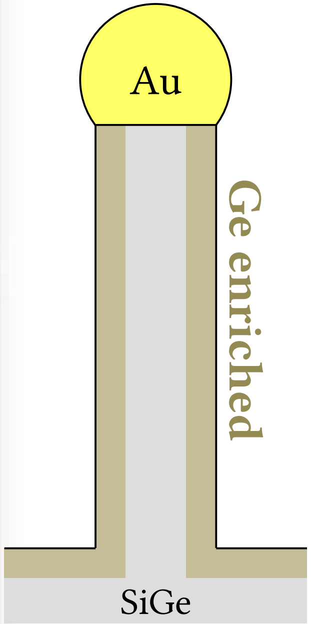

heteroepitaxy

Ion-beam lithography: Au catalyst

Ultimate FIB patterning process

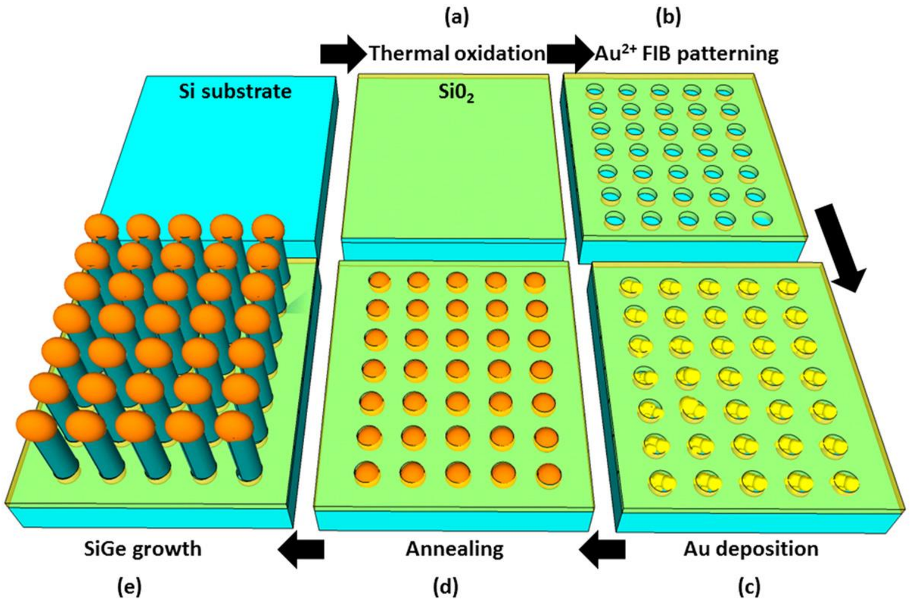

(a) Formation of SiO2 (h_{SiO2} = 5 nm) by RTO

(b) Opening of SiO_2 - free windows by FIB milling

(c) Au deposition by oxydoreduction of gold salts

(d) Phase transition of Au in AuSi clusters by annealing (T_A)

(e) MBE growth of SiGe NWs at T_A

Ion-beam lithography: Au catalyst

Au salts oxidoreduction (galvanic displacement)

$$\mathrm{AuCl_4}^- + 3\,\mathrm{e}^- \longrightarrow \mathrm{Au(s)} + 4\,\mathrm{Cl}^- \qquad \text{with} \quad E^0_{\mathrm{Au^{3+}/Au}} = 0.94\,\mathrm{V}$$

$$\mathrm{Si} + 2\,\mathrm{H_2O} \longrightarrow \mathrm{SiO_2} + 4\,\mathrm{e}^- \qquad \text{with} \quad E^0_{\mathrm{Si^{2+}/Si}} = -0.84\,\mathrm{V}$$

Not selective nor limited

Selective and self limited

Diluted HF

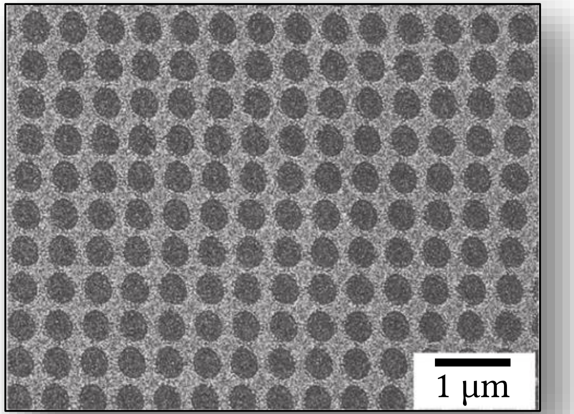

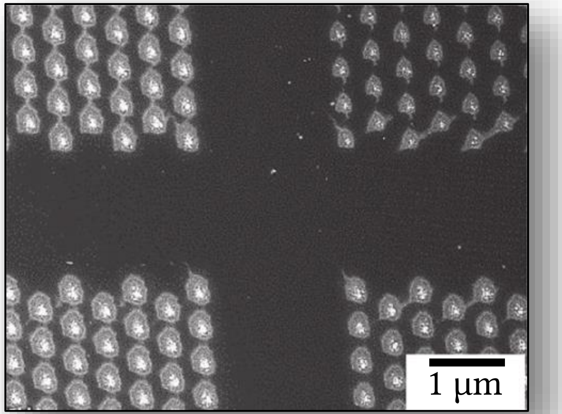

No HF

Au thickness ~5nm

Au clusters diameter
- ≈ 20 nm in pattern
- ≈ 40 nm out of pattern

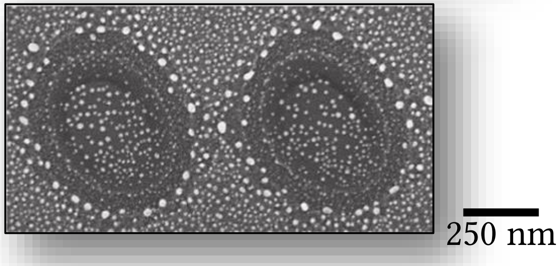

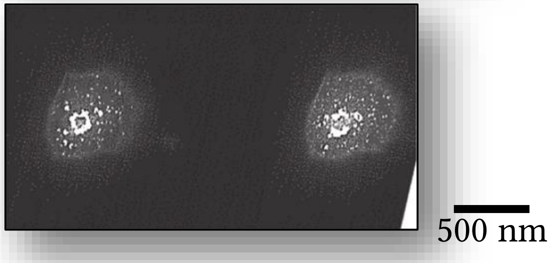

Ion-beam lithography: Au catalyst

Dose influence (pA/cm−2)

2.8×10^{15}

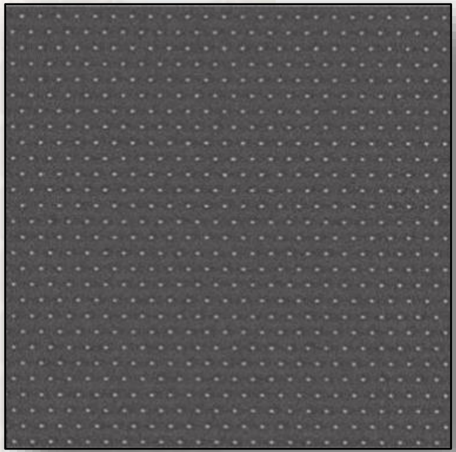

5.5×10^{15}

8.3×10^{15}

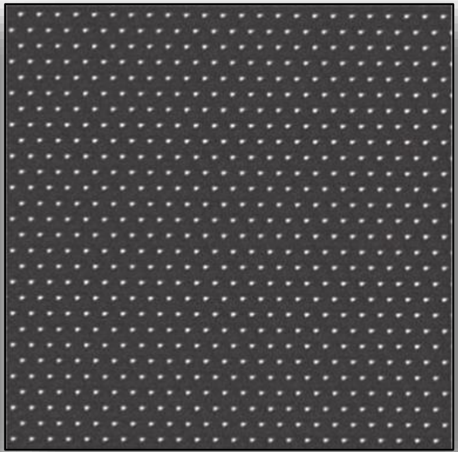

11×10^{15}

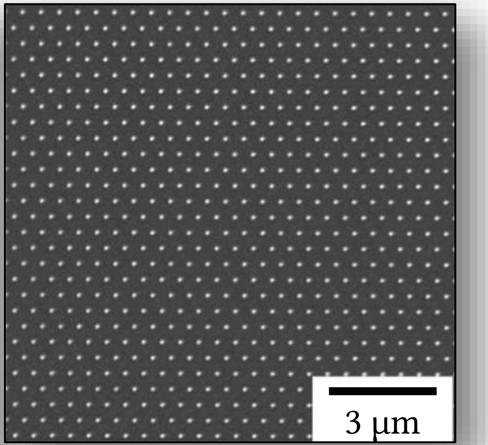

SEM - BSE

SEM - BSE

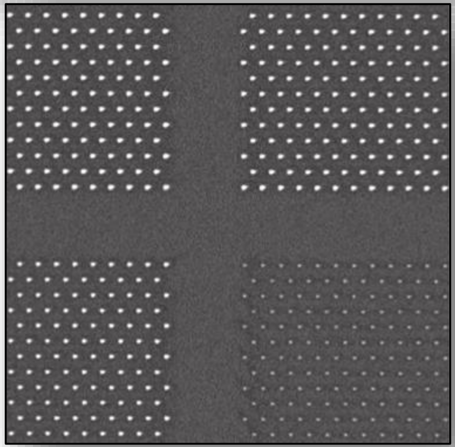

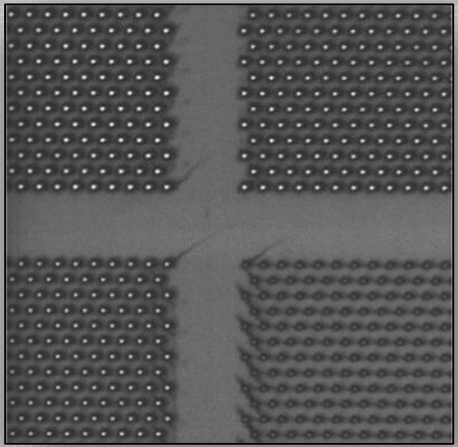

SEM - SE

Ion-beam lithography: Au catalyst

Annealing

T_A = 550 °C

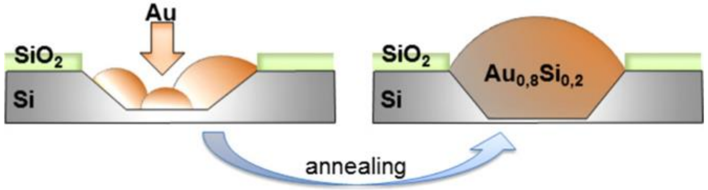

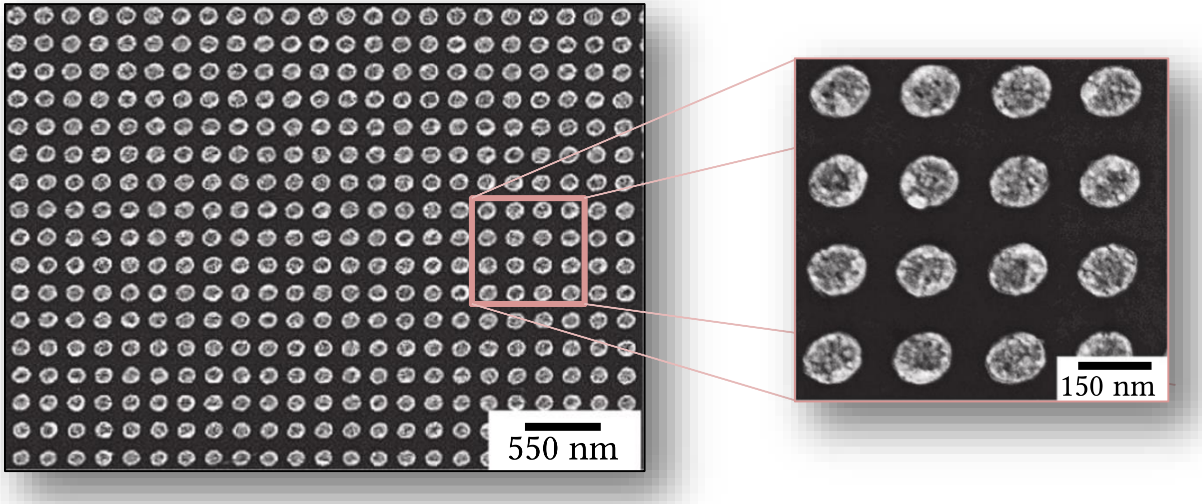

Ion-beam lithography: Au catalyst

MBE growth

$T_{Growth} = 550$ °C

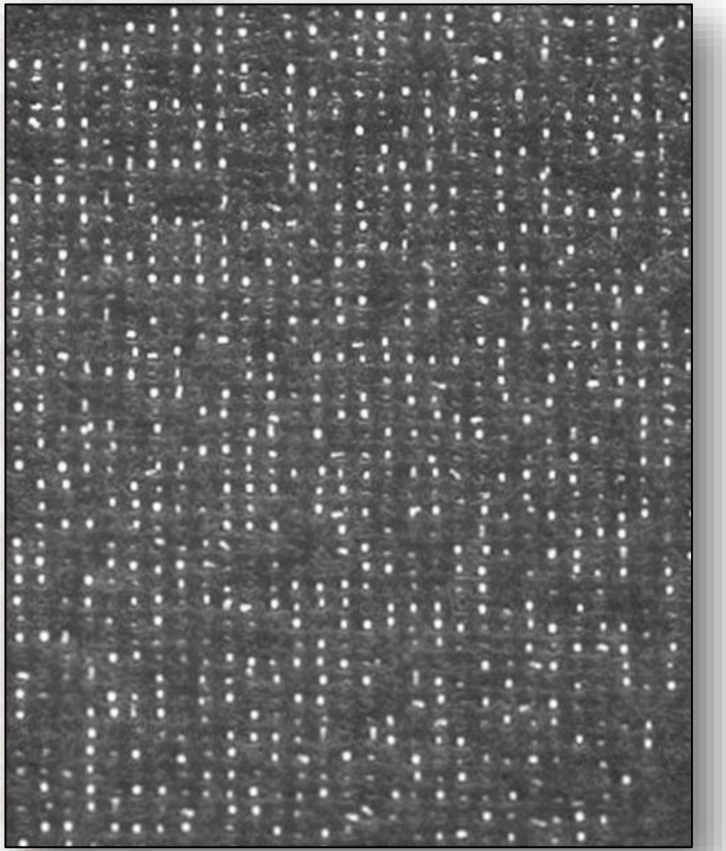

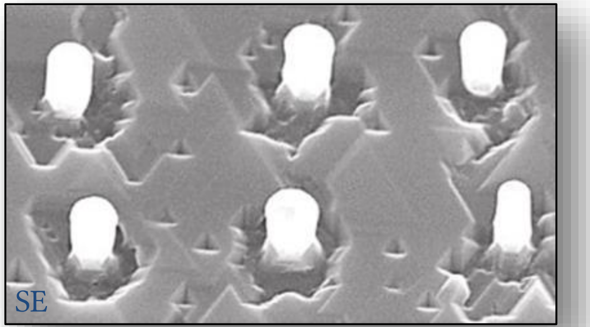

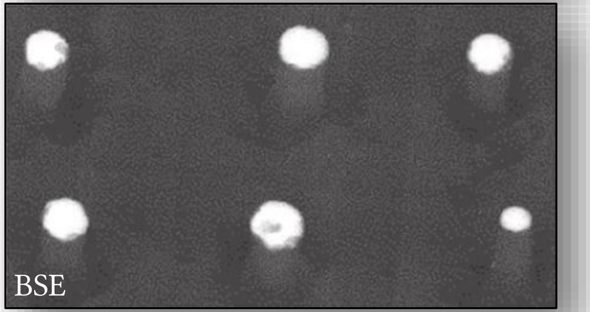

Nanowires height: $h = 200$ nm

Dewetting process organization

Heating ultra-thin films on oxide

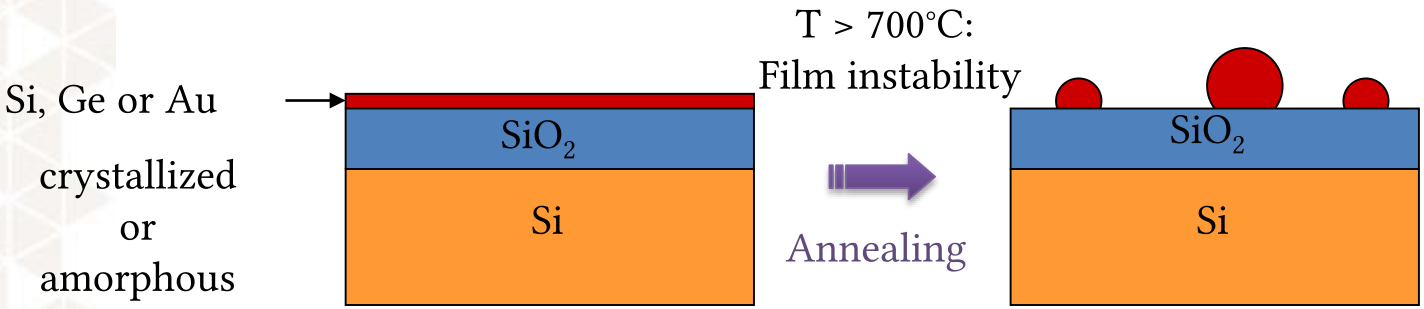

Dewetting process organization

Chemical potential

$$\mu^\beta = \underbrace{\mu^\beta_\mathrm{m}(T)}_{\text{Original }\beta\text{ phase chemical potential}} + \underbrace{\frac{1}{2}C^\beta\varepsilon^2}_{\text{Elastic strain energy density}} - \underbrace{\sigma_\mathrm{n}\Omega^\beta}_{\text{Work (pV)}} + \underbrace{\left[\left(\gamma^{\alpha\beta} + \frac{\mathrm{d}^2\gamma^{\alpha\beta}}{\mathrm{d}\theta_1^2}\right)\frac{1}{R_1} + \left(\gamma^{\alpha\beta} + \frac{\mathrm{d}^2\gamma^{\alpha\beta}}{\mathrm{d}\theta_2^2}\right)\frac{1}{R_2}\right]\Omega^\beta}_{\text{Surface energy (including anisotropy)}}$$

Original β phase chemical potential

Work (pV)

Surface energy (including anisotropy)

- Ω: atomic volume (or molecular)
- R_i: main radius of curvature
- θ_i: surface orientation

Elastic strain energy density

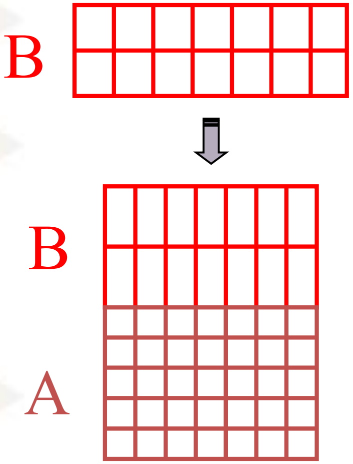

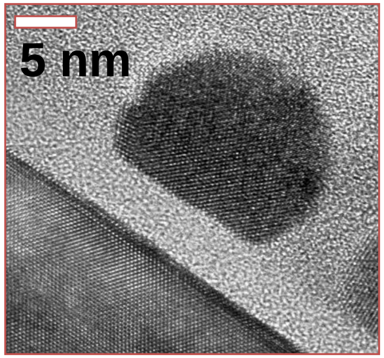

+ Scattering Barriers

Surface defects, steps, …

Growth and self-organisation of SiGe nanostructures
J.N. Aqua, I. Berbezier, L. Favre, T. Frisch, A. Ronda, Phys. Rep. (2013)

Dewetting process organization

Dewetting process as a function of temperature (SOI)

SOI 11 nm T = 750°C

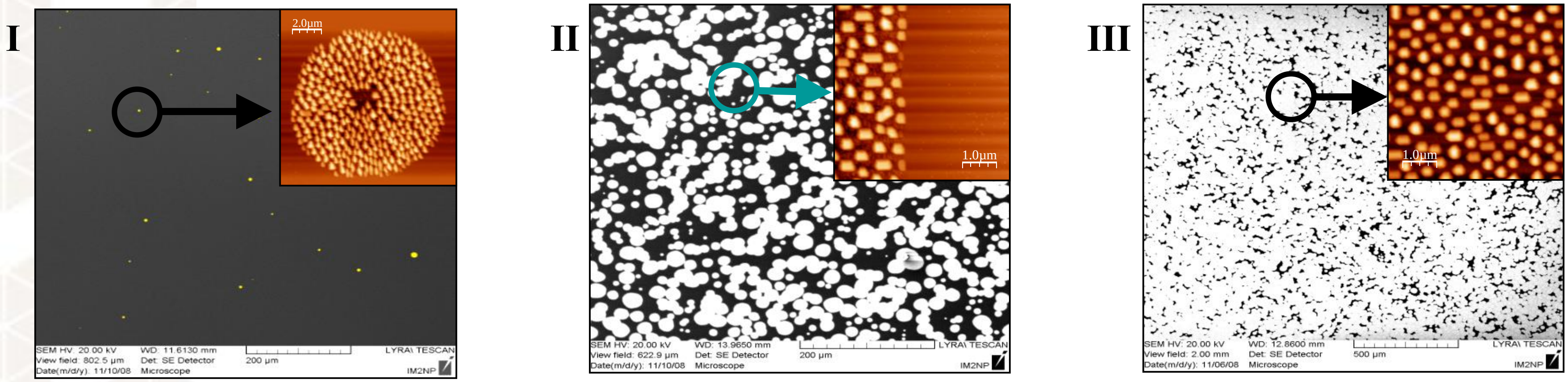

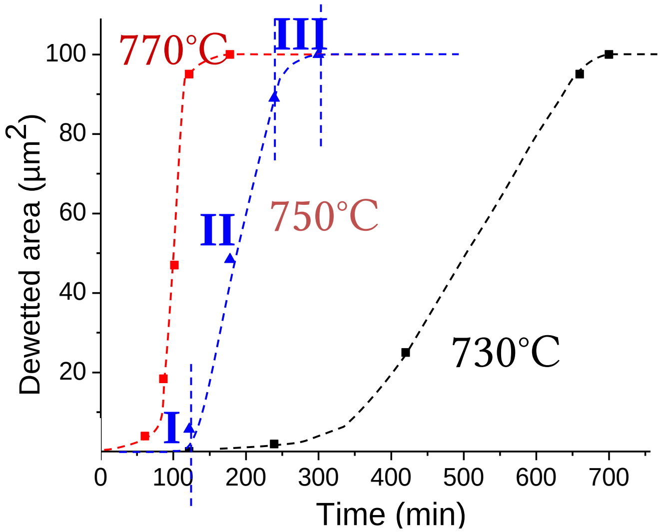

(I) Holes nucleation

(II) Film retraction and holes nucleation

(III) Dewetted areas coalescence

M. Aouassa, L. Favre, A. Ronda, H. Maaref and I. Berbezier, *New J. Phys.*, **14**, 063038 (2012)

Dewetting process organization

Heating ultra-thin films on oxide

Nucleation rate

$$\tau = \tau_0 \exp\left(-\frac{E_h}{k_\mathrm{B}T}\right)$$

G_H : hole nucleation barrier

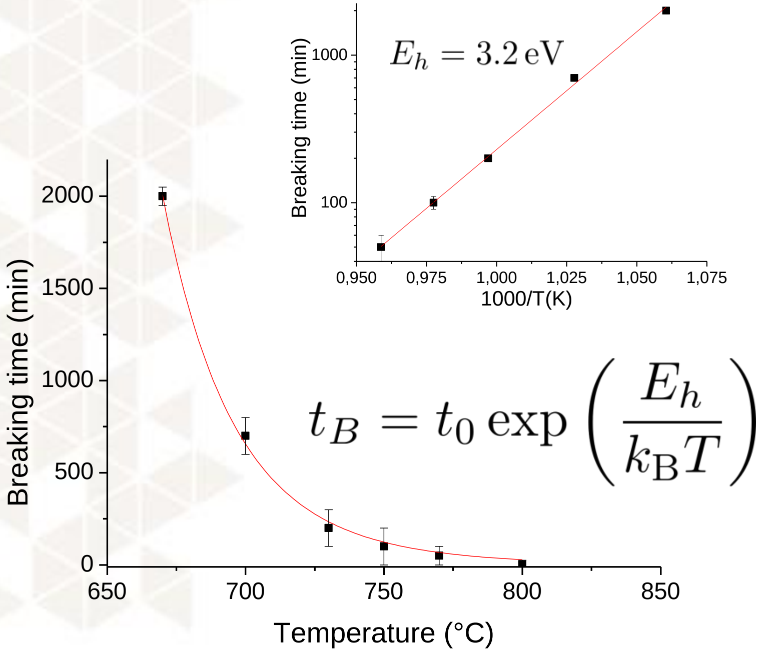

$$E_h = 3.2\,\mathrm{eV}$$

$$t_B = t_0 \exp\left(\frac{E_h}{k_\mathrm{B}T}\right)$$

Dewetted front of pa-Si

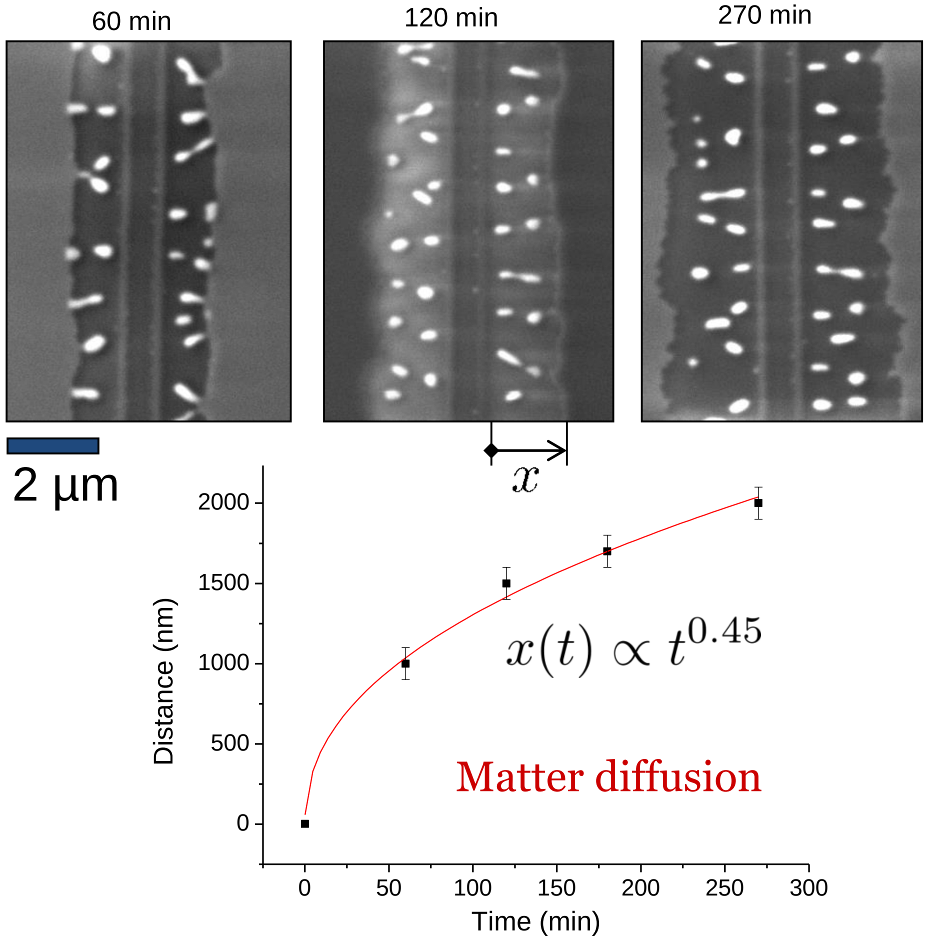

$$x(t) \propto t^{0.45}$$

Matter diffusion

Dewetting process organization

Dewetting process as a function of film thickness and temperature (SOI)

Motion of the dewetted front as a function of the nominal thickness

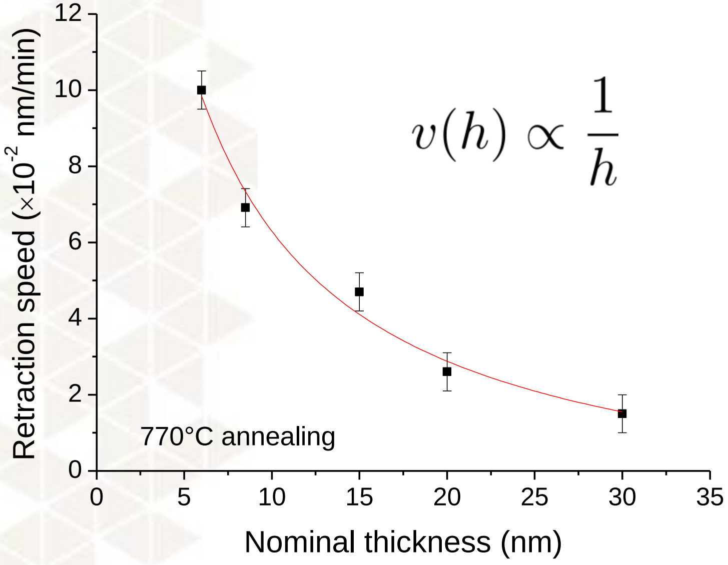

- Matter conservation law
- Consistent with a diffusion limited dewetting mechanism

Dewetting speed as a function of the temperature for c-Si and am-Si

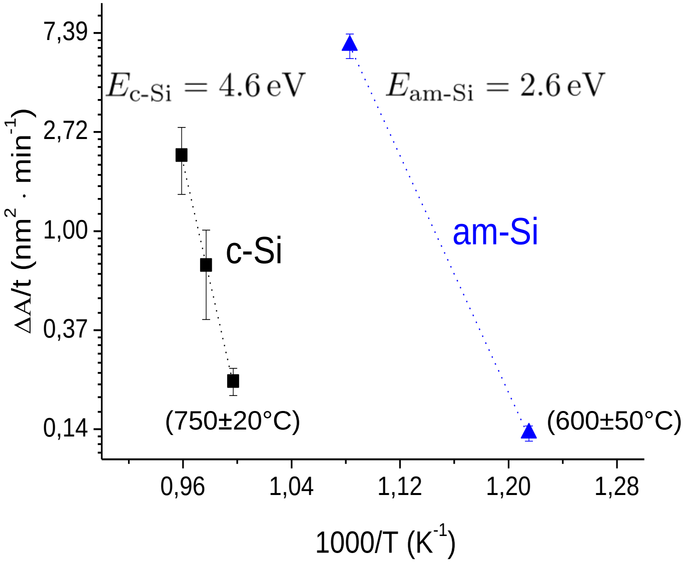

- am-Si films dewet almost instantly: no breaking time
- Activation energy is much smaller for am-Si
- Dewetting speed of am-Si is higher c-Si by two orders of magnitude (at 730°C)

Dewetting process organization

Dewetting process as a function of time (SOI)

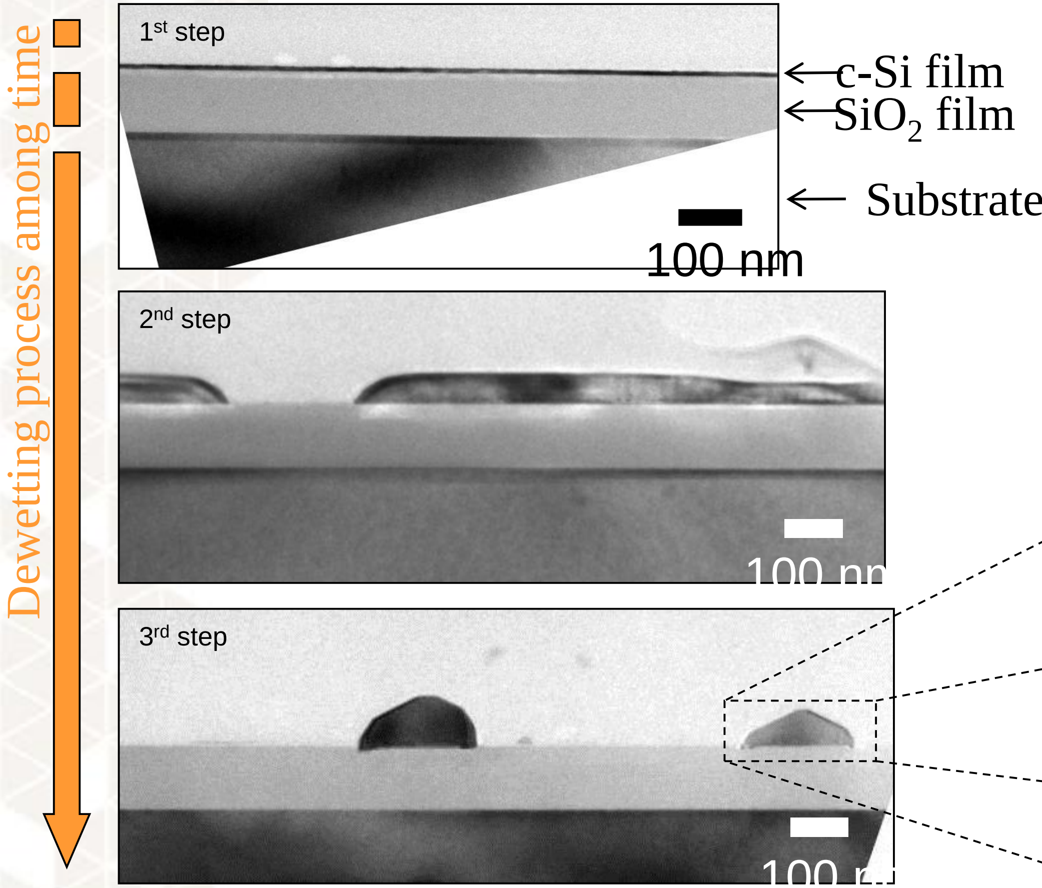

- 3rd step: coalescence

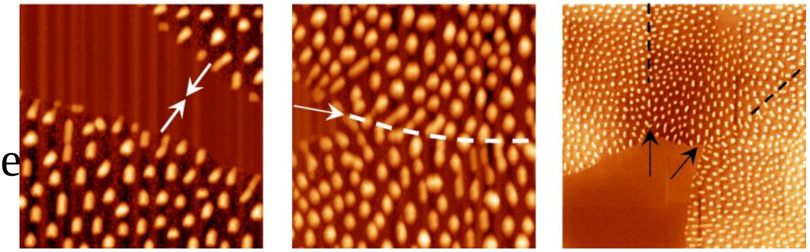

- dots merging
- reorientation

- facetted dots

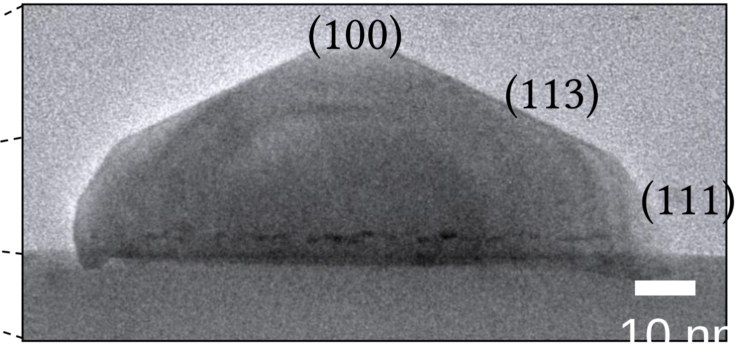

Dewetting process organization

Dewetting process as a function of time (SOI)

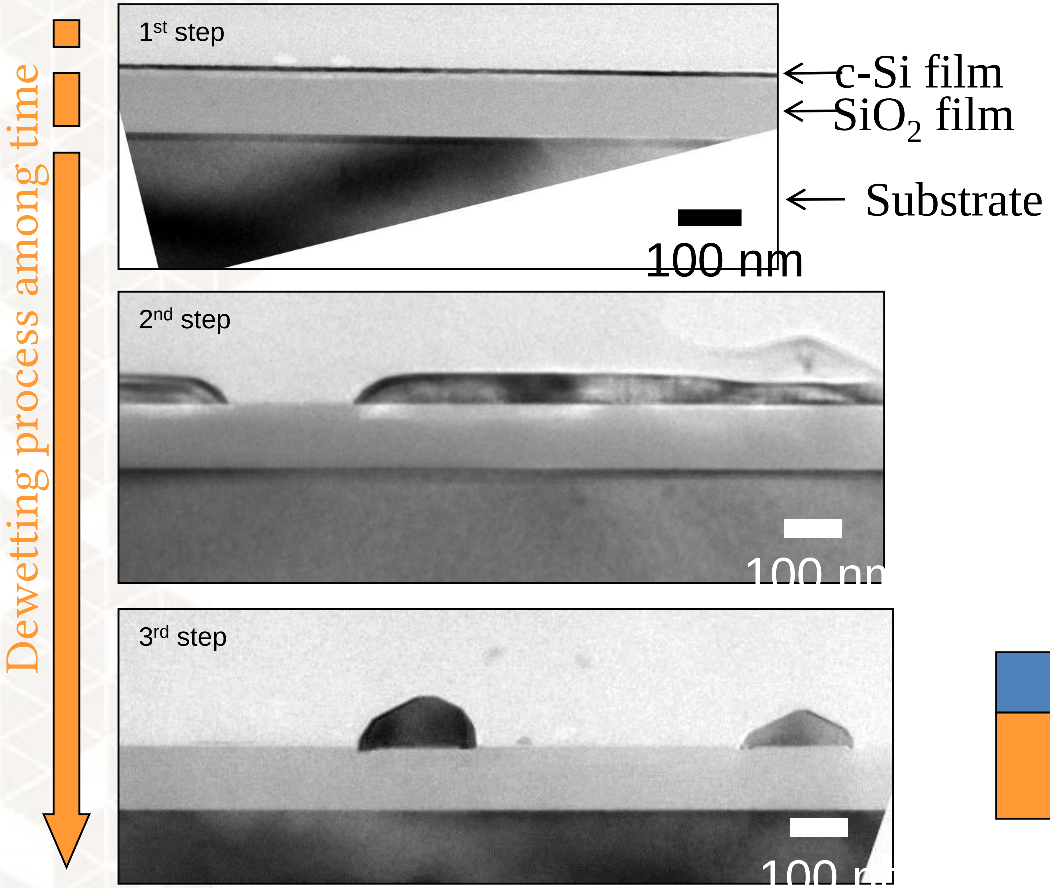

- 2nd step: film retraction
  - flat film
  - thickening on large scale
  - no rim (Mullins model)

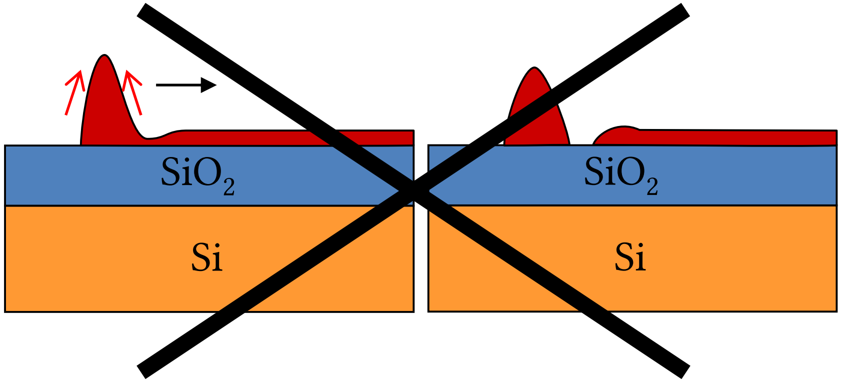

Dewetting process organization

Annealing of SOI layer (11 nm thick)

750°C

Holes nucleation:

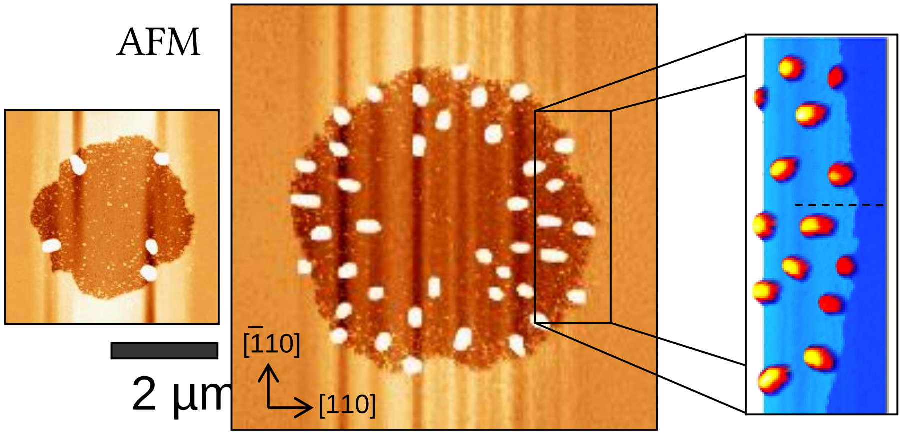

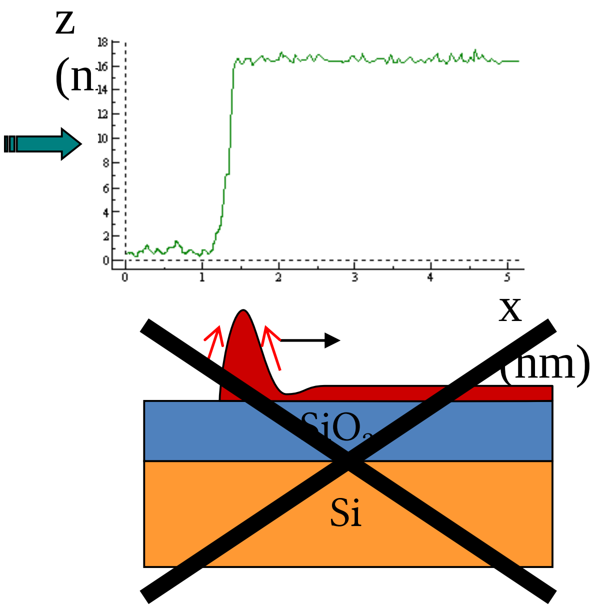

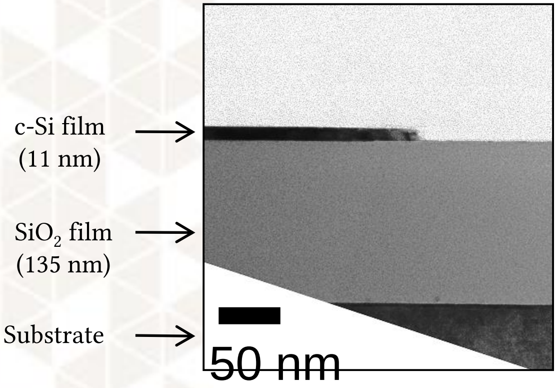

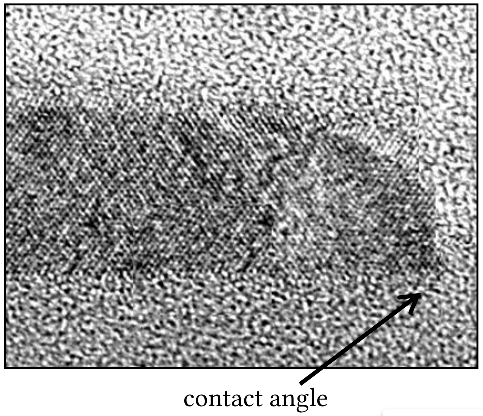

- No rim
- No edge faceting
- Matter diffusion:

$$x(t) \propto t^{0.45} \approx t^{0.5}$$

Front propagation by surface diffusion

Dewetting process organization

Dewetting process as a function of layer thickness (SOI)

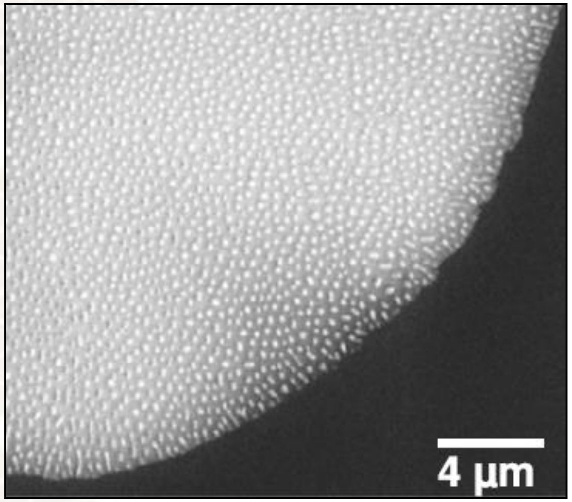

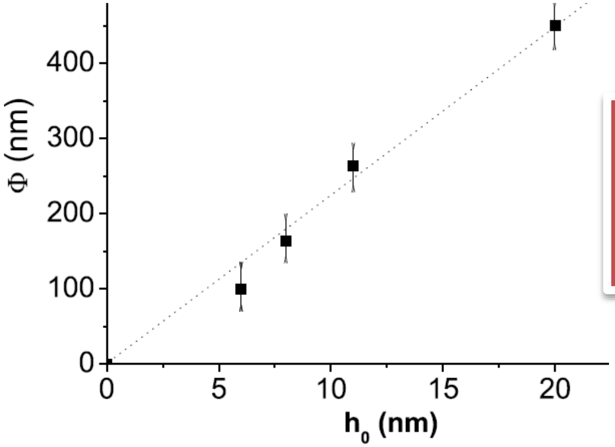

Dots diameter is almost a linear function of initial Si layer thickness h_0

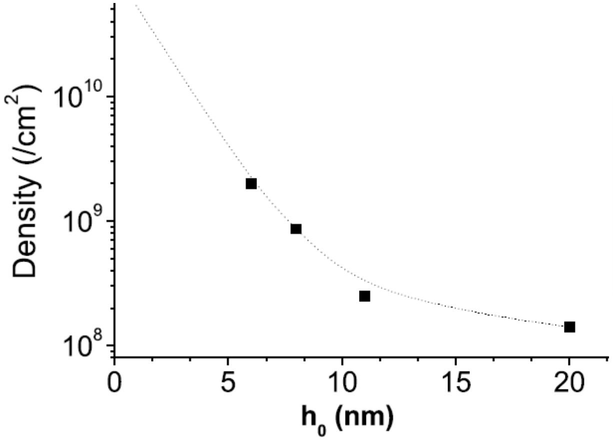

Dots density and dots diameter cannot be varied separately

Dewetting process organization

Dewetting process as a function of layer thickness (am-GeOI)

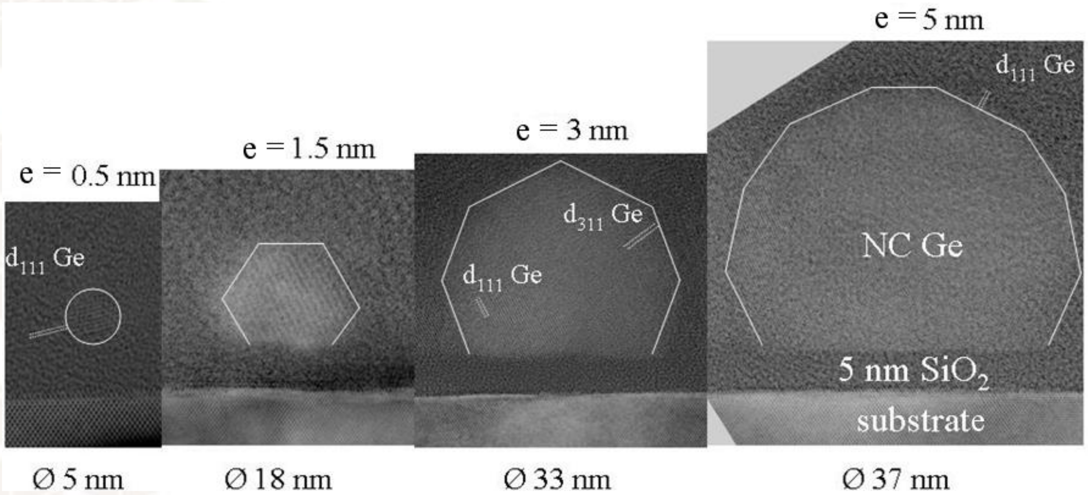

Dots diameter is a function of Ge initial layer thickness

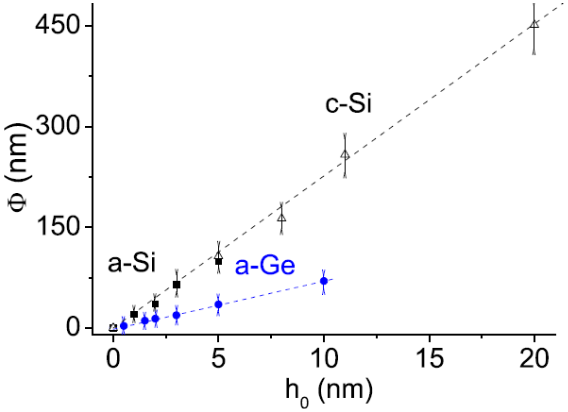

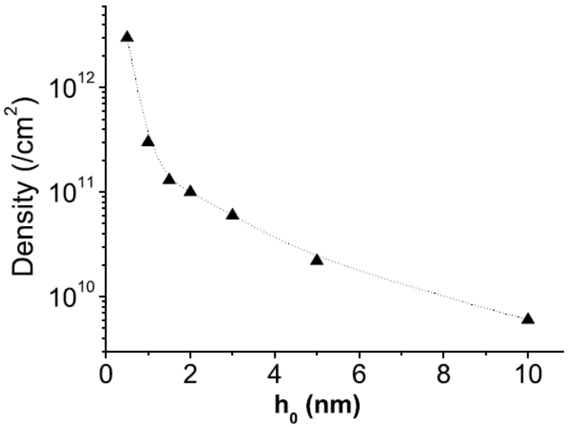

I. Berbezier, M. Aouassa, A. Ronda, L. Favre, M. Bollani, R. Sordan and A. Delobbe, *J. Appl. Phys.*, **113**, 064908 (2013)

M. Aouassa, I. Berbezier, L. Favre, A. Ronda, M. Bollani, R. Sordan, A. Delobbe, and P. Sudraud, *Appl. Phys.Lett.*, **101**, 013117 (2012)

Dewetting process organization

Lithography + Annealing

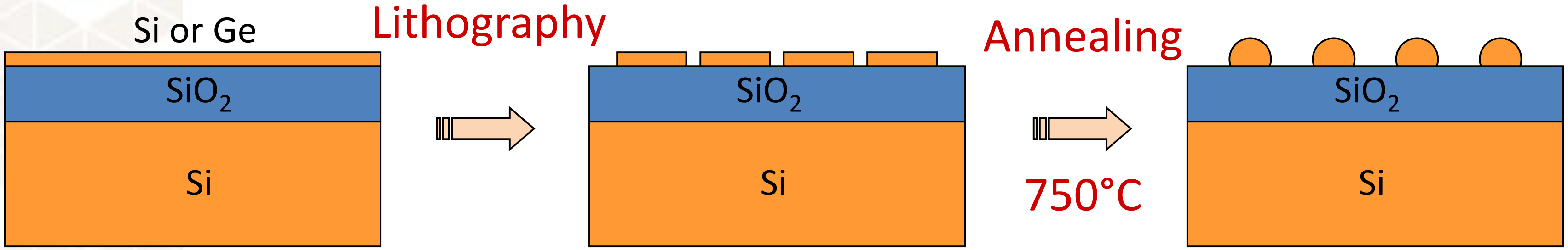

Crystalline or amorphous thin layer

Without lithography

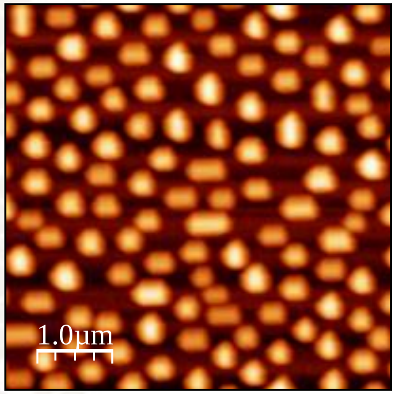

With lithography

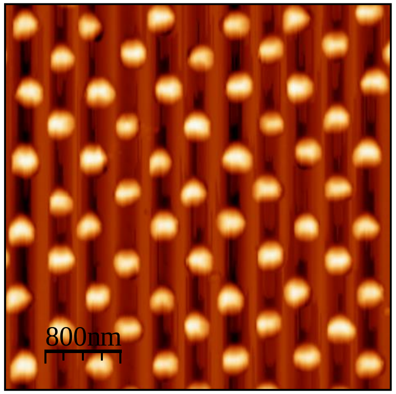

- Organization
- Narrow size distribution
- Dots shape

Dewetting process organization

Lithography + Annealing (c-Si)

Patterns geometry influence

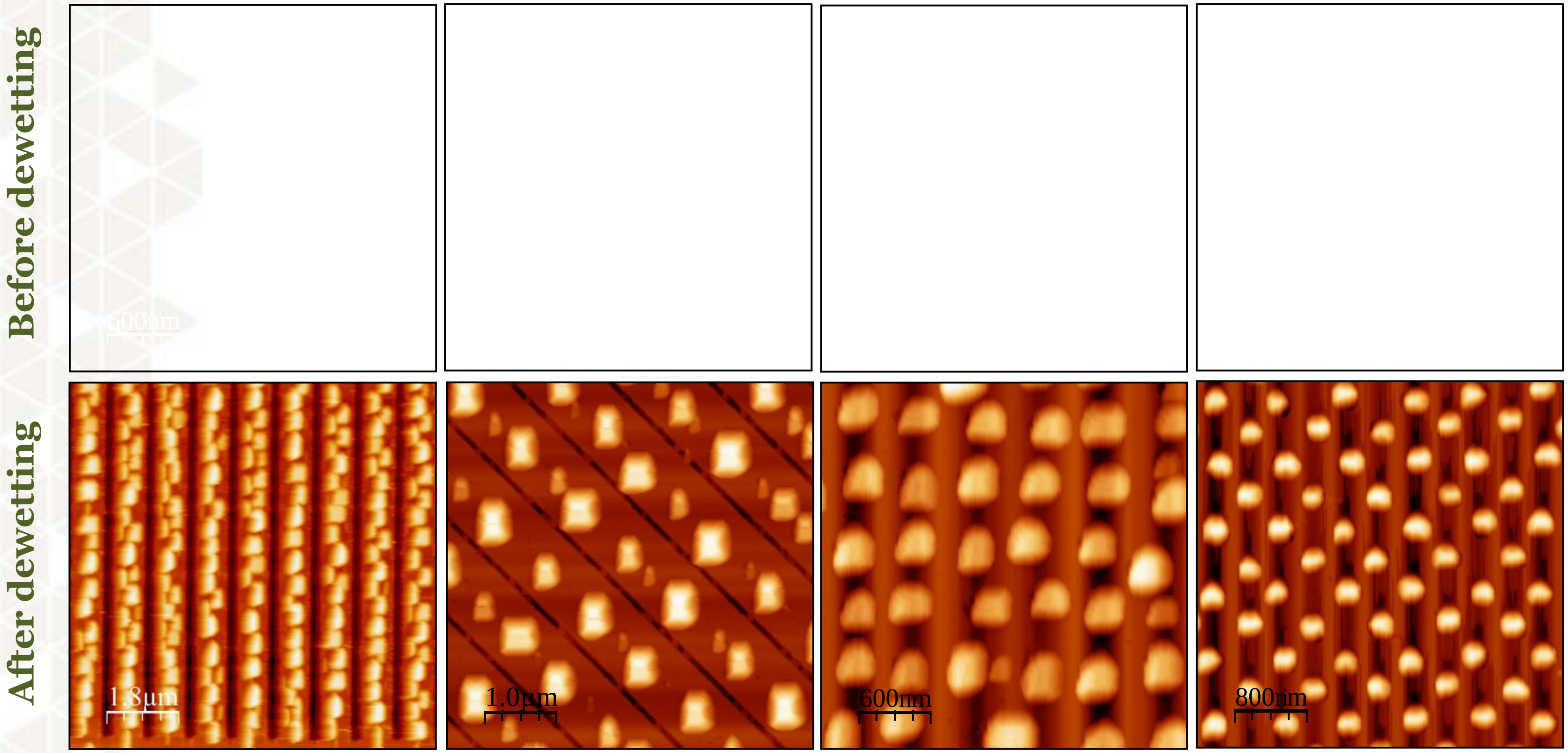

Dewetting process organization

Annealing of SOI layer (c-Si)

Morphology evolution

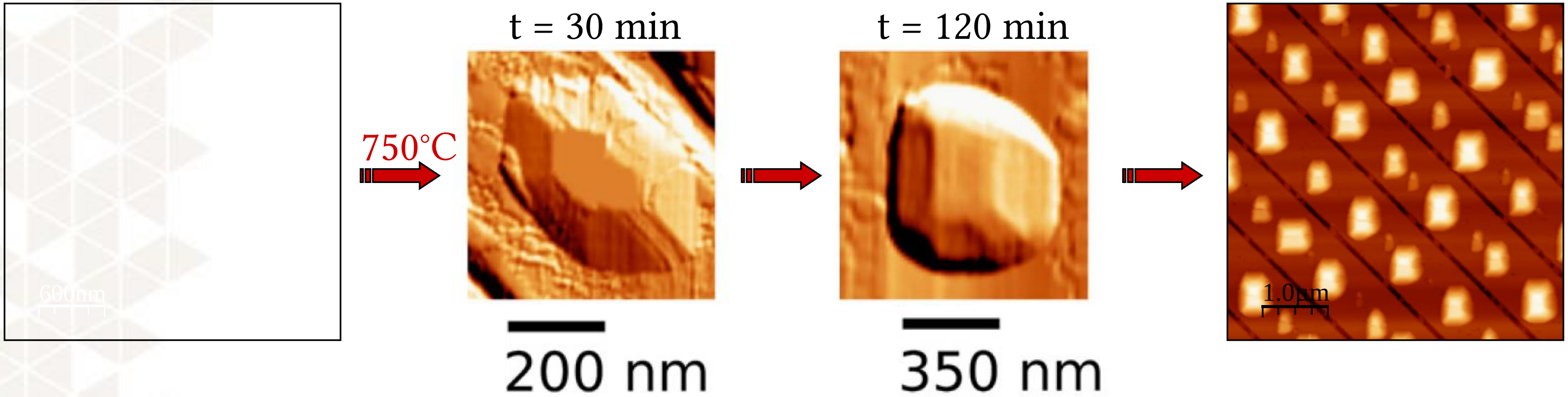

Dewetting process organization

Amorphous Ge layer annealed on SiO2 substrate : organized droplets

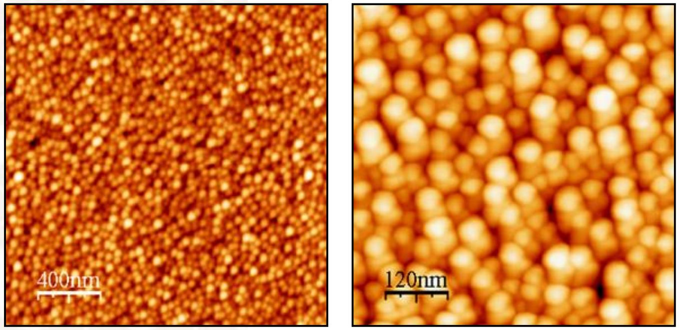

Planar SiO_2 Substrate

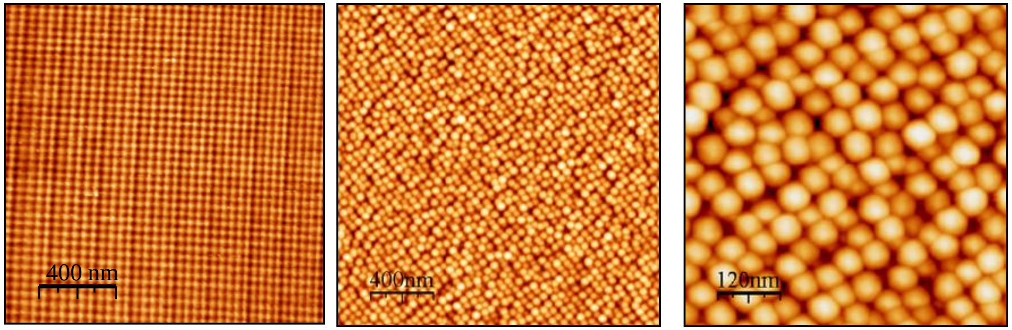

before deposition

Ga ions patterned SiO_2 Substrate

TEM cross section

Application:
floating gate memories

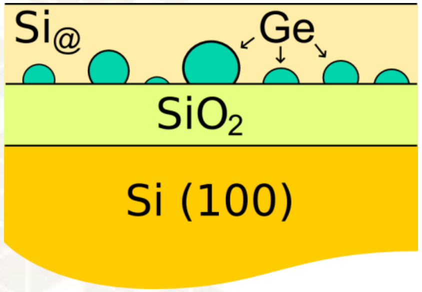

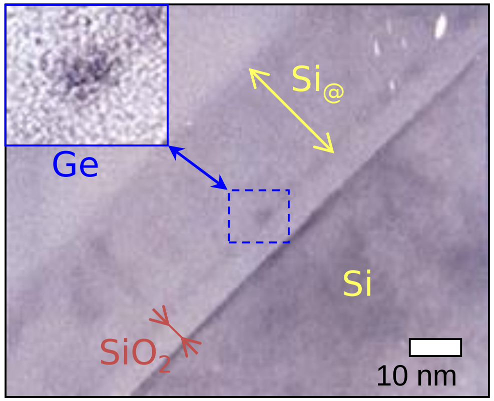

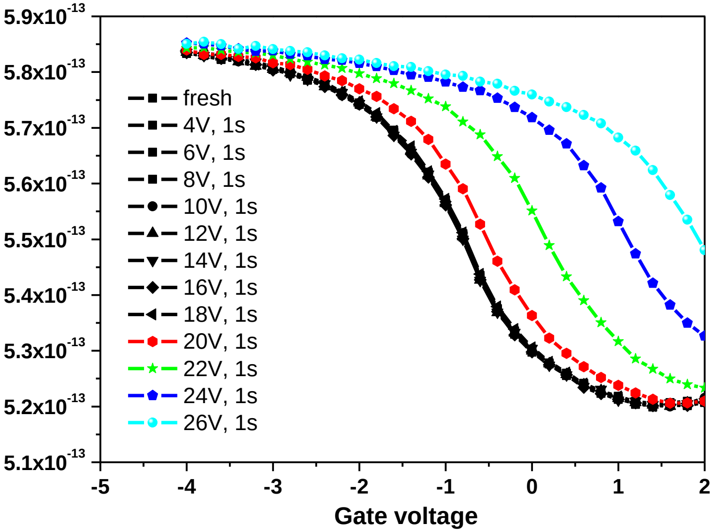

Ge layer thickness	0.5 nm
Ge dots diameter (TEM)	2.5 nm

Tuned diameter

Karmous *et al.* Phys. Rev. B (2006)

Dewetting process organization

c-SI dewetting: optical dewetting (M. Naffouti & M. Abbarchi)

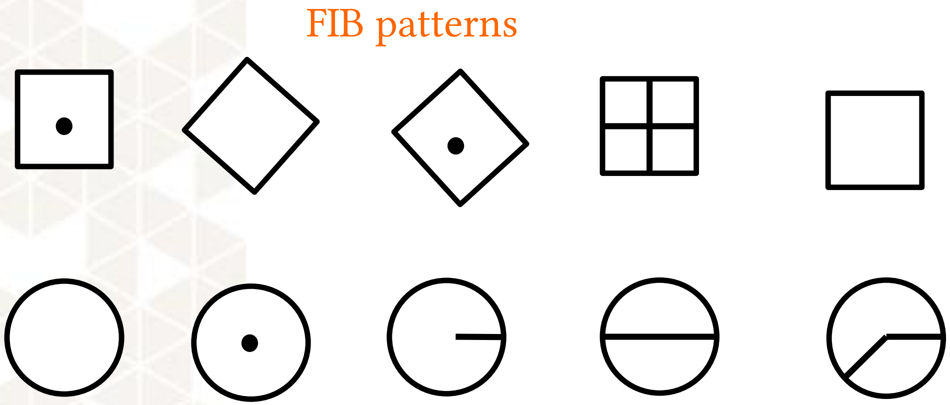

- Structures perimeter (matter conservation)
  ⇒ Dots size
- Dewetting front motion
  ⇒ Dots on pattern center
- Adding punctual defect
  ⇒ Dots position control
- Orientation pattern/crystallographic axes
  ⇒ Dots position

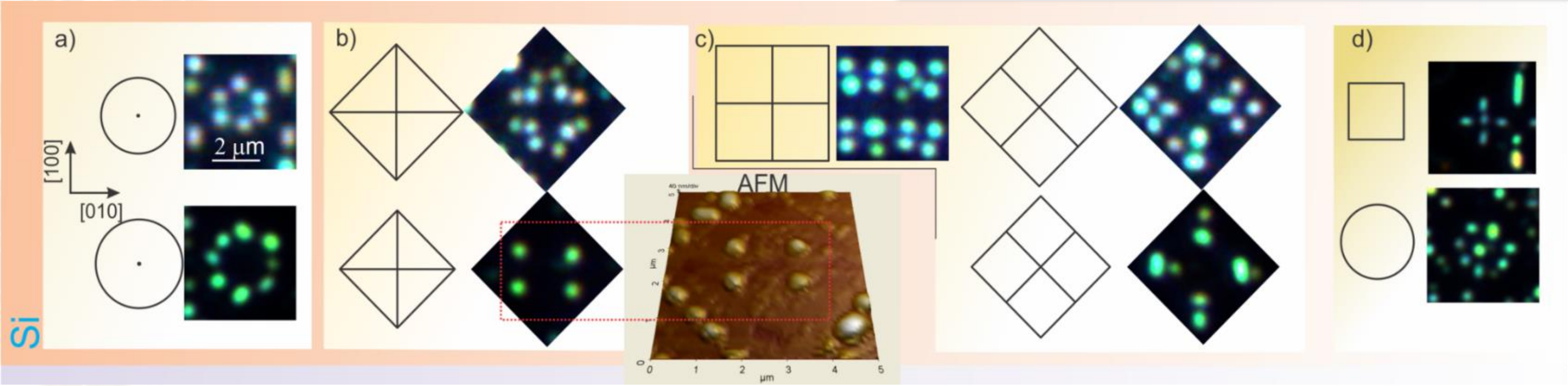

Dark field images of a partially dewetted SOI layer
SOI substrate (Si: 12 nm / SiO_2: 25 nm), 800°C - 60 minutes annealing)

M. Abbarchi *et al.*, ACS Nano, **8** (11), 11181 (2014)

Synopsis

Introduction

- Usual Si cleaning process
- Bottom-up is not, yet, efficient

Ion beam lithography

- Fast review of lithography technics
- Focused Ion Beam principles
- High resolution
- Limits: surface and volume defects

Using Focus Ion Beam for surface preparation

- Gold dewetting
- Au dots
- Silicon dewetting

Conclusion

Conclusion

FIB nanopatterning

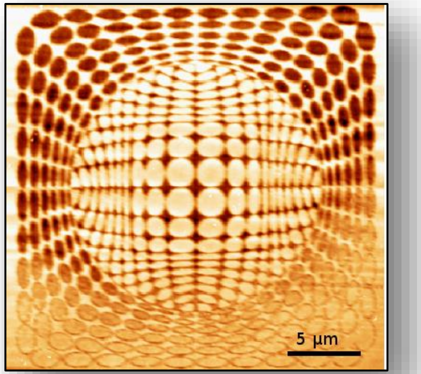

- **Critical parameters**
  - Minimum dose: swelling vs milling
  - Ion focusing
  - Excavated volume: linear with current and time
- **Sacrificial layer**
  - High resolution: 15 nm diameter
  - Compatible with Au salt galvanic displacement

- VLS Nanowires growth ready

Conclusion

FIB assisted Au catalyst dewetting

- **Critical parameters**
  - ❖ Initial Au layer thickness
  - ❖ Pitch pattern
  - ❖ Dewetting temperature
- **AuSi droplets**
  - ❖ Perfect ordering
  - ❖ Narrow size distribution
  - ❖ VLS Nanowires growth ready

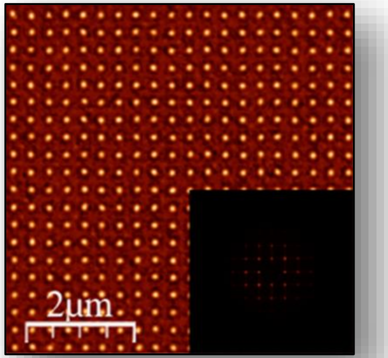

- Extendable to many metal catalyst systems

Conclusion

Next FIB generation

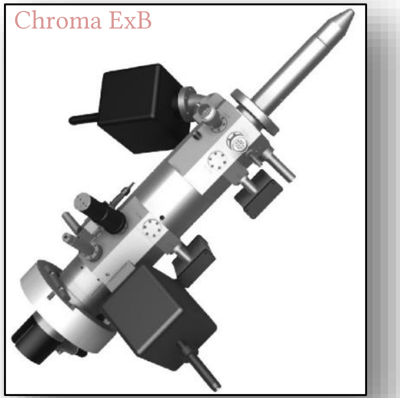
Chroma ExB

- **Ion beam column**
  - Enhancing optics resolution
  - Variable working voltage: limit induced defects

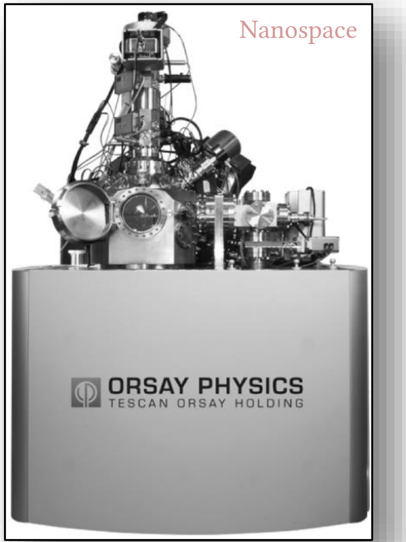
Nanospace

- **UHV compatible**
  - Milling and MBE growth successive steps
  - No oxidation
  - No contamination

- Ultinatool project (IM2NP, LAAS, Orsay Physics, Riber)

Acknowledgements

M. Abbarchi

(Assistant professor)

J.-N. Aqua

(Assistant professor)

I. Berbezier

(Professor)

T. David

(Post Doc.)

A. Ronda

(Engineer)

A. Benkouider

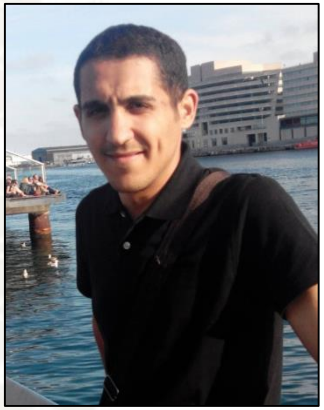

(PhD)

J.-B. Claude

(PhD)

K. Liu

(PhD)

M. Naffouti

(PhD)

Institut Matériaux Microélectronique Nanosciences Provence

Thank you for your attention

Linking fundamental research to applications within our fields of expertise

www.im2np.fr